Contents

Publication policy

The ECMWF Newsletter is published quarterly. Its purpose is to make users of ECMWF products, collaborators with ECMWF and the wider meteorological community aware of new developments at ECMWF and the use that can be made of ECMWF products. Most articles are prepared by staff at ECMWF, but articles are also welcome from people working elsewhere, especially those from Member States and Co-operating States. The ECMWF Newsletter is not peer-reviewed.

Editor: Bob Riddaway

Typesetting and Graphics: Rob Hine

Any queries about the content or distribution of the ECMWF Newsletter should be sent to Bob.Riddaway@ecmwf.int

Contacting ECMWF

Shinfield Park, Reading, Berkshire RG2 9AX, UK

Fax: . . . . . +44 118 986 9450

Telephone: National 0118 949 9000

International . . . . . +44 118 949 9000

ECMWF website . . . . . http://www.ecmwf.int

Front cover

Pictorial description of the concept behind the THORPEX Interactive Grand Global Ensemble (TIGGE).

EDITORIAL

ECMWF and GMES

The Global Monitoring for Environment and Security (GMES), initially a joint initiative from the European Union (EU) and the European Space Agency (ESA), is one of the two EU space programme flagships. Its main focus, through its core services, is to provide services related to environmental issues in support of policy makers' needs. A second goal will be to provide, through downstream developments, services to all potential users of environmental information. GMES is being implemented within four pilot services in the areas of emergency response, land monitoring, marine services and atmospheric chemistry. Two new services are being prepared in the areas of security and climate.

It is clear that what GMES has to deliver is, by and large, similar to what meteorologists have developed over the last decades in the weather area. GMES services are based on defining and collecting data, either from space or in-situ observing systems, and then processing and distributing the information. The meteorological community holds large amount of data necessary for those services. It has developed the expertise for developing, collecting, co-ordinating and processing such data and then developing services to users. It is therefore not a surprise that the European Meteorological Community is increasingly involved in GMES. EUMETSAT will be the operational space agency for marine and atmosphere services. The meteorological services are involved, through EUMETNET, in the development of the in-situ component of GMES. They are also involved in the emergency response service.

ECMWF is making a major contribution GMES. In fact it was one of the pioneers in these developments, thanks to the visionary action of Tony Hollingsworth.

ECMWF is primarily involved in the atmospheric services, as coordinator of the current project GEMS and of the proposed follow-up MACC (Monitoring Atmospheric Composition and Climate) – see for example the article about GEMS aerosol analyses starting on page 20 of this issue of the ECMWF Newsletter. In addition ECMWF is contributing to the following components of GMES.

- Marine services (seasonal forecast, waves)
- Land monitoring (global assimilation of satellite-derived vegetation information and computation of associated CO_2 fluxes)
- Emergency response (support to medium-range flood forecast and observation targeting)

ECMWF will also have a role in the development of climate services as they will include a reanalysis component for climate-change monitoring.

The coming months will be crucial for the future of GMES with important decisions expected concerning the GMES governance, long-term funding, data policy and, more directly for us, the shaping of future operational atmospheric services. It is the right moment for the European Meteorological Community to ensure that the value of the investments made by the Member States in the European Meteorological Infrastructure will be further enhanced by contributing to the development of new services in GMES. In addition, this will contribute strongly to another strategic goal which is to further develop our relationship with the EU institutions and ensure that we meet the EU increasing needs in our field of expertise. ECMWF will play its role in this important development.

Dominique Marbouty

Changes to the operational forecasting system

DAVID RICHARDSON

Implementation of Cy33r1

A new cycle of the ECMWF forecast and analysis system, Cy33r1, was introduced on 3 June 2008. The resolution of the limited area wave model was increased from 25 km to 10 km. The main changes included in this cycle are:

- Improved moist physics in tangent linear/adjoint model used in 4D-Var assimilation.
- Re-tuned entrainment in convection scheme.
- Bug fix to scaling of freezing term in convection scheme.
- Additional shear term in diffusion coefficient of vertical diffusion.
- Increased turbulent orographic form drag.
- Fix for soil temperature analysis in areas with 100% snow cover.
- Change in surface roughness for momentum, and change in post-processing of two-metre temperature and specific humidity.
- Assimilation of AMSR-E and TMI radiances in 1D+4D-Var; assimilation OMI ozone data.
- Usage of all four wind solutions for QuikSCAT in assimilation, rather than only two previously.
- Extended coverage and increased resolution for the limited area wave model.
- Improved shallow water physics and modified advection scheme for ocean wave models.
- Introduction of two new wave model parameters: maximum wave height and corresponding wave period.

Evaluation of Cy33r1

Evaluation from four months of deterministic forecasts shows a modest but significant positive impact on northern hemisphere and European scores in the troposphere. Similar results were obtained for three weeks of EPS testing.

New items on the ECMWF website

ANDY BRADY

New and modified wave forecast charts

There have been some additions and modifications to the wave plots section of the chart catalogue. There are new plots to show mean wave period and direction, and the existing plots for significant wave height and mean direction have been modified. These changes took effect from the 12 UTC run on 6 April 2008.

- www.ecmwf.int/products/forecasts/d/charts/medium/deterministic/range/wave_period_dir/
- www.ecmwf.int/products/forecasts/d/charts/medium/deterministic/range/wave_height_dir/

Forecast charts for ACMAD

Two further deterministic forecast plots, rainfall and MSLP together with 2-metre temperature and 30-metre wind over the African area have been added. ACMAD users also now have access to:

- Forecasts from the Post-AMMA Severe Weather Forecast Demonstration Project (SWFDP) project.
- Monthly forecasts of the Madden-Julian Oscillation (MJO).
- www.ecmwf.int/products/forecasts/d/charts/medium/deterministic/range/msl_24hrain_acmad/
- www.ecmwf.int/products/forecasts/d/charts/medium/deterministic/range/t2m_30mwind_acmad/

ECMWF seasonal forecasts

Several types of skill measures are now displayed in conjunction with the seasonal forecast charts. Verification is performed in cross-validation mode using the 25 years of hindcast data. GPCP data is used to validate precipitation while a combination of ERA-40 and operational analyses is used to verify all the other atmospheric parameters. The skill measures include verification scores for both deterministic and probabilistic forecasts. The Hurricane/Typhoon frequency and Accumulated Cyclone Energy (ACE) have recently been published in addition to the tropical storm frequency and mean location of tropical storm genesis. Lastly, the EUROSIP charts have been modified. The tercile summary has been added which was part of a package of changes to (a) introduce Météo-France system 3 as the new operational Météo-France model and (b) modify plot suites where needed so that all of the plots are consistent with the new standards introduced by the ECMWF System 3. Because the list of plots is different, some changes in the plot locations have been made. Consequently a check needs to be made of any page links or bookmark/favourites that have been established.

- www.ecmwf.int/products/forecasts/d/charts/seasonal/forecast/seasonal_range_forecast/group/seasonal_charts_2tm/
- www.ecmwf.int/products/forecasts/d/guide/seasonal/forecast/seasonal_range_forecast/group_trop/
- www.ecmwf.int/products/forecasts/d/charts/seasonal/forecast/eurosip/mmv2/param_euro/seasonal_charts_2tm/

ECMWF Reanalysis (ERA) Interim Project

ERA-Interim products for the period 1989–1998 are publicly available on the ECMWF Data Server. All fields are provided at 1.5° resolution. They include instantaneous and accumulated surface fields and upper-air parameters on 37 pressure levels as well as on isentropic and potential

vorticity surfaces. More information about ERA-Interim is also available.

- www.ecmwf.int/research/era/do/get/era-interim
- data.ecmwf.int/data/

New forecast charts for WMO members

Two new forecast wave plots have been added: wave height and direction together with wave mean period and direction. Also there are new areas (Africa and Global) for EPS probabilities added specifically for WMO Members.

- www.ecmwf.int/products/forecasts/d/charts/medium/deterministic/range/wave_height_dir_wmo/
- www.ecmwf.int/products/forecasts/d/charts/medium/deterministic/range/wave_period_dir_wmo/
- www.ecmwf.int/products/forecasts/d/charts/medium/eps/probabilities/probas_gusts_gts/
- www.ecmwf.int/products/forecasts/d/charts/medium/eps/probabilities/probas_rain_gts/

ECMWF Corporate Brochure

The ECMWF Corporate Brochure was released in March 2008. The brochure contains a high level overview of ECMWF and its activities.

- www.ecmwf.int/about/corporate_brochure/2007/Corporate-brochure.pdf

69th Council session on 9–10 June 2008

MANFRED KLÖPPEL

Chaired by its President, Dr Adérito Vicente Serrão from Portugal, the ECMWF Council held its 69th session in Reading on 9–10 June 2008.

For the first time, a representative from the European Commission participated to a Council session. In addressing the Council, Dr Paul Weissenberg (DG Enterprise and Industry – Director for Aerospace, Security, Defence and Equipment) emphasised that the European Commission regards ECMWF as an asset in the context of the 'Global Monitoring for Environment and Security' (GMES). He noted that the core service on atmosphere could be built upon the Centre's leadership.

Besides several decisions on financial and staff matters (for example approval of Reports from the Co-ordinating Committee on Remuneration), the main results of this session were as follows.

- **Global Monitoring for Environment and Security**. The Council considered ECMWF's future involvement in the GMES, in particular related to governance and data policy. The Council underlined the need to demonstrate vis-à-vis the European Commission that the European Meteorological Infrastructure (EMI), comprising ECMWF, EUMETSAT and European National Meteorological Services (EUMETNET), should play a prominent role within GMES.

Dr Adérito Vicente Serrão (President of the ECMWF Council), Mr Dominique Marbouty (Director of ECMWF) and Dr Paul Weissenberg (DG Enterprise and Industry – Director for Aerospace, Security, Defence and Equipment) at the ECMWF Council meeting held on 9–10 June 2008. Photograph provided by Detlev Frömming, DWD.

- **Amendments to the Convention**. Good progress had been made to the ratification process within Member States. The following 13 Member States have already ratified the amended Convention: Finland, Denmark, Norway, United Kingdom, the Netherlands, Switzerland, Italy, Spain, Luxembourg, France, Sweden, Germany and Greece. The Council started considering the accession process for new Member States.
- **Co-operation Agreements**. The Director was authorised to negotiate an agreement for scientific and technical co-operation with Tunisia.
- **Financial Matters**. The Council took note of the Auditor's Report regarding the financial year 2007 and gave discharge to the Director in respect of the implementation of the budget for 2007. The Council also considered preliminary estimates of Member States' contributions to the 2009 budget.
- **Products of the Centre**. The Council agreed to add monthly forecasts to the catalogue of archived data and approved some additions to the catalogue of real-time products.

Dr Martin Miller (Head of Model Division at ECMWF) gave a presentation to Council delegates on '*How realistic is the IFS (Integrated Forecast System) model today*'. He showed the substantial progress made in the last few years to the representation of clouds, precipitation and surface parameters. These developments contributed to improved forecasts, including those of severe weather.

Exploratory analysis and verification of seasonal forecasts with the KNMI Climate Explorer

GEERT JAN VAN OLDENBORGH (KNMI), CAIO A. S. COELHO (CPTEC), FRANCISCO J. DOBLAS-REYES (ECMWF)

ECMWF has produced seasonal forecasts since 1997. The current seasonal forecast system, System 3, has been described in the ECMWF *Newsletter No. 110* (winter 2006/2007). The UK Met Office and Météo-France also run their own seasonal forecast systems.

A European multiple-forecast system has been created as a result of research carried out as part of the EU-project DEMETER (*Palmer et al.*, 2004, *Bull. Am. Meteorol. Soc.*, **85**, 853–872). This project has shown that a multi-model ensemble is often more skilful than a single model. The combined predictions from these three systems are disseminated as the EUROSIP (European Seasonal to Inter-annual Prediction) ensemble.

Even more than for weather forecasts, the skill of seasonal forecasts strongly depends on location, season and year. When using these forecasts it is therefore important to assess the likely skill in the area and season under consideration from past performance. Most seasonal forecast centres therefore offer graphical collections of skill measures with the model documentation. However, these are difficult to compare because different methods are used to compute and represent the estimates of forecast quality. Also the results are often not readily available for the region and season of interest for a specific user.

A web-based exploratory analysis tool, the KNMI Climate Explorer (climexp.knmi.nl), has been created. From this site a user can produce a plethora of skill estimates for single-model and multi-model ensembles in a consistent way, for any region and season. In this way the forecast quality of the different systems can be assessed when making a specific seasonal forecast.

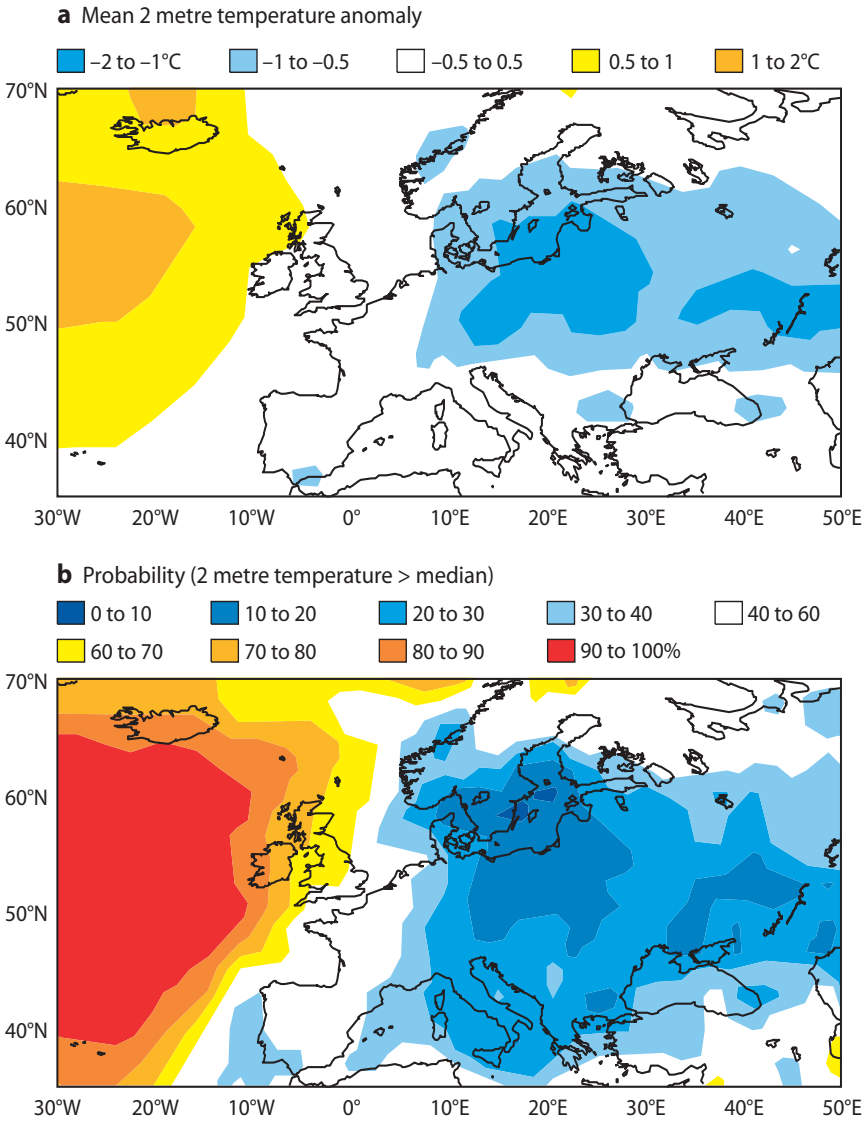

Figure 1 Near-surface temperature forecast for spring 2006 (March to May) from the EUROSIP forecast starting on 1 February 2006. (a) Ensemble-mean forecast of the average temperature anomaly. (b) Probability of temperature above the climatological median.

The website also allows an investigation of the physical mechanisms responsible for the skill exhibited by the forecasts: ENSO teleconnections, persistence of anomalies, global warming, etc. Users can produce correlation plots, regressions, composites and extreme value analyses, mainly using monthly-mean data.

At the moment the Climate Explorer has available the hindcasts and past forecasts from the operational models at ECMWF, UK Met Office, International Research Institute for Climate and Society (IRI) and National Centers for Environmental Prediction (NCEP). Also there are multi-model hindcasts from the DEMETER and ENSEMBLES projects which are funded by the EU. Data from other centres have been requested; the Météo-France hindcasts should be available soon.

The Climate Explorer has been linked to the ENSEMBLES THREDDS server at ECMWF – that was described in *ECMWF Newsletter No. 113* and

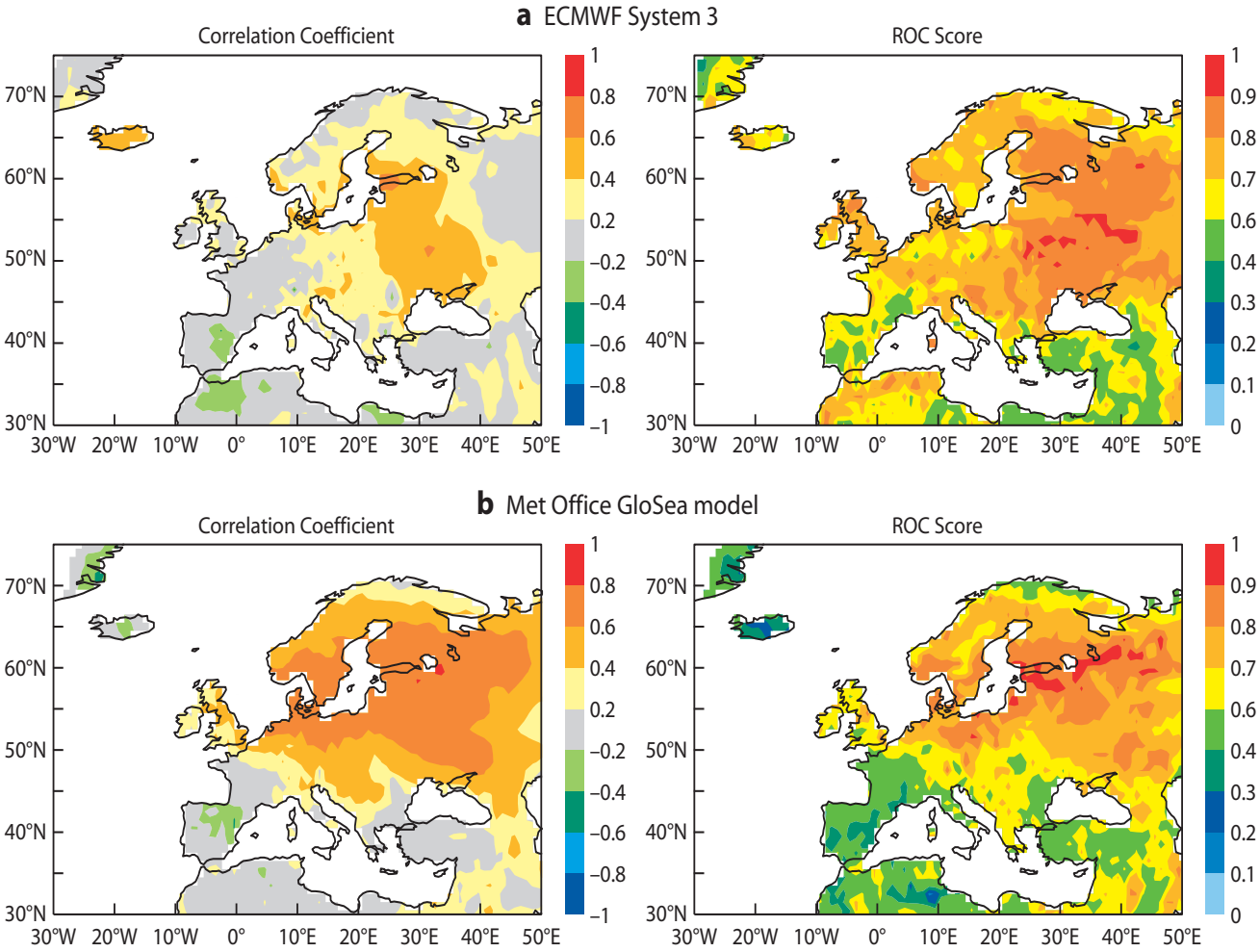

Figure 2 Correlation coefficient of the ensemble-mean forecasts (left) and ROC score for probability forecasts of above normal temperature (right) for (a) ECMWF System 3 and (b) Met Office GloSea System 3 for spring 2006 (March to May, with start date 1 February).

No. 114. With this link any two-dimensional section of the latest version of the ENSEMBLES seasonal-to-decadal dataset can be readily analyzed without the KNMI server having to locally store the model data. The forecasts can be compared to various reanalyses and analyses (including ocean data), as well as station data. Usually the output is in the form of maps or time series, although more advanced options are also available.

As an example we consider the near-surface temperature forecast for spring 2006 in Europe. Figure 1(a) shows the ensemble-mean EUROSIP forecast for the average temperature anomaly in March–May that was available February 15. Also the probability of above normal temperatures is displayed in Figure 1(b). Both plots show a clear signal for a cold spring in Eastern Europe.

Figure 2 shows two measures of skill for the spring 2006 forecasts from ECMWF's System 3 and the UK Met Office GloSea model, namely the correlation coefficient for the ensemble mean forecast and the ROC (Relative Operating Characteristic) score for the probabilistic forecast of above normal temperatures. All these plots were generated using the Climate Explorer and can be easily reproduced or modified by any user of this website. The forecast quality estimates give a clear indication of the skill of the forecasts for Eastern Europe for spring, giving credibility to a forecast of an event that was actually cold over the region. Recently there have been investigations to reveal the source of this skill (e.g. *Shongwe et al.*, 2007, *Mon. Wea. Rev.*, **135**, 4185–4201) and the KNMI Climate Explorer will contribute significantly to this type of study.

This is only one illustration of the use of the KNMI Climate Explorer. It is a very useful tool for investigating the skill of seasonal forecasts and its physical basis. As such the Climate Explorer is in operational use at KNMI, and we hope it will be useful for others involved in research, development and forecasting.

Optimisation and improvements to scalability of 4D-Var for Cy33r2

DEBORAH SALMOND, MATS HAMRUD, GEORGE MOZDZYNSKI

To keep the forecast and 4D-Var components of the Integrated Forecast System (IFS) running within the tight time-schedule for operations it is necessary to have a continuing programme of work on optimisation to offset costs of new scientific developments. These improvements are both to single processor performance and to the scalability of the parallelisation across multiple processors.

Recent optimisations based on detailed profiling of 4D-Var for Cy33r2 of the IFS – with particular attention to scalability of some of the message passing – have achieved a 7% reduction in elapsed time for a run of T799L91 4D-Var on 48 nodes (768 processors). This is the number of nodes of the IBM Power5+ currently used to run 4D-Var in operations. The total elapsed time for the 4D-Var run was reduced from 57:44 minutes to 53:20 minutes, and the overall percentage of peak obtained was increased from 7% to 7.5%.

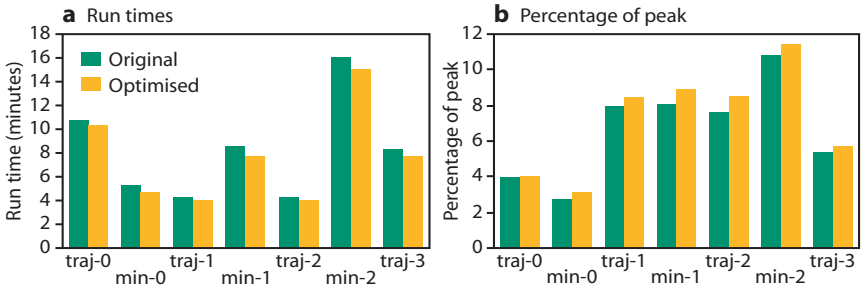

Run times (left panel) and percentage of peak (right panel) for the various steps of a T799L91 4D-Var run on 48 nodes.

The figure shows elapsed times and the percentage of peak for the various steps of 4D-Var for the original and the optimised code. This clearly illustrates the beneficial impact of the optimisation.

World Modelling Summit for Climate Prediction

RENATE HAGEDORN, MARTIN MILLER, TIM PALMER

The World Modelling Summit for Climate Prediction was hosted by ECMWF from 6 to 9 May 2008. It was fully-funded through wide-ranging international sponsorship, and jointly organized by the World Climate Research Programme (WCRP), the World Weather Research Programme (WWRP), and the International Geosphere-Biosphere Programme (IGBP). The goal of the summit was to address the threat of the consequences of global climate change by developing a strategy to revolutionize climate prediction for the 21st century.

140 participants from 19 countries, representing the global weather and climate community, attended the summit. During the opening session, introductory talks were given by distinguished speakers including Michel Jarraud (Secretary-General of WMO), Jeffrey Sachs (Director of the Earth Institute) and Chris Llewellyn-Smith (former Director of CERN). This was followed by a number of presentations related to the main themes of the summit, given by speakers from both the meteorological and computing communities. They

covered themes which included:

- The current status of weather and climate modelling and strategies for seamless prediction.
- Strategies for next-generation modelling systems.
- Prospects for current high-end computer systems.
- Strategies for model evaluation and experimentation.
- Strategies for revolutionizing climate prediction.

In essence, these themes dealt with how to enhance human and computing resources and what could be the requirements and possible organizational frameworks in the future.

The various themes were discussed in more depth during the breakout group sessions on the third day of the summit, and on the final day a draft of the summit statement was developed in plenary session. This draft version has now been finalized by the organizing committee of the summit. The statement contains 12 conclusions which can be found on the website of the summit (URL given below).

Overall it was felt that the summit was a very successful event in many respects. Not least it was a first step in bringing together the weather and climate community with a view to achieving the common goal of providing society with reliable regional predictions of climate change at all timescales that are necessary to develop mitigation and adaptation strategies.

The summit attracted considerable interest amongst the scientific and more general media. A press briefing held in London was attended by journalists from major UK print media, TV stations and international news agencies. Furthermore, the scientific journal *Nature* reported on the summit in its issue published on 15 May with an editorial and two other articles.

More information on the summit can be found on its website:

http://wcrp.ipsl.jussieu.fr/Workshops/ModellingSummit/index.html

This includes the final summit statement, a number of background documents and a link to the presentations and reports of breakout groups.

Operational assimilation of GRAS measurements at ECMWF

SEAN HEALY

ECMWF started assimilating bending angle profiles from the GRAS GPS radio occultation (GPSRO) receiver on MetOP-A on 20 May 2008. GRAS was declared operational by EUMETSAT on 17 April 2008 – it is the first fully operational GPSRO mission. GRAS provides around 650 bending angle profiles per day, and they have a small positive impact on stratospheric temperature forecasts.

GPSRO bending angle profiles have been assimilated operationally at ECMWF since 12 December 2006 (*ECMWF Newsletter No. 111*). The measurements are globally distributed, have good vertical resolution and an all weather capability. They provide information about the atmosphere that is complementary to that derived from satellite radiance measurements. Furthermore, GPSRO measurements can be assimilated without bias correction. This means that they provide an "anchor point" for the Variational Bias Correction scheme (VarBC, *ECMWF Newsletter No. 107*) in the stratosphere that prevents the bias corrected radiances drifting towards the forecast model climatology. GPSRO measurements also have important reanalysis applications.

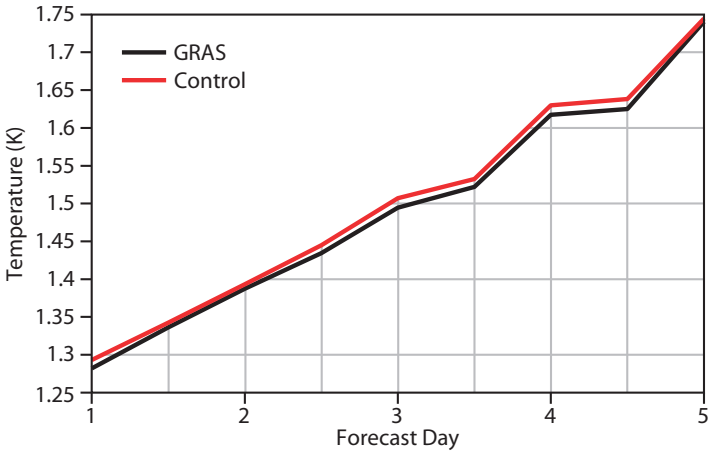

The root mean square temperature error at 50 hPa in the northern hemisphere, verified against radiosonde temperature observations. The black line shows the results when the GRAS measurements are assimilated and the red line is for the control experiment.

ECMWF typically assimilates around 2,000 bending angle profiles per day from the six satellites in the COSMIC GPSRO constellation. We assimilate bending angles as a function of impact parameter, which is a variable that measures how close the tangent point of the ray gets to the surface (*ECMWF Newsletter No. 111*). For profiles from the COSMIC constellation we can assimilate bending angles from the surface up to a height of 40 km.

It is not currently possible to use GRAS measurements in the mid and lower troposphere because of known biases. The GRAS Product Processing Facility (PPF) at EUMETSAT is still evolving and improving. This is evident in the time series of observation statistics calculated daily by the GRAS Satellite Application Facility (SAF), which are available on the web at www.grassaf.org. The current GRAS processing is based on the "phased-lock-loop" method to track the GPS signals, and the inversion of the measurements uses the geometrical optics approximation. This approach

is known to introduce biases in the troposphere and consequently it is difficult to use the GRAS measurements in this region. However, EUMETSAT is already working on the implementation of more advanced processing methods based on wave optics, which will mitigate these problems.

ECMWF has performed a 54-day 4D-Var forecast impact experiment with the GRAS measurements, covering the period 25 February to 18 April 2008. The GRAS bending angles are blacklisted below 8 km in the northern and southern hemispheres, and below 10 km in the tropics. Given the blacklisting, it is not surprising that the results are neutral in the troposphere. However, we have found some improvements in the stratospheric temperatures when verified against radiosonde observations. This is encouraging because the GRAS information content is expected to be good in the stratosphere.

We anticipate further improvements in the GRAS processing at EUMETSAT – including the implementation of wave optics processing – in the coming year. These will enable the exploitation of the measurements in the troposphere.

ECMWF Annual Report for 2007

BOB RIDDAWAY

The *ECMWF Annual Report 2007* has been published. It is intended to be an important way of maintaining the flow of information to all the people and institutions that have an interest in ECMWF.

The report draws attention to some of the key events of 2007 that affected operational activities.

- **Assimilation of radiances from AMSU-A and MHS**. Assimilation of radiances from the Advanced Microwave Sounding Unit (AMSU-A) and from the Microwave Humidity Sounder (MHS) on-board EUMETSAT's polar orbiting MetOp-A satellite, launched on 19 October 2006, became operational (11 January).
- **Upgrade of web services**. A major upgrade of the web service hardware systems was completed resulting in a significant improvement in the response when accessing the web pages (24 January).
- **New seasonal forecast system**. Operational forecasts started using System 3, the new seasonal forecast system (15 March).
- **Assimilation of radiances from HIRS**. Assimilation of radiances from the High-resolution Infrared Radiation Sounder (HIRS) instrument on-board EUMETSAT's polar orbiting MetOp-A satellite, launched on 19 October 2006, became operational (19 March).
- **TIGGE database**. The TIGGE database of operational ensemble forecasts from various global forecasting centres became accessible to scientists in near real-time for research and educational purposes (22 May).
- **Implementation of IFS Cy32r2**. A new cycle of the ECMWF forecast and analysis system was implemented (Cycle 32r2). The changes produced a significant improvement in the forecasts of the tropical troposphere at all forecast ranges (5 June).
- **Upgrade of RMDCN**. A new milestone was reached in the Centre's Regional Meteorological Data Communication Network (RMDCN) with the successful completion of the migration of the architecture from Frame Relay to a new Internet Protocol Virtual Private Network (8 June).
- **Assimilation of data from IASI and ASCAT**. Radiance data from the Infrared Atmospheric Sounding Interferometer (IASI) and surface winds from the Advanced Scatterometer (ASCAT) on-board EUMETSAT's polar orbiting MetOp-A satellite, launched on 19 October 2006, were incorporated into the operational forecasting system (12 June).
- **Implementation of IFS Cy32r3**. A new cycle of the ECMWF forecast and analysis system was implemented (Cycle 32r3). This included significant changes to the model physics with a beneficial increase in model activity globally, particularly in the tropics (6 November).
- **Contract with IBM**. The contract for the Centre's next High Performance Computing Facility was signed with IBM (20 December).

As well as the Annual Report describing the wide range of activities at ECMWF there is particular emphasis on the prediction of severe weather. Indeed ECMWF's strategy puts the early warning of severe weather as its principal goal. In the report there are examples of:

- Good predictions of severe weather: severe storm Kyril over northern Europe in January, high temperatures in Europe in April, heat wave in south-eastern Europe and flooding in England and Wales in June.
- Use of hydrological ensembles for flood prediction.
- Support provided by ECMWF for severe weather events.

The Annual Report can be downloaded from:

www.ecmwf.int/publications/annual_report

The THORPEX Interactive Grand Global Ensemble (TIGGE): concept and objectives

PHILIPPE BOUGEAULT

THE THORPEX Interactive Grand Global Ensemble (TIGGE) is a key component of THORPEX, one of the major components of the World Weather Research Programme (WWRP) of the World Meteorological Organization. TIGGE will contribute to achieving one of the WWRP-THORPEX goals: to accelerate improvements in the accuracy of one-day to two-week high-impact weather forecasts for the benefit of humanity. In addition TIGGE is registered as a specific task for GEO (Group on Earth Observation). It has high relevance to the GEO societal benefit areas that need access to advanced global weather forecasts and the derived products, especially in areas related to risk management, disaster mitigation, energy, health etc.

The objectives of TIGGE are:

- Enhancing collaboration on ensemble prediction, internationally and between operational centres and universities.
- Developing new methods to combine ensembles from different sources and to correct for systematic errors (biases, spread over-/under-estimation).
- Achieving a deeper understanding of the contribution of observation, initial and model uncertainties to forecast error.
- Exploring the feasibility and the benefit of interactive ensemble systems responding dynamically to changing uncertainty.
- Enabling evolution towards an operational system, the "Global Interactive Forecast System (GIFS)".

Phase 1 and Phase 2 of TIGGE

The TIGGE objectives will be reached by a two-phase implementation. In the current Phase 1 data are collected in near-real time at a small number of central data archives using existing network and storage capabilities. They are then made accessible to scientists for research and education through specific data portals. The delay to access any forecast data is 48 hours. The implementation of TIGGE Phase 1 is described in the article in this edition of the *ECMWF Newsletter* which starts on page 10.

In Phase 2, to be developed in the near future subject to the success of Phase 1, the real-time preparation and distribution of multi-model products will be the main focus. This will require substantial software development, specific funding and coordination with the evolving WMO Information System (WIS). Archiving arrangements may also be reviewed in Phase 2.

The highest priority data accumulated in the TIGGE archive are the ensemble forecasts generated routinely (operationally) at major forecast centres around the world. This core data stored in the TIGGE archive is accumulating at a daily rate of approximately 240 GB from ten providers around the world. Additional special datasets may be added in the future for specific research and applications.

The databases and data portals of Phase 1 have been developed by three archive and distribution centres: ECMWF, US National Centre for Atmospheric Research (NCAR) and China Meteorological Agency (CMA). The operational forecasting centres supplying daily forecasts are given in Box A.

TIGGE has strong links with the North American Ensemble Forecasting System (NAEFS). Although NAEFS is initially an operational project, TIGGE and NAEFS share many technical aspects, and NAEFS plans to implement results from TIGGE. It is believed that TIGGE and the NAEFS will ultimately evolve into a single operational system.

Data access

Data providers supply their products to the TIGGE archive centres under an agreed set of rules, which include re-distribution rights. Access is provided for research and education through a simple electronic registration process, with valid e-mail address and acknowledgment of conditions of supply. Under the simple registration process, access is given with a delay (48 hours) after the initial time of the forecast. Real-time access is granted in some cases, e.g. for field experiments and projects of special interest to THORPEX. Registration for real-time access is handled via the THORPEX International Programme Office.

Box A

Centres supplying daily forecasts to the TIGGE archive

- ECMWF
- US National Centers for Environmental Prediction (NCEP)
- Meteorological Service of Canada (MSC)
- Australian Bureau of Meteorology (BoM)
- China Meteorological Administration (CMA)
- Brazilian Centra de Previsao de Tempo e Estudos Climatico (CPTEC)
- Japan Meteorological Administration (JMA)
- Korea Meteorological Administration (KMA)
- Météo-France
- UK Met Office

Box B

TIGGE data portals

Data access is operated via the TIGGE data portals.
- NCAR portal: http://tigge.ucar.edu
- ECMWF portal: http://tigge-portal.ecmwf.int/
- The CMA portal: http://wisportal.cma.gov.cn/tigge/

The functionalities of the data portal are:
- Registration.
- Search, discover, and download files.
- Select data by initialization date/time, data provider, file type and forecast time.
- Check volume and download data.

Data access is operated via the TIGGE data portals at NCAR, ECMWF and CMA. Information about how to access these portals and their functionality are given in Box B. These portals also provide selection of parameter subsets. ECMWF offers grid interpolation and a wide choice of spatial subsets. In the future NCAR and CMA plan to offer these expanded services.

Outlook

TIGGE is considered by THORPEX as paving the way towards a Global Interactive Forecasting System (GIFS). The primary need for further development is to accelerate data exchange between the partners. In the upcoming Phase 2 of TIGGE, which is still subject to funding, requirements for massive data transfers will be alleviated by a distributed data access concept.

It is anticipated that limited-area ensemble prediction systems will also form an important component of the GIFS whose development is dependent upon TIGGE. The priority requirement here is to develop standard formats which will enhance the interoperability of the existing systems. One key objective is to facilitate the use of lateral boundary conditions from various global systems by various limited-area systems. A panel of experts (called TIGGE-LAM) has recently been set-up to organize the limited-area-model component of TIGGE. The three archive centres have accepted in principle to host results from LAM ensemble prediction systems as part of the TIGGE archive for Phase 1.

Data from the TIGGE archive is already being used for a variety of research and development activities. An example of how TIGGE data has been used to study predictability is given in the article starting on page 16 of this edition of the ECMWF Newsletter.

There is no doubt that there are immense benefits in optimizing the use of the output from ensemble prediction systems. Having scientist make full use of the data in the TIGGE archive will help realize those benefits. ECMWF encourages European scientists to engage in using the TIGGE archive to fully assess the merits of multi-model forecasting.

FURTHER READING

WMO, 2005: First Workshop on the THORPEX Interactive Grand Global Ensemble (TIGGE), Final Report. *WMO/TD-No. 1273, WWRP/THORPEX No. 5* (available from www.wmo.int/thorpex).

Implementation of TIGGE Phase I

BAUDOUIN RAOULT, MANUEL FUENTES

THE THORPEX Interactive Grand Global Ensemble (TIGGE) aims to improve the accuracy of high-impact weather forecasts by enhancing the development and use of ensemble predictions through international collaboration. The goal of TIGGE is to collect in near-real-time and store in a common format the outputs of global ensembles run to around 14 days. These outputs would be made available to researchers in operational centres and academic communities. In the longer term TIGGE would be the basis for the development of a prototype for the future Global Interactive Forecasting System (GIFS). More information about the concept of TIGGE and its objectives can be found in the article by Philippe Bougeault in this edition of the *ECMWF Newsletter* (see page 9).

The first workshop on TIGGE was held at ECMWF in March 2005. Its purpose was to collect the views of the community about the aims of the TIGGE science, the requirements for use of TIGGE data and how the associated infrastructure should be designed.

Ten operational centres volunteered to become Data Providers: these are listed in Box A on page 9 of the article by Philippe Bougeault. In addition three centres volunteered to become Archive Centres: CMA (China), ECMWF and NCAR (USA).

On 1 October 2006, three Data Providers started sending the output from their global EPS to the three Archive Centres in near-real-time. Users were provided with access to the archive on 1 May 2007. On 1 February 2008, less than three years after the first TIGGE workshop, the tenth and last of the Data Providers started sending its data in near-real-time to the Archive Centres.

This article describes the work carried out during these three years, the technical choices that have been made, and some of the difficulties that have been encountered.

Requirements

During the first workshop, the goals and requirements of TIGGE were laid out. These are now described.

A key component of TIGGE would be the TIGGE database. This would contain a core dataset consisting of ensemble forecasts generated routinely at different centres. Additional datasets could be added later to respond to requests of the scientific community, especially the THORPEX Working Groups. The database would also consist of a website providing the capability to link to regional and user-specific observational data sets.

TIGGE data would be available to all users for research purposes. Consideration would also be given to the provision of real-time access to data, in particular for demonstration projects and field experiments. The process for obtaining approval for data access would need to be transparent, streamlined and reasonably fast.

To meet user needs, a user-friendly interface to the database should be developed, that enable researchers to obtain subsets of ensemble data, especially over geographic regions of their choice.

Post-processing of archived data would be required before delivery to users. Routines would be needed for grid conversion, format conversion, and for the extraction of sub-areas, parameters and levels, for example. In addition, applications and tools for data processing, tailored to the needs of specific users, could be prepared and shared among users. These tools would need to be catalogued and documented.

Two phases were considered:

- **Phase 1**. The data would be collected in near-real-time (via the Internet) at a small number of central TIGGE data archives.
- **Phase 2**. The TIGGE database would be distributed, and a user would have to retrieve the data from the different Data Providers, using a common interface.

Technical implementation

This first workshop was followed by a meeting of a Working Group on Archiving held at ECMWF on 19–21 September 2005. It included representatives from CMA, ECMWF, NCAR and the North American Ensemble Forecast System (NAEFS). This group established how TIGGE Phase 1 could be implemented. The outcome of this working group was presented at the Implementation Meeting held at ECMWF on 9–10 November 2005. The participants represented both Archive Centres and Data Providers, and addressed the technical issues raised by the two preceding meetings.

Homogeneity of the TIGGE database

For the TIGGE project to succeed, it is paramount that the content of the database is as homogeneous as possible. This would ensure a productive environment with systematic data management and user access to data from many provider centres. The more consistent the archive, the easier it would be to develop applications.

All partners needed to agree on a common way of referencing data within the TIGGE dataset and describe fields using the following attributes: *analysis date*, *analysis time*, *forecast time step*, *origin centre*, *ensemble number*, *level* and *parameter*. In this context "parameter" refers to the physical quantity represented by the field: temperature, pressure etc.

When using fields to create a "grand ensemble", i.e. when considering all members from several Data Providers as a super ensemble, it is essential that they share the same values for the attributes *analysis date*, *analysis time*, *forecast time step*, *level* and *parameter*. Furthermore, all fields had to be provided using the same units. This led to the definition of the TIGGE core dataset to which all Data Providers must adhere (Table 1).

To guarantee the best precision original model grids and resolutions should be preserved if possible. Data Providers would supply interpolation routines for conversion to regular latitude-longitude grids and for point extraction. Archive Centres may endeavour to return data in regular grids using these interpolation routines.

As a common data format it was decided to use GRIB edition 2 – it is the only WMO standard that supports ensemble data without the need of local extensions. Moreover, the NAEFS community is committed to using it. Data Providers would make their data available in the archive format. Requests for clarifications and proposals for new parameters were submitted to the WMO Expert Team on Data Representation systems and Codes; as a result, a substantial number of amendments were made to the Guide to the WMO Table Driven Code Form.

The Archive Centres defined the list of GRIB2 codes, tables and templates to be used for each of the fields of the TIGGE database. They also provided guidelines (best practice) on how all TIGGE fields should be coded in GRIB2, as well as examples of properly encoded model outputs.

Data transfers

It was thought that the available network bandwidth between Europe and the USA is sufficient to meet the needs of TIGGE. However, CMA raised concerns that the current bandwidth between China and Europe as well as between China and the USA (the latter probably being better) would not meet the TIGGE requirements. Nevertheless, the situation was improved by the end of 2006 when CMA joined the GLORIAD network.

After extensive testing, it was decided that IDD/LDM (Internet Data Distribution system, Local Data Manager), an Internet based distribution system developed by UNIDATA, would suit the requirements of TIGGE for data transfer. In particular it would support the parallel transfers needed to exchange the large volumes of TIGGE data.

LDM is a broadcasting system, based on a subscription mechanism: a "downstream" LDM can subscribe to "products" from an "upstream" LDM. When a product is inserted in the upstream LDM, it is automatically

Parameter	Unit
Parameters on a single level	
Mean sea level pressure	Pa
Surface Pressure	Pa
10 m u-velocity	m s^{-1}
10 m v-velocity	m s^{-1}
Surface temperature	K
Surface dew point temperature	K
Surface max temperature	K
Surface min temperature	K
Skin temperature	K
Soil moisture	kg m^{-3}
Soil temperature	K
Total precipitation (liquid + frozen)	kg m^{-2}
Snowfall water equivalent	kg m^{-2}
Snow depth water equivalent	kg m^{-2}
Total cloud cover	0–100%
Total column water	kg m^{-2}
Time-integrated surface latent heat flux	W m^{-2} s
Time-integrated surface sensible heat flux	W m^{-2} s
Time-integrated surface net solar radiation	W m^{-2} s
Time-integrated surface net thermal radiation	W m^{-2} s
Time-integrated outgoing long-wave radiation	W m^{-2} s
Sunshine duration	s
Convective available potential energy	J kg^{-1}
Convective inhibition	J kg^{-1}
Orography (Geopotential height at the surface)	m
Land-sea mask	0–1
Parameters on pressure levels	
Temperature	K
Geopotential height	m
U-velocity	m s^{-1}
V-velocity	m s^{-1}
Specific humidity	kg kg-1
Parameters on potential temperature surfaces	
Potential vorticity on θ = 320 K surface	K m^2 kg^{-1} s^{-1}
Parameters of potential vorticity surfaces	
Potential temperature on 2PVU surface	K
U-velocity 2PVU surface	m s^{-1}
V-velocity 2PVU surface	m s^{-1}

Table 1 List of agreed parameters and their units. Note that temperature, u-velocity, v-velocity and specific humidity are provided on the following isobaric surfaces: 1000, 925, 850, 700, 500, 300, 250 and 200 hPa. The geopotential height is provided on the same surfaces plus 50 hPa. All parameters have to be provided six-hourly. All fluxes are to be accumulated since the beginning of the forecast.

sent to all the downstream LDMs that have subscribed to this product. Unfortunately, such a broadcasting system does not guarantee that products will be received by all downstream LDM, in particular if some are not running. To overcome this problem, a protocol has been defined on top of LDM to exchange fields by specifying a file name convention and a series of messages to request retransmission of missing fields. A complete description of the protocol is available on the TIGGE website.

Operational aspects

For day-to-day operations tools would have to be created to monitor the data transfer within the system. Therefore, each Archive Centre will set up a web page showing volumes, date of data and date of reception for each Data Provider. This information will be used to cross-validate the content at the three archives. In addition the Archive Centres will provide the technical coordination of the project and take on the responsibility of defining the necessary procedures.

Whenever problems arise that prevent data delivery to the Archive Centres, the Data Provider will be responsible for notifying all the Archive Centres (e.g. by sending an e-mail to the appropriate TIGGE mailing list).

The objective is to have complete data at the Archive Centres as an incomplete dataset is often difficult to use, as most of the current tools used for ensemble data assume a fixed number of members from day to day. To ensure the datasets are as complete as possible, Data Providers would endeavour to send missing data to the Archive Centres – even if this means rerunning a forecast cycle.

If an Archive Centre does not receive the expected data from a Data Provider, or if the data are incomplete or corrupted, it will first check with other Archive Centres and determine whether the failure is an isolated case. If it is an isolated case, recovery will be initiated between Archive Centres. If not, the Data Provider must re-initiate the data delivery. In any case, incidents must be investigated and documented. The Archive Centres have agreed to define and collect common metrics that can be used to create combined TIGGE-wide reports. This information will be used as a basis for the further evolutions of the system.

Participation in TIGGE must not interfere with the operational activities of Data Providers: they should be able to upgrade models, introduce higher resolutions, and make all customary changes as needed. Mechanisms should exist which allow new products from the Providers to be easily integrated into the TIGGE Archive Centres. On the other hand, Data Providers must take into account their participation in TIGGE when planning changes to their forecasting systems, and must inform Archive Centres accordingly.

To support the smooth running of TIGGE activities, it was decided that each partner would nominate two contact points: a technical contact point who will be able

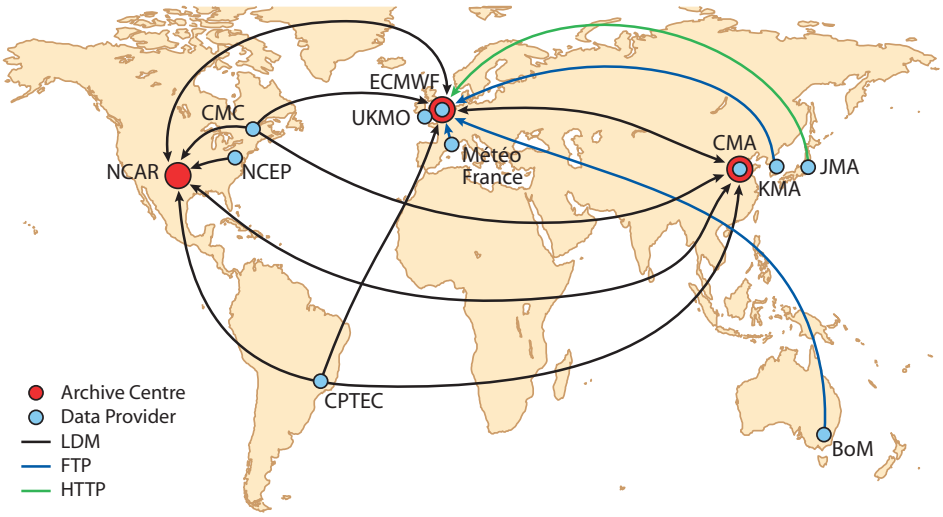

Figure 1 Exchange of data between Data Providers and Archive Centres.

to address operational and technical issues, such as troubleshooting, networking or timeliness of delivery and a scientific contact point who will be able to address issues such as forecast performances or numerical errors.

User access

Access will be provided for research and education through a simple electronic registration process. Once registered, access will be given with a delay of 48 hours after the initial time of the forecast (reference time of data in GRIB2). Registration for real-time access will be handled via the THORPEX International Programme Office.

The Archive Centres will guarantee that user interfaces will present the same information (e.g. same variable names), and that similar requests, although expressed differently, should return identical results.

From planning to implementation

As with any project, there have been a few deviations from the original plans, mainly to accommodate the operational requirements of the Data Providers.

Collaboration

A website has been setup at http://tigge.ecmwf.int. It contains the list of all known contact points for each partner (though this information is password protected). It also contains a comprehensive description of how fields should be encoded in GRIB2, with an example of each field available for download.

A description of the protocol (file names, messages, etc.) that has been built on top of LDM can be downloaded, together with sample scripts implementing the protocol and sample configuration files.

Compliance with the agreed list of parameters

As the first data exchanges were being set up between the partners, it soon became clear that most of the Data Providers could not contribute to the whole of the agreed list of products, mainly because these products were not produced by their models. It was felt that waiting for all partners to upgrade their systems to produce the missing fields was an unnecessary delay in the building of the archive. As all the Data Providers were producing the most important fields (surface temperature, geopotential, winds, etc. on standard levels), a staged approach was chosen. Data Providers would join the project by sending whatever parameters they had, and would add more parameters during the course of the project.

Data transfer

Although LDM was the preferred solution for the exchange of data between the TIGGE partners, it was not always possible for Data Providers to install an LDM server at their site. Some decided to use either FTP or HTTP to transfer the data to one of the Archive Centres which would in turn relay it to the two others. Figure 1 shows the various protocols used between the Data Providers and Archive Centres.

Quality assurance

Good quality assurance procedures are required to guarantee the homogeneity of the dataset. Many tests have been implemented to ensure that the TIGGE database does not contain any badly encoded data that would prevent its use. With such checks in place, researchers can use the archive with confidence.

When a Data Provider starts sending new data to the Archive Centres, all new fields are marked as being in "test" mode. The new fields are checked against the agreed list of TIGGE fields, and then checked for proper encoding and units. Once all the fields have been validated, they are tagged as being in "production" mode and are sent routinely.

Although all the fields have been thoroughly validated during the test phase, changes may be introduced by

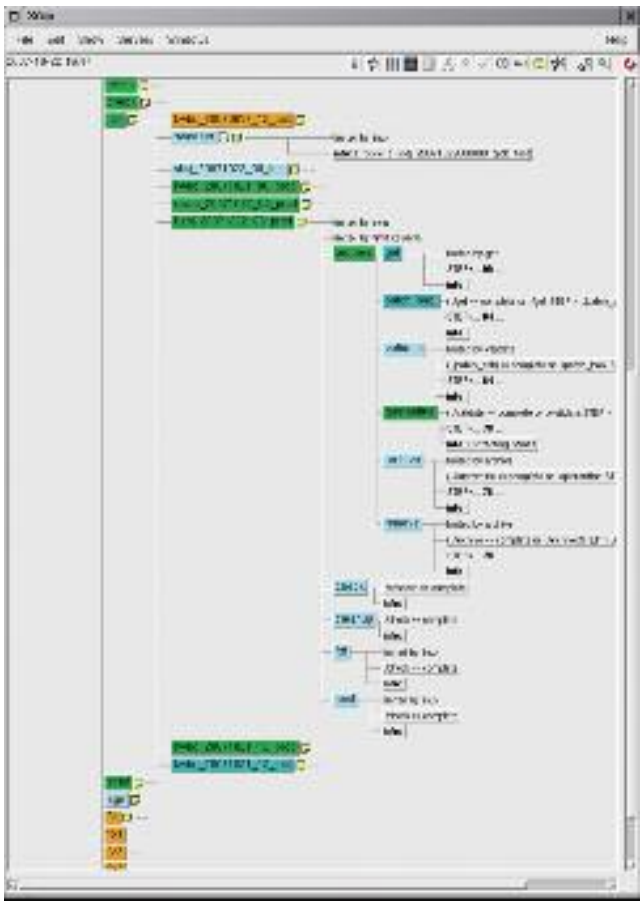

Figure 2 Processing the TIGGE flow.

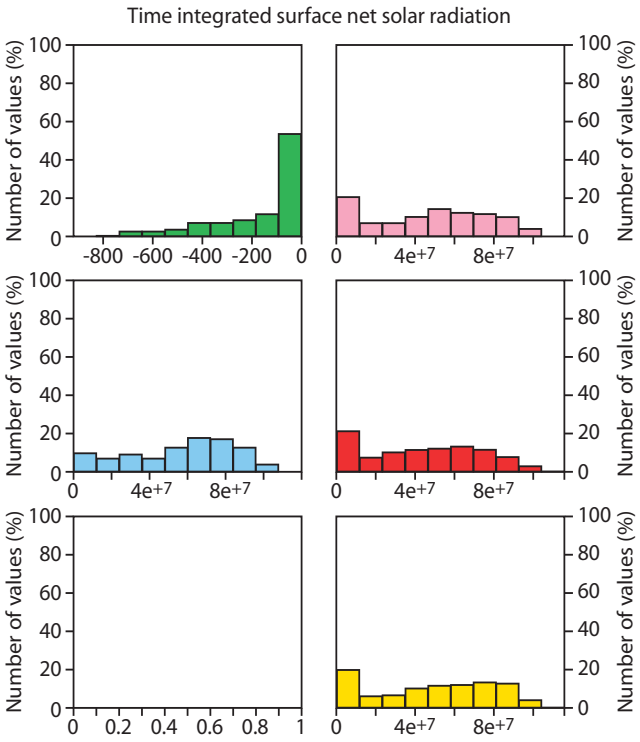

Figure 3 Example of a plot produced every day to compare data from providers. The charts of time integrated surface net solar radiation from various providers indicate an error in the data from one of the data providers (top left chart).

the Data Providers due to evolutions in their operational environments. It is recognised that these changes may subsequently have an unforeseen effect on the TIGGE data exchange. This is why all the fields which are received in production mode are also validated, and any field that fails this validation would be quarantined for further investigation. This guarantees that no unexpected data is able to compromise the homogeneity of the archive. Figure 2 shows a screenshot of SMS, the ECMWF supervisor used to control the flow

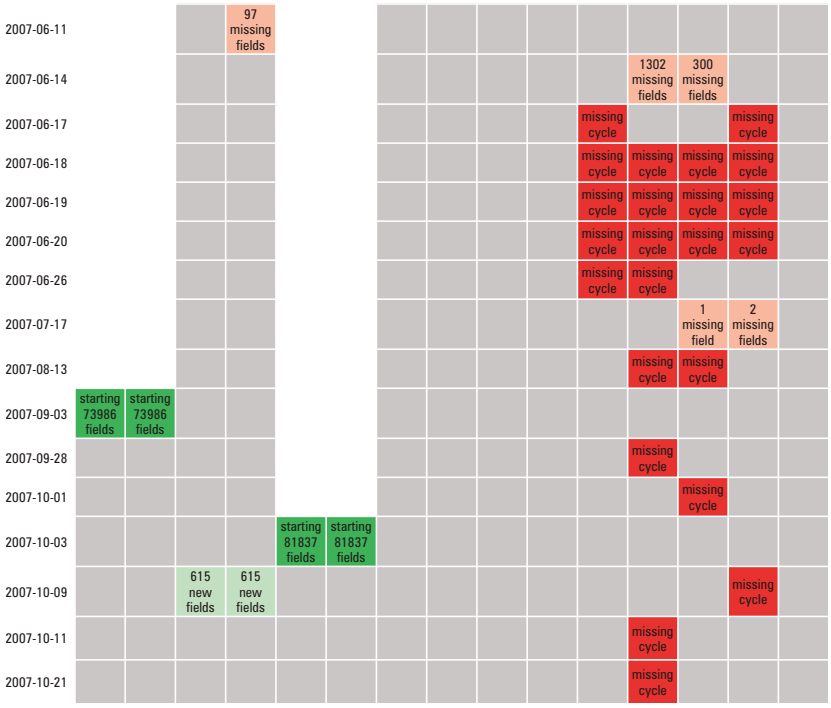

Figure 4 TIGGE history web page.

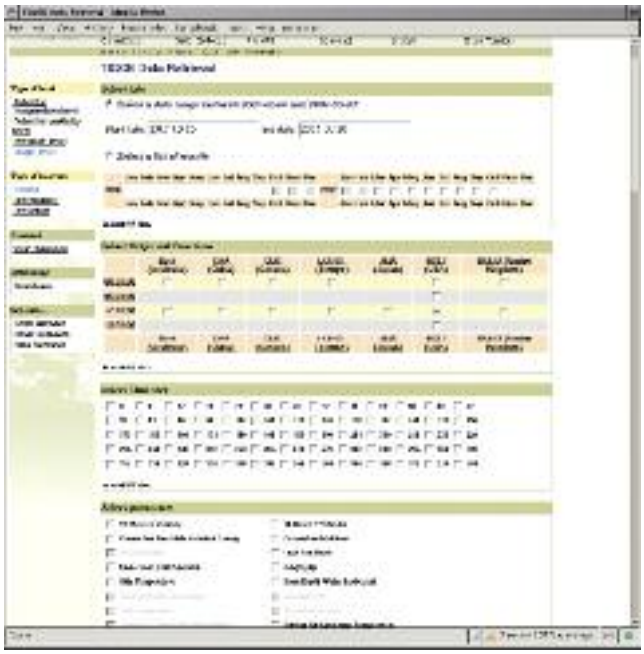

Figure 5 Selection of fields on the TIGGE data portal.

of TIGGE data at ECMWF. The "archive" task will only run once the "validate" and "quarantine" tasks are successful.

To complement the documentation and examples available from the TIGGE website, a series of GRIB2 tools were made available to all the partners. The tools included GRIB1 to GRIB2 converters and validation programmes. For example the tigge_check command will check if a field is correctly encoded and if it is part of the agreed catalogue.

Fields may be properly encoded, and pass checks by validation tools, but their values may still be incorrect. This is usually the case if the units are wrong, or the fields are instantaneous instead of accumulated. To spot these problems, a series of plots are produced every day, comparing the data from all the providers – an example of such a plot is given in Figure 3.

In order to ensure that the TIGGE archive is as complete as possible, a web page has been set up to show the status of availability of each cycle from each Data Provider. This web page (Figure 4) shows the whole history of the dataset: the addition of new fields is indicated, as well as any incidents. It is used by the partners to check the completeness of their contributions to the dataset.

ECMWF's TIGGE portal

The ECMWF TIGGE data portal can be found at http://tigge-portal.ecmwf.int. The portal makes use of the WebMARS framework that has been developed at ECMWF to provide access to the MARS archive for external users. It allows users to select any combination of parameters, origins, levels, time steps and dates, in a very simple manner, by offering a very compact user interface and making use of the AJAX technology to control user selection. This data portal is illustrated in Figure 5.

Users have the possibility of requesting the data in various forms: on a common grid (Figure 6(a)) and on a common area (Figure 6(b)), thus retrieving a very homogeneous dataset that can easily be used. Hundreds of thousands of fields can be sought with a single request (Figure 6(c)).

As the TIGGE database is already very large, and growing, it was necessary to offer access to offline data (on tape). In order to make sure that the TIGGE activity has no adverse impact on ECMWF's core activities, TIGGE retrieval requests are handled by a dedicated SMS and a dedicated MARS server, while re-gridding is performed on a dedicated Linux server. This allows a very fine control of the resources used by this service.

There are around 100 registered users, of which a third are active. Figure 7 shows the country of origin of the registered users (excluding ECMWF internal users).

There has been a considerable growth of active users since the service started (Figure 8(a)). From December 2006 to April 2007 the service was only available inside ECMWF, but it was opened to the external users in May 2007. In addition the number of requests handled per

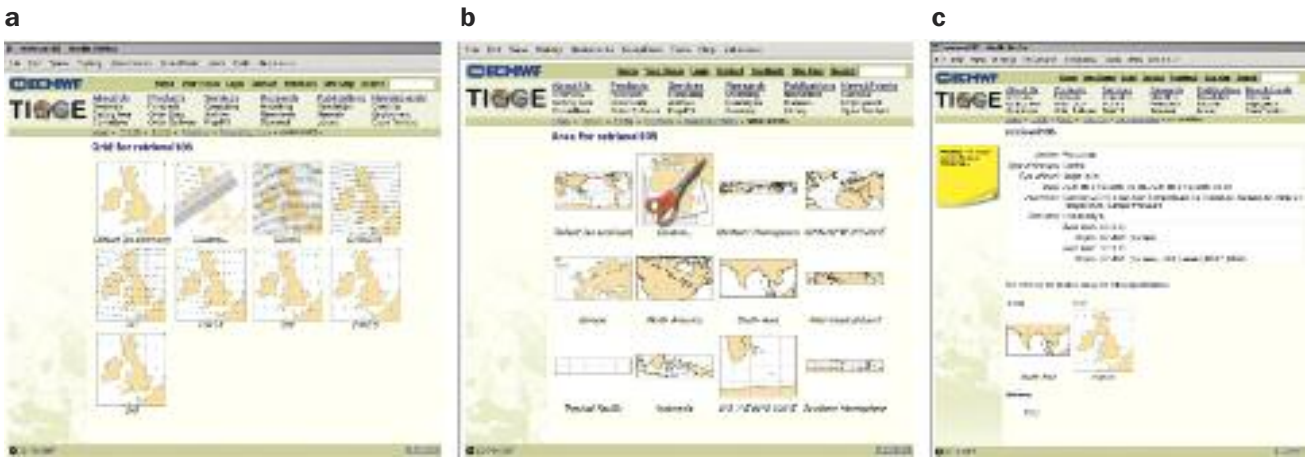

Figure 6 Web pages illustrating the selection of data in terms of (a) the grid and (b) the area and (c) the amount.

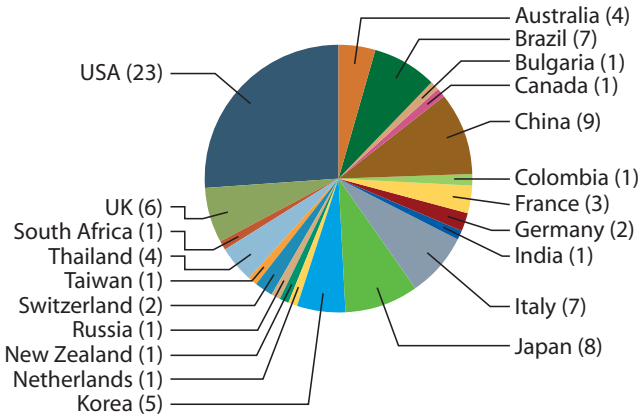

Figure 7 Number of registered users according to their country.

month has increased (Figure 8(b)). These increases are reflected in the amount of data retrieved from the MARS archive (Figure 8(c)) in terms of both the amount of data retrieved from the database and the amount of data delivered to the users. The difference is due to users being given the opportunity to extract sub-areas and change the resolution of the data retrieved.

Success of TIGGE Phase 1

Around 240 GB (~1.6 million fields) are now exchanged routinely each day between ten Data Providers and three Archive Centres in near-real-time. The TIGGE database now contains global EPS data from all ten Data Providers, and holds more than 100 TBytes of data (600 million fields).

Around 100 users have registered with the TIGGE data portal at ECMWF, of which a third are active, generating up to 5,000 requests per month. An example of how the TIGGE data has been used is provided by the articles in this edition of the *ECMWF Newsletter* which describes some predictability studies (see page 16).

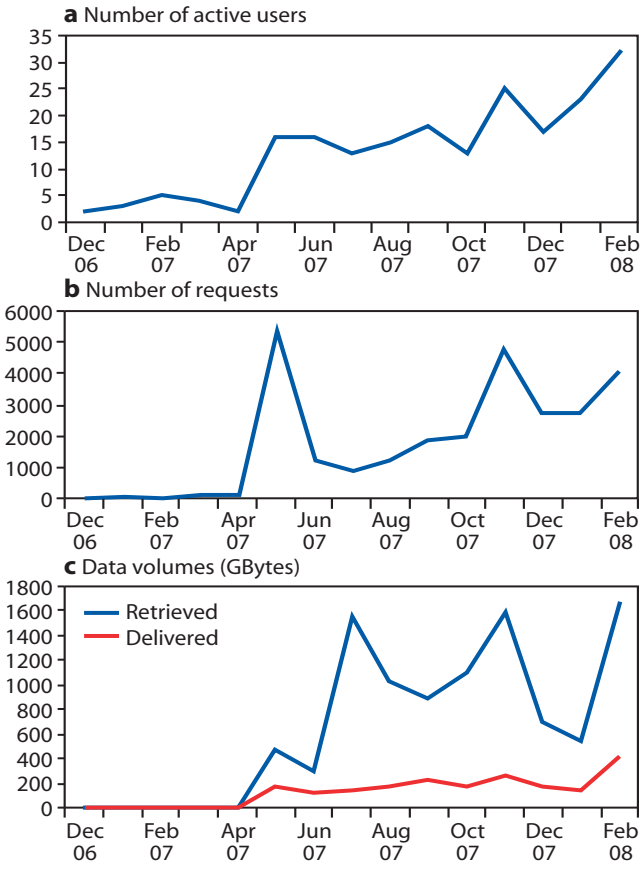

Figure 8 Variation in (a) number of active users (b) number of data requests and (c) data volumes from December 2006 to February 2008.

TIGGE Phase 1 is a truly successful international collaboration – it has only been possible thanks to strict governance by the Archive Centres and a strong commitment from the Data Providers. The TIGGE database now provides an essential tool for the research community, giving THORPEX the means to achieve its goals.

Predictability studies using TIGGE data

ROBERTO BUIZZA, YOUNG-YOUN PARK,
MARTIN LEUTBECHER, FLORIAN PAPPENBERGER

OPERATIONAL medium-range ensemble prediction began in December 1992, when the National Centers for Environmental Prediction (NCEP) and ECMWF began producing global ensemble predictions as part of their operational products. In 1995, the Meteorological Service of Canada (MSC) implemented its ensemble prediction system. Following these examples, six other centres started running global ensemble prediction systems daily. At the beginning of 2008, ten meteorological centres are running a medium-range (i.e. with a forecast length of at least 7 days) global ensemble prediction system. The ensemble systems are based on a finite number of time integrations of a numerical weather prediction model. Most of them are designed to simulate the effect on forecast accuracy of initial uncertainties, with only few of them designed also to simulate the effect of model approximations.

TIGGE, the THORPEX Interactive Grand Global Ensemble, has among its objectives to achieve a deeper understanding of the contribution of initial and model uncertainties to forecast error, and to develop new methods of combining ensembles from different sources

AFFILIATIONS
Roberto Buizza, Martin Leutbecher, Florian Pappenberger: ECMWF, Reading UK.
Young-Youn Park: ECMWF and Korea Meteorological Administration, Seoul, Republic of Korea.

and of correcting systematic errors (biases and spread over- or under-estimation). More information about the concept of TIGGE and its objectives is given in the article by Philippe Bougeault on page 9 of this edition of the *ECMWF Newsletter*.

Here we summarise some preliminary conclusions from two studies using TIGGE data:

- *Park et al.* (2008), who presented some results on comparing and combining ensembles obtained using the TIGGE data available up to December 2007.
- *Pappenberger et al.* (2008), who illustrated how TIGGE weather forecasts can be used in hydrological ensemble prediction for a case of severe flooding that affected Romania in October 2007.

Assessing the strengths and weaknesses of single ensemble systems

For the first time, TIGGE gives access to forecasts generated by different ensemble systems but archived with the same format (GRIB2). Users can easily extract all available ensemble forecasts, and compare the performance of individual systems. Thereby, TIGGE helps to develop an understanding of the strengths and weaknesses of each single system. The TIGGE dataset can also be used to investigate the potential value of calibration methods, and of combining single ensembles into a multi-systems ensemble. An example is given in Figure 1 which uses ensembles from ECMWF, UK Met Office (UKMO), Japan Meteorological Administration (JMA) and China Meteorological Administration.

A comparison was made between the scores of the single ECMWF ensemble, with or without bias correction, with the scores of three bias-corrected combinations:

- Combined ECMWF and UKMO ensemble.
- Combined ECMWF, UKMO and JMA ensemble.
- Combined ECMWF, UKMO, JMA and CMA ensemble.

Note that the scores of the bias-corrected combined ECMWF, UKMO and JMA ensemble are almost identical to those of the bias-corrected combined ECMWF, UKMO, JMA and CMA ensemble. Consequently the results of the combined ECMWF, UKMO and JMA ensemble are not shown in Figure 1.

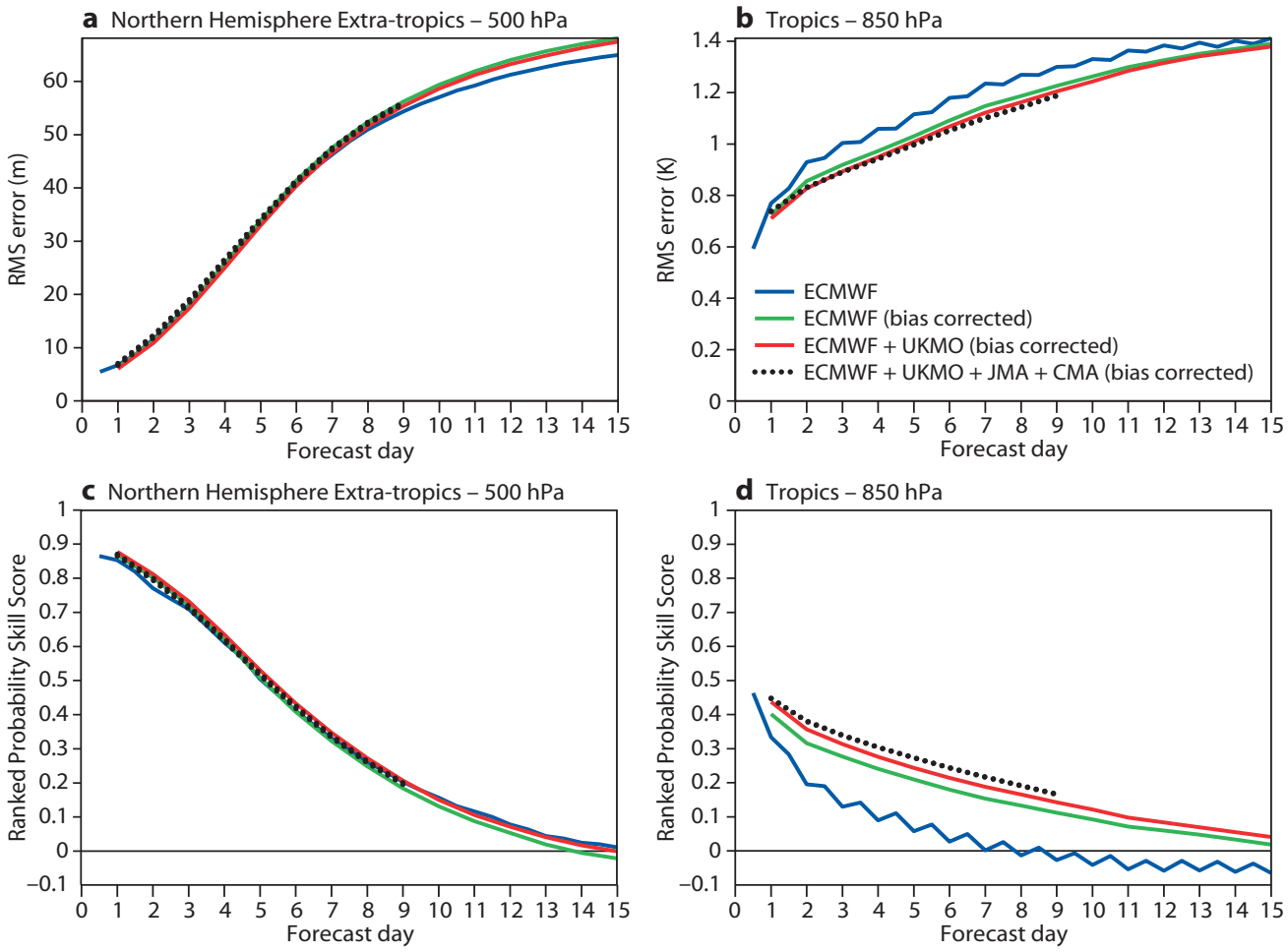

Figure 1 TIGGE combination results for June, July and August 2007 (86 cases): average scores of ECMWF (blue line), bias-corrected ECMWF (green line), bias-corrected combined ECMWF and UKMO (red line) and bias-corrected combined ECMWF, UKMO, JMA and CMA (dotted line), with biases estimated using a 30-day training period. (a) Root-mean-square error of the ensemble mean forecast of 500 hPa geopotential height over the northern hemisphere extra-tropics. (b) Root-mean-square error of the ensemble mean forecast of 850 hPa temperature over the tropics. (c) Rank probability skill score for 500 hPa geopotential height over the northern hemisphere extra-tropics. (d) Rank probability skill score for the 850 hPa temperature over the tropics (from *Park et al.*, 2008).

Results indicate that for the 500 hPa geopotential height over the northern hemisphere extra-tropics the scores of all these ensembles are very close (Figures 1(a) and 1(c)). It is found that all scores are slightly worse than the score of the single ECMWF ensemble without bias correction. By contrast, results indicate that for the 850 hPa geopotential height over the tropics (Figures 1(b) and 1(d)), adding the UKMO and JMA ensembles to the ECMWF ensemble improves the scores, but further adding the CMA ensemble does not bring any extra improvement. It is interesting that most of the improvements are achieved by combining the two ensembles characterized by the most similar performance characteristics (i.e. ECMWF and UKMO ensembles), while the addition of a third ensemble does not bring any extra improvement.

To further illustrate the impact of merging two ensembles with similar characteristics, Figure 2 compares the performance of the ECMWF ensemble without bias correction with three other ensembles:

- UKMO ensemble without bias correction.
- Combined ECMWF and UKMO ensemble with bias correction.
- Combined ECMWF and UKMO ensemble without bias correction.

For the 500 hPa geopotential height over the northern hemisphere extra-tropics (Figures 2(a) and 2(c)), results show that the single ECMWF ensemble performs better than the single UKMO ensemble. Also in the short-range the combined bias-corrected ECMWF and UKMO ensemble performs best, but in the long range the combined non-bias-corrected ECMWF and UKMO ensemble has the best performance. By contrast, for the 850 hPa temperature over the tropics (Figures 2(b) and 2(d)) it is the combined ECMWF and UKMO ensemble with bias-correction that outperforms the other systems.

In general, the preliminary results obtained by *Park et al.* (2008) indicate that, for the variables considered in their study, it is over the tropics where the perform-

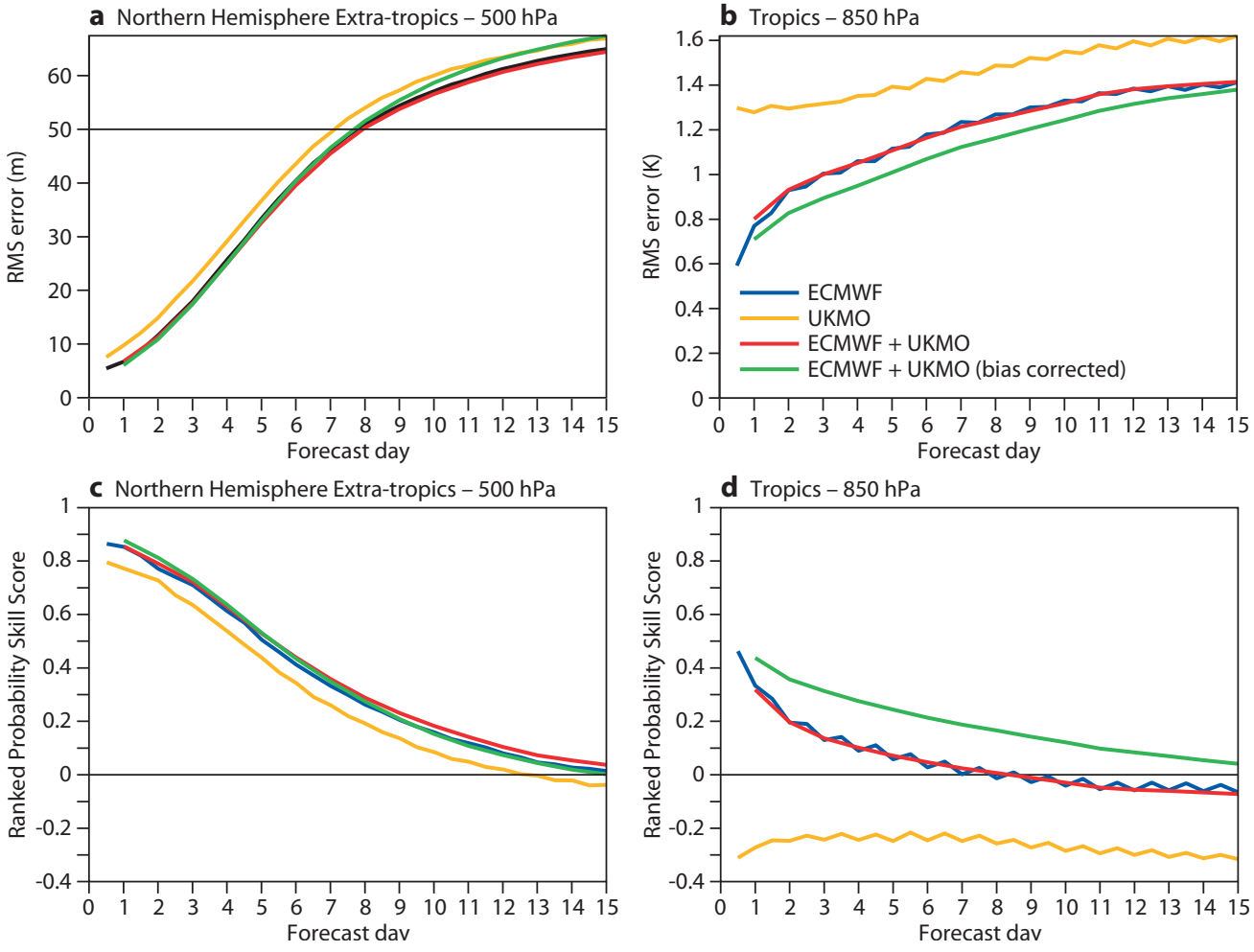

Figure 2 TIGGE combination results for June, July and August 2007 (86 cases): average scores of ECMWF (blue line), UKMO (yellow line), combined ECMWF and UKMO (red line) and bias-corrected combined ECMWF and UKMO (green line), with biases estimated using a 30-day training period. (a) Root-mean-square error of the ensemble mean forecast of the 500 hPa geopotential height over the northern hemisphere extra-tropics. (b) Root-mean-square error of the ensemble mean forecast of the 850 hPa temperature over the tropics. (c) Rank probability skill score for the 500 hPa geopotential height over the northern hemisphere extra-tropics. (d) Rank probability skill score for 850 hPa temperature over the tropics (from *Park et al.*, 2008).

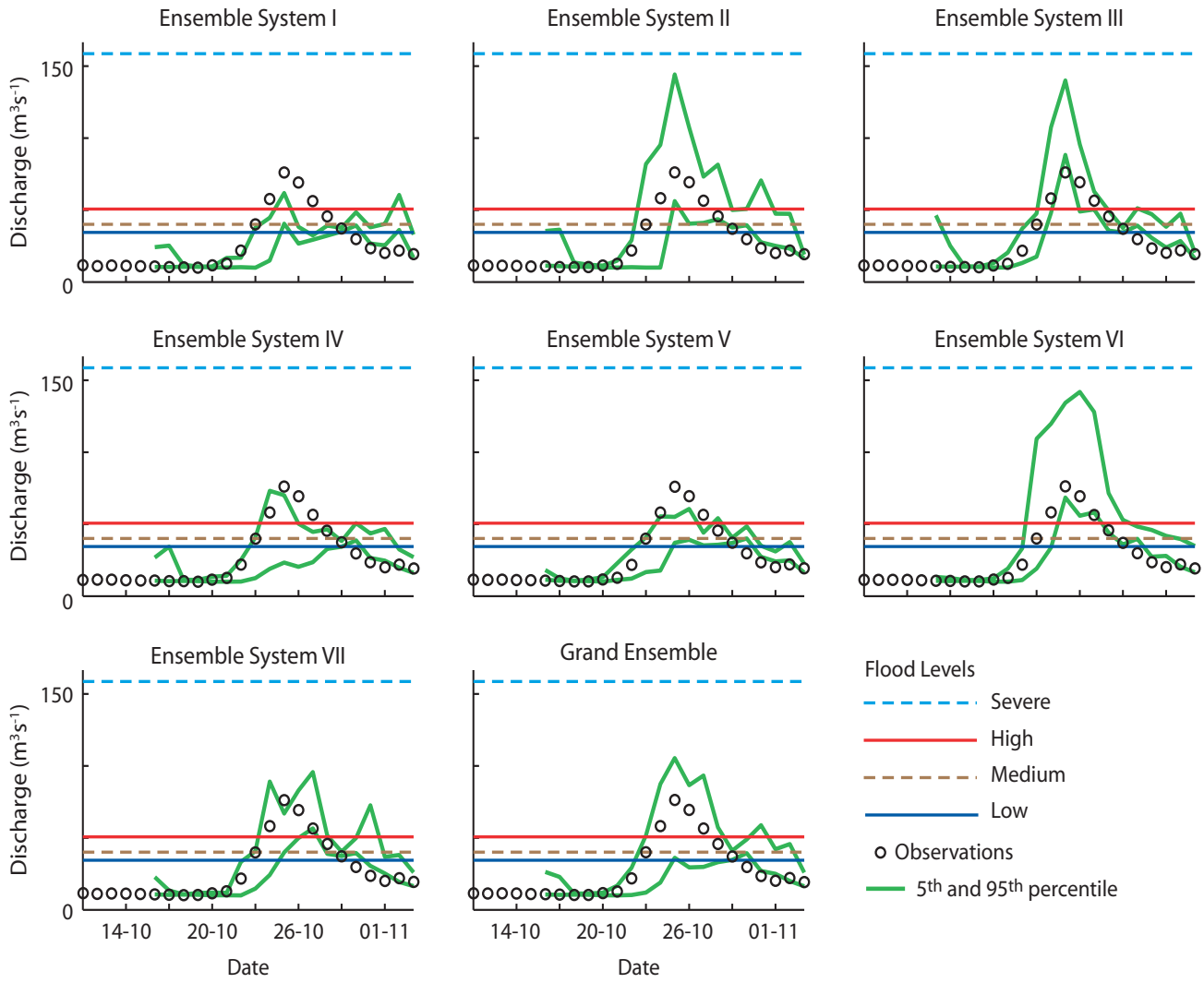

Figure 3 The 5th and 95th percentile of discharge predictions of the different forecasts with a 5 day lead time. The horizontal lines indicate the four warning thresholds (from *Pappenberger et al.*, 2008).

ance of the ensembles differs most. Also it is over the tropics where the benefit of combining them is the highest. Overall, these preliminary results indicate that care must be taken when combining ensemble systems. It appears that the largest benefit of merging ensembles is for the prediction of, for example the 850 hPa temperature over the tropics, an area where the largest variability in the performance of the single ensembles have been detected. Refer to *Park et al.* (2008) for a more complete discussion of these and related issues.

Using TIGGE data in hydrological probabilistic prediction

Pappenberger et al. (2008) illustrated how TIGGE weather forecasts can be used to drive the European Flood Alert System (EFAS), a flood prediction model developed as an initiative of the European Commission. EFAS has been running on a pre-operational basis at the EU's Joint Research Centre (JRC) since 2005, driven by Deutscher Wetterdiens (DWD) and ECMWF rainfall forecasts. It provides local water authorities with probabilistic flood forecasting information up to 10 days in advance based on four warning thresholds (low, medium, high and severe). More precisely, *Pappenberger et al.* (2008) discussed the potential of using grand-ensembles for early flood warnings by evaluating flood forecasts based on TIGGE data for the floods on several tributaries to the Danube in Romania (Siret, Jiu, Olt and Arges) in October 2007.

Figure 3 shows EFAS discharge forecasts driven from the single TIGGE ensembles and for a grand-ensemble which includes all the single ensemble forecasts for a 5-day lead time. It is essential to correctly represent the onset of the rising limb of the flood hydrograph to allow flood preparedness and disaster mitigation. All six single ensemble distributions and the grand-ensemble distribution predict the onset of the rising limb correctly in terms of timing and discharge thresholds. However, some of them fail to include the observed hydrograph at the onset and peak time. None of the forecasts perform very well for the lower end of the recession limb.

It is found that the ensemble spread widens with lead time and thus more observations are bracketed. The

widening distribution also means that a lower percentage of discharge predictions are above the warning thresholds. This has important implications for issuing warnings – at long lead times there will be fewer ensemble members that will be able to trigger such warnings and this should be taken into account (this is recognised in the EFAS system). Overall, using the grand-ensemble consistently gives a good prediction of the flood hydrograph, apart from the falling recession limb.

The potential value of TIGGE data for predictability studies

Scientists are encouraged to access the TIGGE database, and try to answer some of the key questions which are still outstanding in ensemble prediction. TIGGE gives users access to many ensemble systems, but it is still not clear whether there is one method which is most efficient to calibrate and combine single ensembles to generate grand-ensemble products, or whether different methods should be used for different variables, areas and users. Also there is still the unanswered question about whether a single system can perform as well as a grand-ensemble system. This brings us to a fundamental question about the simulation of model approximations in ensemble prediction: is using a multi-system ensemble the best approach to simulate the effect of model uncertainty on forecast quality? Alongside these and other key predictability questions, the TIGGE database can also help users become more familiar with ensemble products, test the development of new products and foster a more intense exploitation of a probabilistic approach to weather prediction.

FURTHER READING

Pappenberger, **F.**, **J. Bartholmes**, **J. Thielen**, **H.L. Cloke**, **R. Buizza** & **A. de Roo**, 2008: New dimensions in early flood warning across the globe using grand-ensemble weather predictions. *Geophys. Res. Lett.*, doi:10.1029/2008GL033837, in press, available online (also published as *ECMWF Tech. Memo No. 558*).

Park, **Y.-Y.**, **R. Buizza** & **M. Leutbecher**, 2008: TIGGE: preliminary results on comparing and combining ensembles. *Q. J. R. Meteorol. Soc*, submitted (also published as *ECMWF Tech. Memo. No. 548*).

GEMS aerosol analyses with the ECMWF Integrated Forecast System

ANGELA BENEDETTI, JEAN-JACQUES MORCRETTE, OLIVIER BOUCHER, ANTJE DETHOF, RICHARD ENGELEN, LUKE JONES, JOHANNES W. KAISER, MARTIN SUTTIE AND THE GEMS TEAM

ENVIRONMENTAL monitoring will become an integral part of the ECMWF mission under the new convention that is undergoing ratification by the Member States. One of the major EU-funded projects dedicated to this goal is GEMS which deals with global and regional earth-system (atmosphere) monitoring using satellite and in-situ data. GEMS is being undertaken by thirty-two European partners with expertise in various aspects of atmospheric composition monitoring.

As part of ECMWF's contribution to GEMS, a 4D-Var reanalysis for the years 2003–2007 is currently being run to estimate atmospheric greenhouse gases (carbon dioxide and methane), reactive gases (carbon monoxide, ozone etc.) and aerosols using satellite-based observations. In parallel, an aerosol-only reanalysis is being run for the years 2003–2004. Near real-time forecasts of these tracers are also being performed both on global and on regional (European) scales. Preliminary results for both reanalyses and forecasts can be found at http://gems.ecmwf.int.

This short note focuses on describing the development and implementation of the aerosol component of the 4D-Var assimilation system.

The aerosol analysis system

The aerosol species included in the analysis are sea salt, desert dust, black carbon, organic matter and sulphates. Stratospheric background aerosol can be also activated. However, the background values for 2003–2004 are so small that it has been decided to run the reanalysis without stratospheric aerosols. Some of the key features of the analysis system are as follows.

- The emission sources for the various aerosol species are defined either using established emission inventories (black carbon, organic matter and sulphates) or through parametrizations (sea salt and desert dust) which involve model variables such as surface winds and soil moisture, amongst others.
- All aerosols species are subject to horizontal and vertical advection, diffusion and aerosol-specific physical processes such as sedimentation and wet/dry deposition.
- For organic matter and black carbon, both the hydrophobic and the hydrophilic components are considered.
- Desert dust and sea salt are represented with three size bins whose limits are chosen to include 10%, 20% and 70% of the total mass.

The analysis is performed on the total aerosol mixing ratio which is calculated as the sum of all species. The background fractional contributions are then used to re-distribute the analysis increments of total mixing ratio into the single species. This is achieved primarily

through an aerosol mass adjustment using observations of total aerosol optical depth derived from the Moderate Resolution Imaging Spectroradiometer (MODIS) instrument on-board of the NASA Terra and Aqua satellites. The aerosol observations are processed through the operational pathway and ingested in the 4D-Var system where they are processed with an ad hoc observation operator specifically designed for aerosol optical depth. This operator uses pre-computed values of aerosol optical properties, specific to the different aerosol species at the wavelength of interest (at present, 550 nm), in combination with the first-guess values of the aerosol mixing ratios from the model to calculate a profile of extinction. This extinction profile is then vertically integrated to obtain the aerosol total optical depth.

Initial test analyses showed anomalous increments in total aerosol mixing ratio, and consequently in aerosol optical depth, over the polar regions. The values produced in the analysis were clearly unrealistic, with optical depths reaching values as large as 3 over the north pole, where they should be around 0.1–0.2. Several experiments were conducted to understand the reason for these large increments, including:

- Data denial experiments.

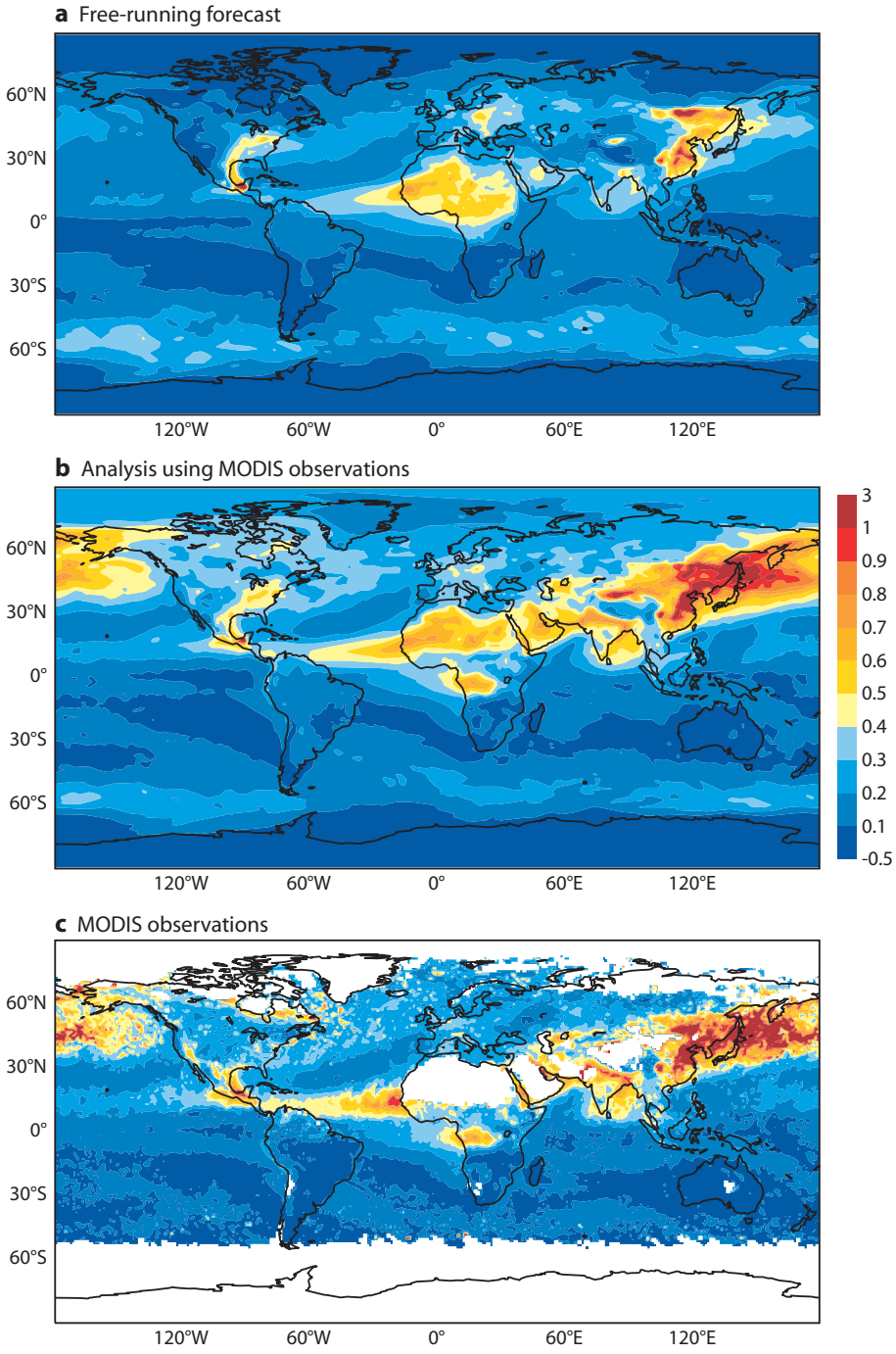

Figure 1 Comparisons of simulated aerosol optical depths from the new aerosol module implemented in the IFS model: (a) free-running forecast, (b) analysis using MODIS collection 5 observations, and (c) MODIS average optical depth for the month of May 2003.

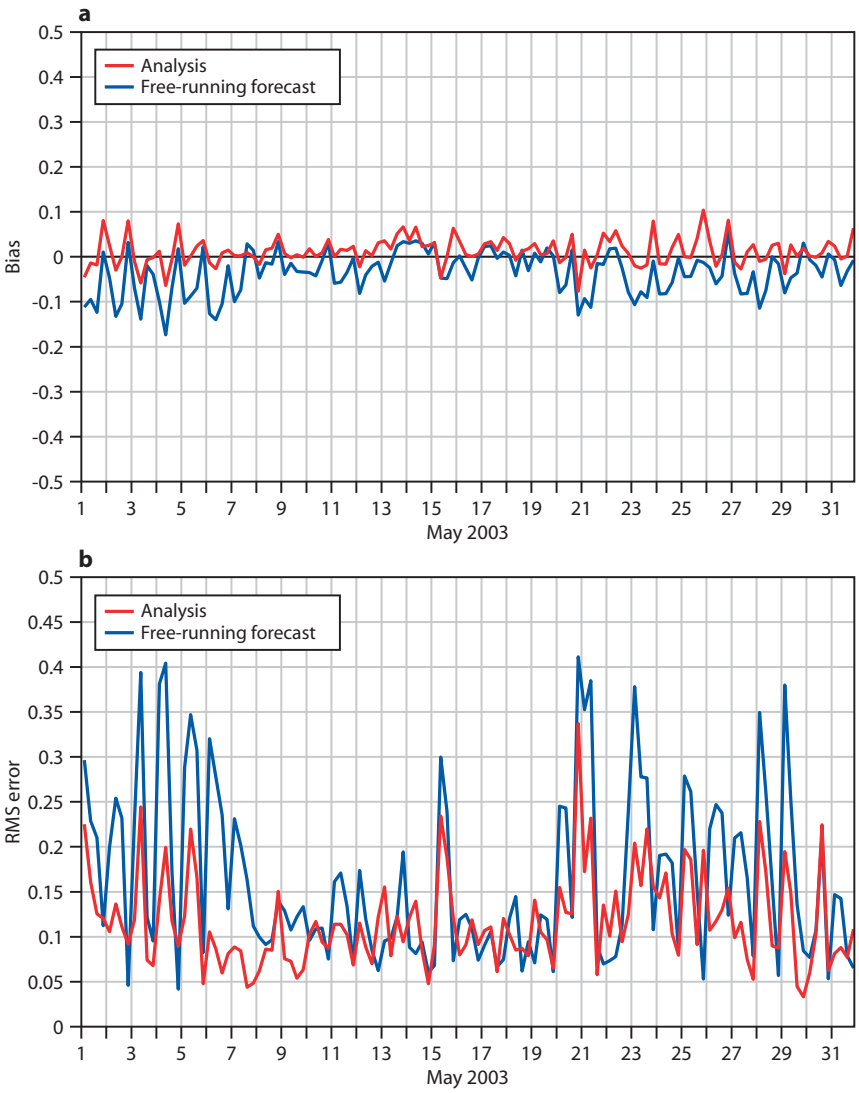

Figure 2 (a) Bias and (b) RMS error of free-running forecast (blue) and analysis (red) of aerosol optical depths at 550 nm with respect to AERONET ground observations for May 2003.

- The implementation of aerosol loss parametrizations in the minimisation.
- The redefinition of the background error statistics.

The last of these proved to be the solution to the problem.

The old background aerosol statistics had been calculated with a preliminary model version which included only sea salt, desert dust and a generic continental background aerosol type; hence they had become outdated for the improved aerosol model. New statistics have been calculated with the current model version. Comparisons with the old set of statistics show dramatic differences both in the standard deviation and in the vertical and horizontal correlations. Specifically the new standard deviation is one order of magnitude smaller than the old one, indicating that the model has a smaller degree of variability in the aerosol forecasts at 24 and 48 hours. This, in turn, translates into a smaller background error, which is more realistic given the improvements implemented in the current aerosol model. With this new background error, the analysis, while still drawing to the observations, takes the model background constraint more into account. This is extremely important, especially in areas that are data-limited such as the polar regions where the aerosol analysis could be severely under-constrained.

First results

The current analysis configuration includes the new aerosol background statistics. Also it includes the error analysis for MODIS optical depth data over ocean developed at the Laboratoire d'Optique Atmosphérique (LOA), which is a partner in the project. The aerosol data in the analysis come from MODIS collection 5 (see http://modis.gsfc.nasa.gov/).

Figure 1 shows quantitative comparisons between a 'free-running' forecast of aerosol optical depth without any assimilation and the analysis of optical depth from assimilated MODIS observations. The MODIS observations are also shown as reference. Optical depth retrievals are assimilated over both land and ocean. The three-hourly forecasts of optical depth from the

free-running model and from the analysis are averaged over May 2003.

Results show that the analysis is very effective in bringing the model aerosol optical depth closer to the observations. The assimilation generally improves the aerosol distribution, especially over areas with extensive biomass burning and other anthropogenic sources. These are not captured as well in the free-running simulation, mainly because of inadequate definition of the sources for these anthropogenic emissions. Note, however, the overall skill of the forecast model in predicting the general distribution of the aerosol fields which provides a good first-guess for the analysis.

Figure 2 shows some preliminary comparisons of the free-running forecast and analysis of aerosol optical depths with AERONET independent data for May 2003. Forty-one sites, as evenly distributed over the globe as possible, were chosen for the comparison. Both plots

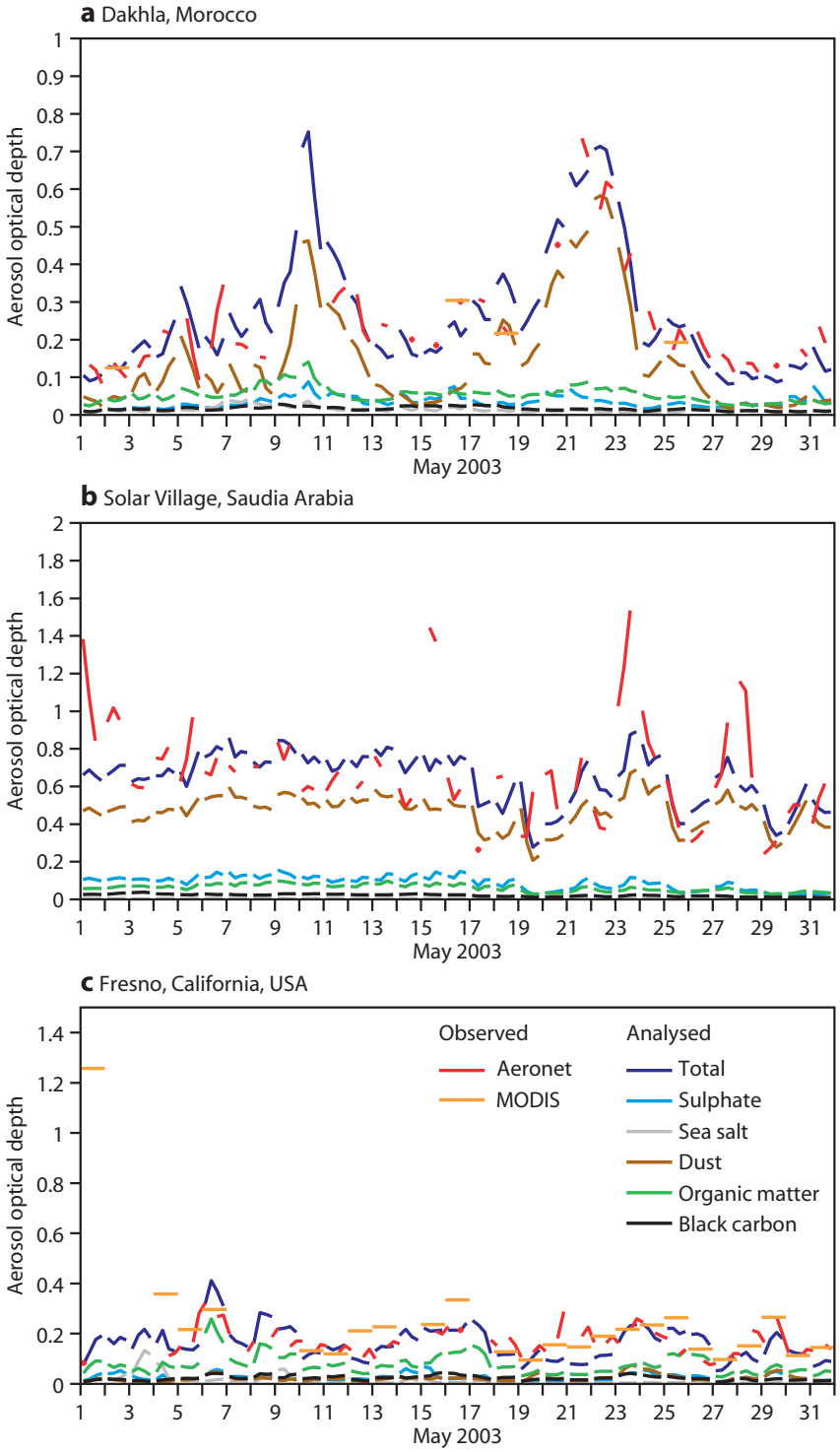

Figure 3 Comparisons of analysed aerosol optical depths at 550 nm with AERONET and MODIS observations for (a) Dakhla (Morocco), (b) Solar Village (Saudi Arabia) and (c) Fresno (California).

show that the analysis is closer to the AERONET observations, with the analysis displaying a lower bias and Root Mean Square (RMS) error than the free-running forecast.

As a further example, Figure 3 compares the analysed optical depth at 550 nm with the observed aerosol optical depth over the AERONET sites of Dakhla (Morocco), Solar Village (Saudi Arabia) and Fresno (California). Note that the analysis is able to reproduce the observed variability and intensity of the dust episodes at Dakhla and Solar Village, despite the lack of MODIS data (not available over bright surfaces).

The GEMS aerosol reanalysis for 2003–2004 will be completed in August 2008. An in-depth review of the results and comparisons with yet more independent datasets is needed for a final assessment of the quality of the analysis. This will involve several of the partners in the GEMS project. Preliminary results are, however, encouraging and show a good degree of skill in the analysis to provide initial conditions for improved forecasts of atmospheric aerosol fields.

FURTHER READING

Benedetti, **A.** & **M. Fisher**, 2007: Background error statistics for aerosols. *Q. J. R. Meteorol. Soc.*, **133**, 391–405.

Hollingsworth, **A.**, **R. J. Engelen**, **C. Textor**, **A. Benedetti**, **O. Boucher**, **F. Chevallier**, **A. Dethof**, **H. Elbern**, **H. Eskes**, **J. Flemming**, **C. Granier**, **J.W. Kaiser**, **J.-J. Morcrette**, **P. Rayner**, **V.-H. Peuch**, **L. Rouil**, **M. G. Schultz**, **A. J. Simmons** & **the GEMS Consortium**, 2008: The Global Earth-system Monitoring using Satellite and in-situ data (GEMS) Project: Towards a monitoring and forecasting system for atmospheric composition. To appear in the *Bull. Am. Meteorol. Soc.*

Morcrette, **J.-J.**, **L. Jones**, **J. W. Kaiser**, **A. Benedetti** & **O. Boucher**, 2007: Toward a forecast of aerosols with the ECMWF Integrated Forecast System. *ECMWF Newsletter No. 114*, 15–17.

Diagnosing forecast error using relaxation experiments

THOMAS JUNG, TIM PALMER,
MARK RODWELL, SOUMIA SERRAR

DESPITE substantial improvements in model formulation, data assimilation systems and observing systems, forecasts are still prone to failures. For example, extended-range forecasts (beyond 10 days) of the extratropical flow have moderate skill at the best of times. Apart from being of purely academic interest, understanding the origin of forecast error is the first step towards possible future improvements of the forecasting system. One important piece of information about forecast error is *where* it originates. If it turns out, for example, that extended-range predictability in the extratropics is primarily limited by model errors in the tropics then future model development should focus on exactly this region.

In this study we apply the so-called relaxation technique (also know as nudging technique), where prognostic fields are relaxed towards ERA-40 reanalyses produced at ECMWF (see Box A for details). The aim is to investigate how much of the extratropical forecast error in 30-day integrations originates in the tropics and how much in the stratosphere. These regions are two parts of the atmosphere with (theoretically) enhanced extended-range predictability. The relaxation technique is also applied in a case study to investigate the potential seasonal predictability of the cold European winter of 2005/06.

Origin of extratropical forecast error in 30-day integrations

To investigate the origin of extratropical forecast error during boreal winter a large set of 30-day control and relaxation experiments has been carried out using model cycle Cy32r1 at a resolution of T159 (about 125 km) and with 60 vertical levels (T159L60). For each of the experiments a total of 88 30-day forecasts were carried out. Forecasts were started on the 15th of the months: November, December, January and February, for each of the winters from 1980/81 to 2001/02. The initial conditions were taken from ERA-40 reanalysis data and in most experiments initial sea surface temperature (SST) and sea ice fields were persisted throughout the forecast. A control integration with observed SST and sea ice fields was also carried out in order to quantify the influence that knowledge of the lower boundary conditions has on atmospheric forecast skill.

The relaxation experiments can be divided into three groups depending on the region being relaxed: tropics, northern hemisphere troposphere and northern hemisphere stratosphere. Additional experiments were carried out to investigate the relative importance of different tropical regions and to study the sensitivity to the strength of the relaxation. A more detailed description of the relaxation formulation is given in Box A. Also the various 30-day experiments are summarized in Table 1.

Tropical skill scores

Figure 1 shows mean absolute forecast error of 5-day averaged tropical velocity potential (divergent flow) and stream function (rotational flow) fields at the 200 hPa level. The control integration (CNT/PER-SST) shows increasing forecast error throughout the 30-day forecast period. Prescribing SST fields (CNT/OBS-SST) reduces these errors slightly, particularly for the tropical rotational winds. "Moderately" relaxing ($\lambda = 0.1$) the tropics towards ERA-40 during the course of the integration

Box A

Relaxation Formulation

In the relaxation experiments the model is drawn towards the analysis during the course of the integration. In this way it is possible to reduce forecast error in specific regions, such as the tropics, in some controlled way. The relaxation experiments are carried out by adding an extra term of the following form to the ECMWF model:

$$-\lambda(\mathbf{x}-\mathbf{x}^{\mathrm{ref}})$$

The model state vector is represented by $\mathbf{x}$ and reference field towards which the model should be drawn (here analysis data) by $\mathbf{x}^{\mathrm{ref}}$. The strength of the relaxation is determined by λ, which generally can be a function of the variable, region (both the horizontal and vertical) and spatial scale (e.g., planetary scales only) considered. The units of λ are in $(\text{time step})^{-1}$. For a time step of one hour, for example, a value of $\lambda = 0.1$ indicates that at each time step the model is "corrected" using 10% of the departure of $\mathbf{x}$ from $\mathbf{x}^{\mathrm{ref}}$.

In this study the relaxation is carried out in grid point space in order to allow for localization. Parameters being relaxed include u, v, T and $\ln p_s$; the same λ is used for each of these parameters. The reference fields used in this study (i.e. ERA-40 reanalyses and operational analyses) are available at 6-hourly intervals only. Since a time step of 1 hour is used in the integrations linear interpolation is applied to the reference fields.

When applying masks to localize the relaxation, care has to be taken in order to reduce adverse effects close to the relaxation boundaries. Here the transition from relaxed to non-relaxed regions is smoothed using the hyperbolic tangent. The smoothing in the horizontal is carried out over 10° belts, both in longitude and latitude. Boundaries stated in the text refer to the centre of the respective 10° belt. The transition in the vertical is smoothed over about 8 model levels, which corresponds to a pressure interval of about 200 hPa close to the tropopause in the 60-level model used in this study.

Experiment	Comment	Relaxation region	Relaxation strength
CNT/PER-SST	Control run with persisted SSTs	–	–
CNT/OBS-SST	Control run with observed SSTs	–	–
TROP	Relaxation in the tropics	20°S–20°N, 180°W–180°E, all levels	$\lambda = 0.1$, $\lambda = 1.0$
NH	Relaxation of the troposphere (northern hemisphere)	20°–90°N, 180°W–180°E, p>300 hPa	$\lambda = 0.1$, $\lambda = 1.0$
STRAT	Relaxation of the stratosphere (northern hemisphere)	20°–90°N, 180°W–180°E, p<70 hPa	$\lambda = 0.1$, $\lambda = 1.0$
MCIN	Relaxation over the tropical Africa, Indian Ocean and Maritime Continent	20°S–20°N, 0°–140°E, all levels	$\lambda = 0.1$
TPAC	Relaxation over the tropical Pacific	20°S–20°N, 140°E–90°W, all levels	$\lambda = 0.1$
SAAT	Relaxation over tropical South America and the tropical Atlantic	20°S–20°N, 90°E–0°, all levels	$\lambda = 0.1$

Table 1 Summary of 30-day forecast experiments. All experiments are based on a resolution of T159 with 60 levels in the vertical using model cycle Cy32r1. Lower boundary conditions were persisted throughout the forecast for all relaxation experiments.

(TROP/0.1) is sufficient to reduce the forecast error of tropical velocity potential and stream function fields substantially throughout the forecast, thereby illustrating the effectiveness of the relaxation formulation.

Also shown in Figure 1 are mean absolute forecast error for an experiment in which the troposphere over the northern hemisphere has been relaxed towards ERA-40 (NH/0.1). Interestingly, "knowledge" of the extratropical circulation is particularly beneficial when it comes to predicting the rotational wind component in the tropics; the influence on the divergent component seems to be less pronounced. These results are in line with the notion that the extratropics affect the tropics on intra-seasonal time scales primarily through equatorward travelling extratropical Rossby wave trains.

Northern hemisphere Z500 skill scores

Figure 2 shows mean absolute forecast error of 5-day averaged northern hemisphere geopotential height fields at the 500 hPa level (Z500, hereafter) for various experiments. The control integrations with persisted and observed SST/sea ice fields (CNT/PER-SST and CNT/OBS-SST) show that it takes about 30 days for forecast error to saturate and that knowledge of the lower boundary conditions increases the skill in the extended-range slightly; knowledge of true rather than persisted lower boundary conditions in the short-range and medium-range, on the other hand, provides little, if any, benefit.

Relaxing either the tropics or the stratosphere (TROP and STRAT integrations), leads to a substantial reduction in Z500 forecast error. In relative terms the forecast error reduction is largest in the extended-range (beyond D+10), where it amounts to about 10–20% of the forecast error of the control integration for TROP/1.0 and STAT/1.0. The "delayed" positive impact of the relaxation in the tropics and stratosphere can be explained

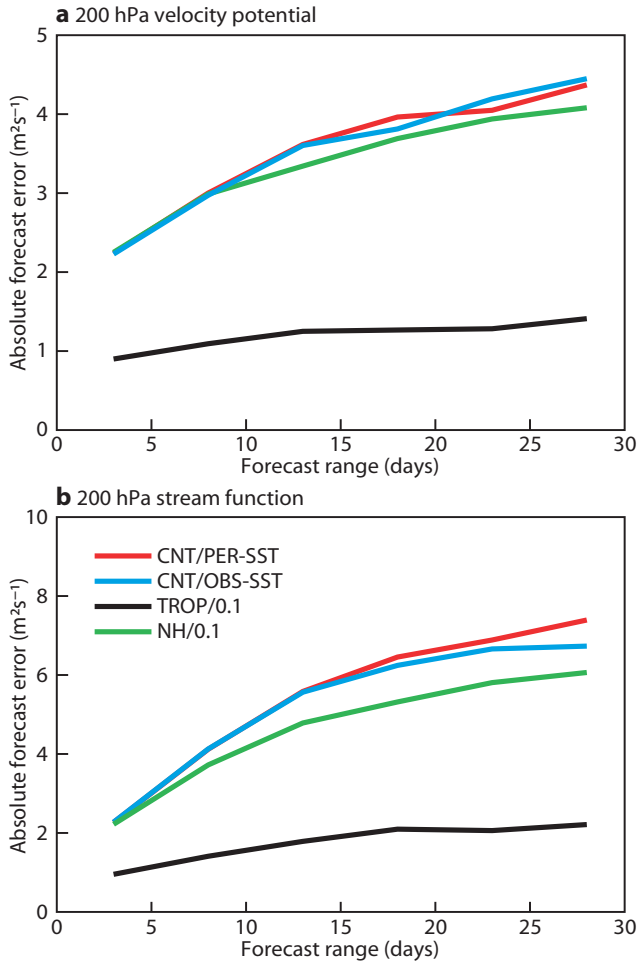

Figure 1 Mean absolute error of 5-day averaged forecasts of (a) velocity potential and (b) stream function at 200 hPa in the tropics (10°S–10°N) for control forecast with persisted (CNT/PER-SST) and observed (CNT/OBS-SST) SSTs as well as for experiments with the tropics (TROP/0.1, 20°S–20°N) and northern hemisphere extratropics (NH/0.1, 20°N–90°N) relaxed towards ERA-40 reanalysis data.

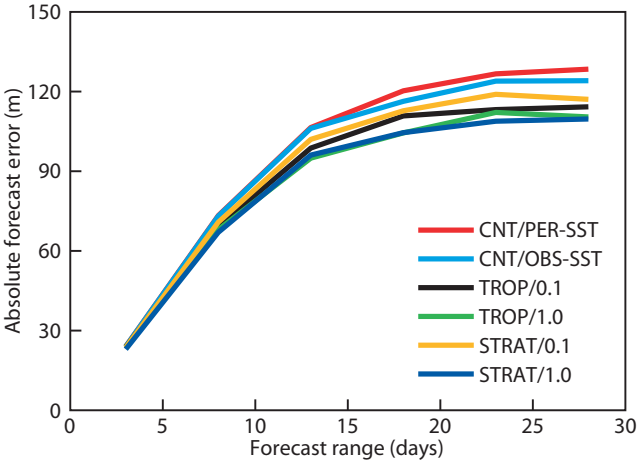

Figure 2 Mean absolute error of 5-day averaged forecasts of northern hemisphere (north of 40°N) 500 hPa geopotential height fields (in metres): control forecast with persisted (CNT/PER-SST) and observed (CNT/OBS-SST) SSTs as well as experiments with the tropics (TROP/0.1 and TROP/1.0) and extratropical stratosphere (STRAT/0.1 and STRAT/1.0) relaxed towards ERA-40 reanalysis data.

by the fact that forecasts are still quite successful in the short-range and medium-range (i.e., the relaxation has little work to do) and that it takes some time for the signal (reduced forecast error) to propagate from the tropics and stratosphere, respectively, into the northern hemisphere troposphere (e.g. *Jung & Barkmeijer*, 2006).

Figure 2 also reveals that the magnitude of Z500 forecast error reduction in the northern hemisphere troposphere depends somewhat on the strength of the relaxation coefficient λ. For a value of $\lambda = 1.0$ relaxing the tropics and northern hemisphere stratosphere leads to similar forecast error reductions throughout the 30-day forecast period. For a value of $\lambda = 0.1$ the tropics appear to be more efficient than the stratosphere in reducing Z500 forecast error.

Regional impacts of tropical and stratospheric relaxation

So far the focus has been on forecast error of the northern hemisphere as a whole. In order to identify possible regional differences in the relaxation experiments "difference maps" of mean absolute Z500 forecast error between the relaxation integrations for the tropics (TROP/1.0) and stratosphere (STRAT/1.0) and the control integration (CNT/PER-SST) have been produced (Figures 3(b) and 3(c)). For reference, mean absolute forecast errors for the control integration are also shown (Figure 3(a)).

Not too surprisingly, the tropical relaxation experiment (Figure 3(b)) leads to substantial forecast error reduction in the northern hemisphere subtropics, which is adjacent to the region where the model has been relaxed towards ERA-40. The fact that the forecast error reduction with tropical relaxation appears to be largely "confined" to the subtropics might also be explained by the presence of strong subtropical wave guides (e.g. *Branstator*, 2002). In the eastern North Pacific and the central North Atlantic, however, the "signal" appears to be spreading from the tropics into the northern hemisphere mid-latitudes. Western Europe appears to be benefiting in particular from an improved representation of the tropical circulation. This is true from the medium-range well into the extended-range. The Z500 forecast error reduction is largest just west of the British Isles in an area which is known for the frequent occurrence of persistent small-scale ridges ("blocking") and troughs which tend to produce high-impact weather over Western Europe (e.g. UK floods in autumn 2000). North America is the other area in the northern hemisphere mid-latitudes which benefits from improved forecasts in the tropics.

In the medium-range the stratospheric relaxation experiment leads to the largest forecast error reduction in high latitudes (Figure 3(c)). This is consistent with the initial tropospheric response found in the ECMWF model as a result of changes in the strength reduction of forecast error is found over large parts of the northern hemisphere mid and high latitudes. Interestingly, Europe is also one of the key-beneficiaries

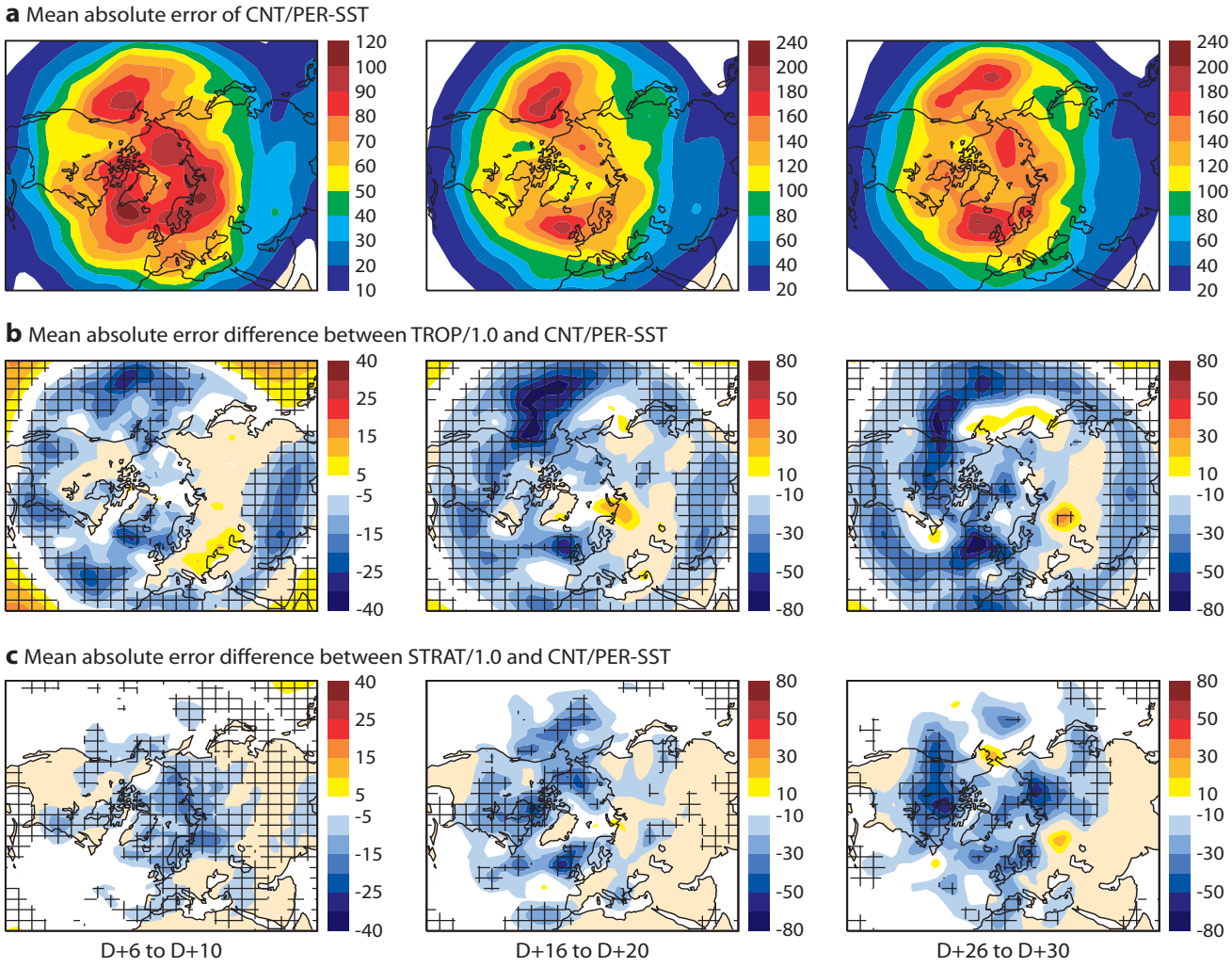

Figure 3 (a) Mean absolute forecast error of 500 hPa geopotential height field (in metres) for the control integration with persisted SSTs (CNT/PER-SST). (b) Mean absolute forecast error between the relaxation experiments TROP/1.0 and the control integration. (c) As (b) but for experiment STRAT/1.0. Results are shown for averaged data: D+6 to D+10 (left), D+16 to D+20 (middle) and D+26 to D+30 (right). Differences significant at the 95% confidence level (two-sided t-test) are hatched.

of a better representation of the stratospheric circulation, both in the medium-range and extended-range.

Further exploring the tropical influence

Having demonstrated the beneficial impact for Z500 forecasts over Western Europe and North America from improved forecasts of the tropical atmosphere, it is interesting to investigate from which part of the tropics the forecast improvement originates. To this end, three additional relaxation experiments were carried out (see also Table 1). The three tropical regions being relaxed are:

- 0°–140°E: Africa, Indian Ocean and Maritime Continent (MCIN).
- 140°E–90°W: Tropical Pacific (TPAC).
- 90°W–0°: South America and Atlantic (SAAT).

An investigation of the forecast error for these experiments in the tropics shows that the forecast "improvement" is largely confined to the relaxation regions (not shown). This shows that it is possible to trace extratropical forecast error reduction back to different tropical regions.

Figure 4 shows the impact of the various tropical relaxation experiments (with λ=0.1) on mean absolute Z500 forecast error over the northern hemisphere. Forecast improvement for MCIN is largely confined to the Asian subtropical Jet Stream and the North Pacific region throughout the 30-day forecast (Figure 4(b)). Although there appears to be some influence in the North Atlantic by D+26 to D+30, forecast error reduction is relatively small compared to the experiment in which the whole tropical belt has been relaxed (Figure 4(a), right panel). Relaxing the tropical Pacific, TPAC, leads to forecast improvements from the eastern North Pacific, over North America into the North Atlantic region. A similar forecast error reduction is found for SAAT. In both experiments, TPAC and SAAT, Z500 forecast in the North Atlantic region are already improved in the medium-range; the largest signal, however, is found in the extended-range (both, in absolute and relative terms).

A comparison of Figure 3(b) with Figure 4(a) gives a more detailed picture of the sensitivity of the reduction of Z500 forecast error to the exact choice of λ for

the tropical relaxation experiment. In general, increasing λ from 0.1 to 1.0 leads to a further reduction of forecast error; this further reduction, however, is small compared to the reduction achieved with λ=0.1, and the spatial structure of forecast error reduction is similar for either of the values.

The role of the Madden-Julian Oscillation

Previous studies have highlighted that the Madden-Julian Oscillation (MJO), the dominant atmospheric phenomenon in terms of intra-seasonal tropical variability (e.g. *Zhang*, 2005), gives rise to strong extratropical teleconnections, particularly in the North Pacific region. It seems likely, therefore, that improved prediction of the MJO would lead to improved medium-range and extended-range forecasts in the extratropics (see also *Jones et al.*, 2004), a notion that also features prominently in the THORPEX International Science Plan (*Shapiro & Thorpe*, 2004). Indeed, if extratropical forecast error in the control integration is considered

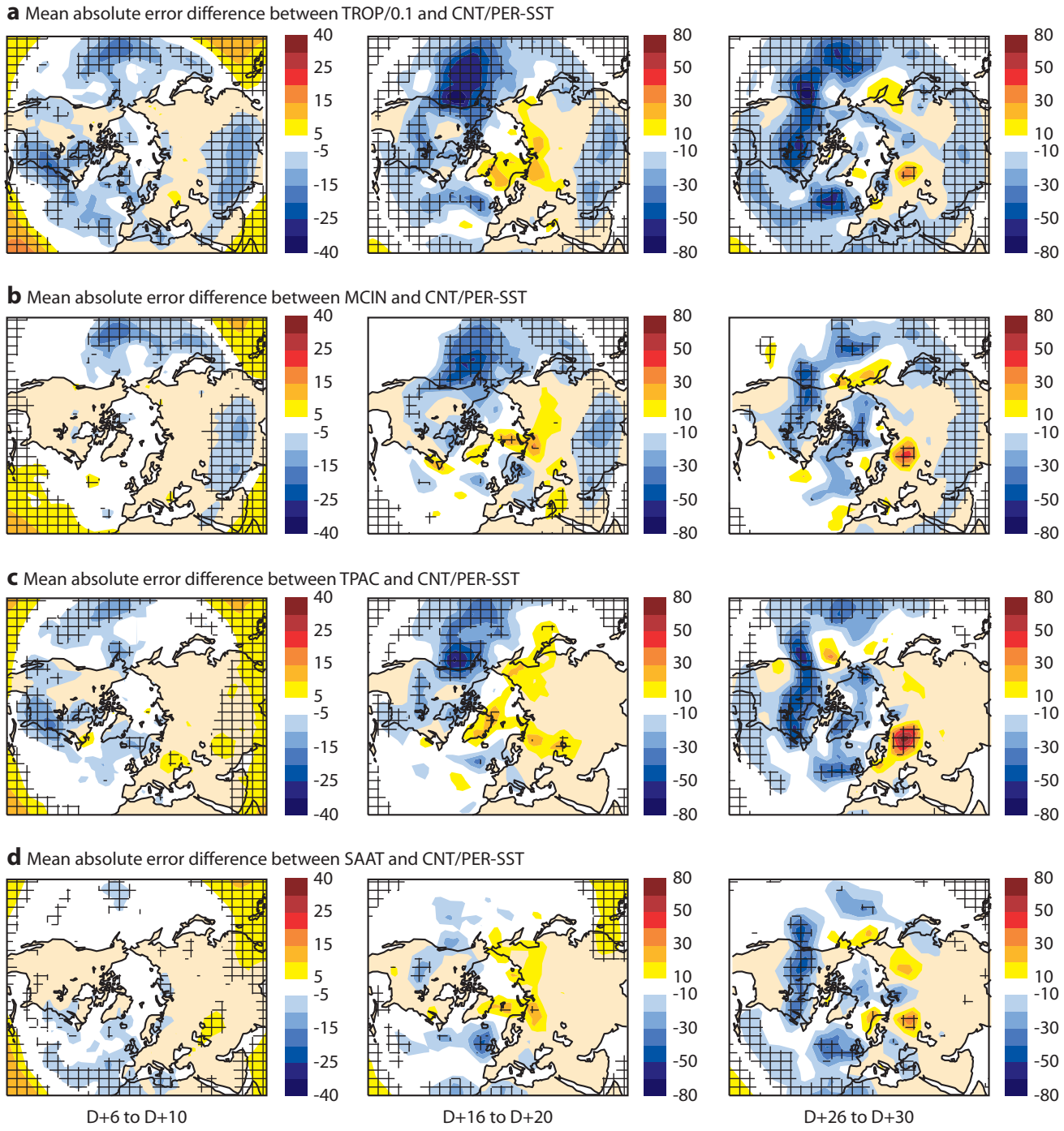

Figure 4 Mean absolute forecast error (in metres) between the relaxation experiments confined to (a) tropics (TROP), (b) Indian Ocean/Maritime Continent (MCIN), (c) central tropical Pacific (TPAC) and (d) tropical South America/tropical Atlantic (SAAT) and the control integration (CNT/PER-SST). All relaxation experiments are based on λ=0.1. Results are shown for averaged data: D+6 to D+10 (left), D+16 to D+20 (middle) and D+26 to D+30 (right). Differences significant at the 95% confidence level (two-sided t-test) are hatched.

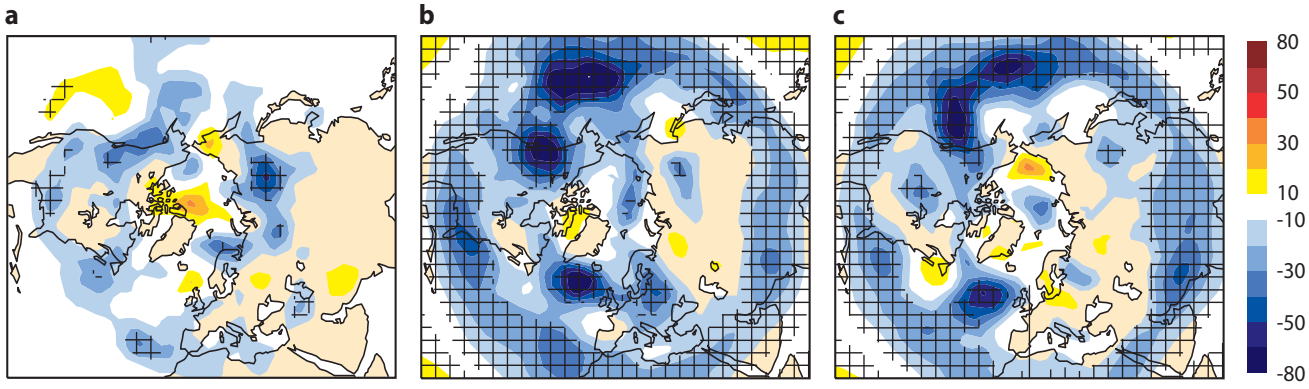

Figure 5 (a) Difference in mean absolute forecast error of 5-day averaged 500 hPa geopotential fields (in metres) between episodes with active and non-active MJO for the control experiment (CNT/PER-SST). Also shown are differences between tropical relaxation (TROP/1.0) and control experiments for (b) non-active and (c) active MJO episodes. The active (non-active) MJO sample comprises n=22 (n=27) 30-day forecasts for each of the experiments. To increase the sample size forecast errors were computed by aggregating all D+16 to D+20, D+21 to D+25 and D+26 to D+30 forecasts.

separately for periods with active and non-active MJO then it turns out that forecast error is smaller during active MJO spells (Figure 5(a)). It is tempting to assume that the beneficial impact that relaxing the tropics has on extratropical forecast skill (see previous discussion) is a result of "improved forecasts" of the MJO. This notion is supported by previous studies (e.g., *Ferranti et al.*, 1990; *Jones et al.*, 2004). Here, the classification into active and non-active MJO periods was done subjectively by inspecting individual Hovmöller diagrams of bandpass-filtered (30–60 days) tropical velocity potential anomalies at the 200 hPa level from ERA-40.

If improvements in the prediction of the MJO were the main contributor to the reduction of extratropical forecast errors when relaxing the tropics, then we would expect the relaxation to improve primarily during active MJO periods. Comparing the differences in mean absolute errors between the tropical relaxation (TROP/1.0) and control experiment for non-active MJO (Figure 5(b)) and active MJO (Figure 5(c)) shows that this is not the case. Forecast error reduction of Z500 in the northern hemisphere extratropics is comparable for active and non-active MJO periods. This shows that there are other aspects of the tropical atmosphere as well that, if simulated more realistically, would lead to more skilful extratropical forecasts. Examples for such tropical aspects include mean systematic error and a wide spectrum of tropical convectively coupled waves.

The fact that it is not just the MJO that leads to extratropical forecast error reduction in the relaxation experiments of this study may be interpreted as indirect evidence for the relatively high quality of the ERA-40 reanalysis in the tropics. Operational analysis fields in the 1980s (based on Optimal Interpolation), as used in the study of *Ferranti et al.* (1990), do capture main features associated with the MJO. There are large differences, however, between these old operational analyses and ERA-40 re-analyses on other spatial and temporal scales (not shown). So, the fact that Ferranti et al. found such an important role of the MJO might be explained by the relatively poor representation of the analysis of other aspects of the tropical circulation. Furthermore, improvements in MJO prediction in our control experiments relative to the comparable experiments of Ferranti et al., who used a much older model cycle, may explain the relatively less important role that the MJO plays in our experiments. Indeed, *Vitart et al.* (2007) show that there is useful skill in predicting the MJO up to D+15 to D+20 in a recent model version of the ECMWF model.

The cold European winter of 2005/06 – a case study

The winter of 2005/06 was marked by the frequent occurrence of Euro-Atlantic blocking episodes, which led to anomalously cold conditions over large parts of Europe. The observed seasonal mean Z500 anomaly, shown in Figure 6(a), clearly reflects the anomalous atmospheric condition during December to February 2005/06. Did the operational ECMWF seasonal forecasting system predict the observed anomalies? Figure 6(b), which shows the ensemble mean anomaly based on ECMWF seasonal forecasts started on 1 November 2005, gives some evidence for a reduction of the climatological westerly winds over Europe. The predicted ensemble mean anomaly, however, is rather small (about 6 times smaller than the observed anomaly) and it is not statistically significantly different from climatology (not shown).

To evaluate the forecast performance of the operational ECMWF seasonal forecasting system for the cold European winter of 2005/06 it is necessary to understand the "origin" of the observed anomaly. Was the observed anomaly a result of internal dynamics of the extratropical atmosphere (suggesting weak, if any, predictability on seasonal time scales), or was the anomaly "externally" forced?

Figure 7 shows observed SST anomalies for December to February 2005/06. SST Anomalies were present in all ocean basins, including a moderate La Niña event in the tropical Pacific. The winter of 2005/06 was also marked by the occurrence of a strong stratospheric

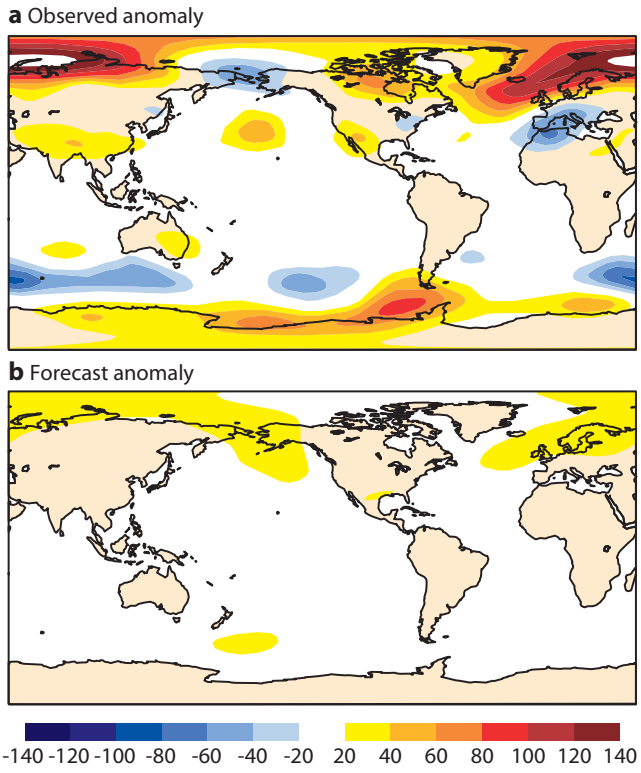

Figure 6 500 hPa geopotential height anomaly (in metres) for the winter December to February 2005/06: (a) observed and (b) ensemble mean from the operational ECMWF seasonal forecasting system (starting on 1 November 2005).

warming event at the end of January 2006 which lasted for more than four weeks, which might be seen as an alternative explanation for the increased frequency of occurrence of Euro-Atlantic blocking events.

In order to understand the origin of the anomalously cold winter 2005/06, a large number of seasonal forecast experiments with and without relaxation have been carried out using a T95L60 resolution and observed lower boundary conditions. A set of calibration runs covering winters of the period 1990/91 to 2005/06 was carried out in order to obtain the model's climatology. For the winter of 2005/06 a set of seasonal ensemble forecasts was then carried out. The ensembles were generated by starting forecasts in 6-hourly intervals from 12 UTC on 16 November to 12 UTC on 20 November 2005 giving a total of 17 ensemble members. In the relaxation experiments the model was relaxed towards interpolated (T95L60) operational analysis fields. A relaxation coefficient of λ=0.1 has been used in all relaxation experiments. A summary of all forecast experiments is given in Table 2.

Tropospheric response

Figure 8 shows observed Z500 anomalies for December to February 2005/06 along with those obtained from the various seasonal forecast experiments. Prescribing observed SST anomalies, Figure 8(b), produces rather weak Z500 anomalies. There is some evidence for weakening of the climatological westerly winds over Europe; the anomalies, however, are hardly statistically significant (at the 95% confidence level). Prescribing the tropics (Figure 8(c)), on the other hand, leads to very realistic circulation anomalies over Europe, both in terms of amplitude and spatial structure. Does this mean that the observed anomalies originated from the tropics? Figure 8(d) shows that by prescribing the northern hemisphere stratosphere, similar Z500 anomalies can be produced in the Euro-Atlantic region. This raises the question whether the anomalous cold European winter of 2005/06 originated in the tropics and/or the polar stratosphere.

Stratospheric response

Observed and simulated anomalies of the stratospheric polar vortex, expressed in terms of geopotential height fields at the 50 hPa level (Z50 hereafter), are shown in Figure 9. The control experiment (Figure 9(b)), with observed SSTs, clearly fails in simulating the anomalously weak stratospheric polar vortex. Interestingly, the weak

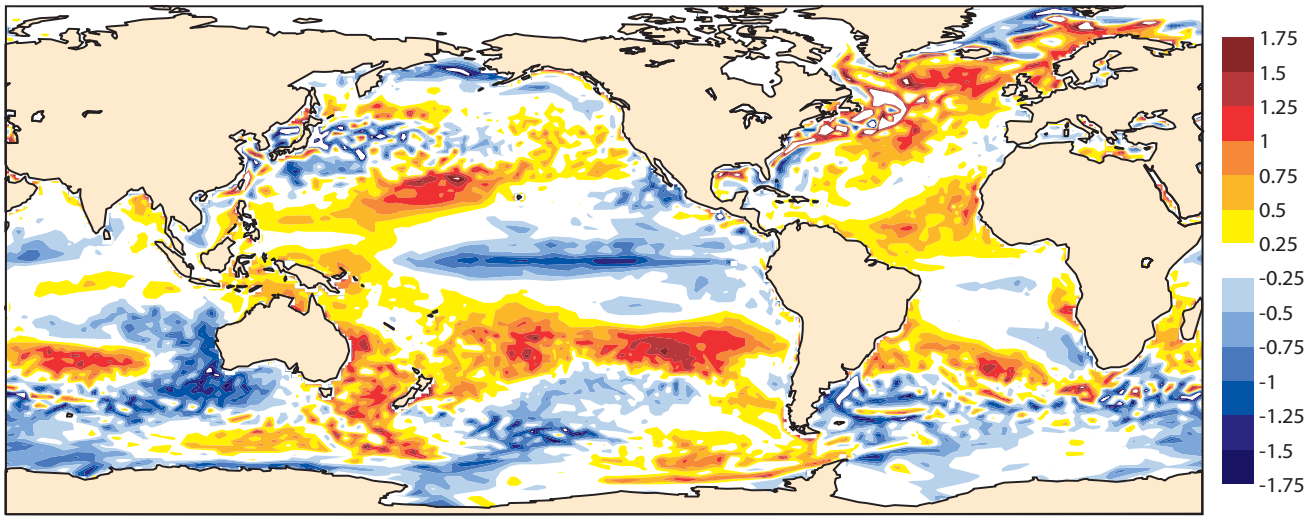

Figure 7 Observed SST anomalies (in K) for December to February 2005/06.

Experiment	Comment	Relaxation region(s)	Relaxation strength
CAL	Calibration run, observed SSTs, 1990/91 to 2005/06	–	–
CNT	Control ensemble without relaxation, observed SSTs, December to February 2005/6	–	–
TROP	Tropical relaxation ensemble, observed SSTs, December to February 2005/06	20°S–20°N, 180°W–180°E, 0°–140°E, 140°E–0°, whole atmosphere, troposphere only	$\lambda = 0.1$
STRAT	Stratospheric relaxation ensemble (NH), observed SSTs, December to February 2005/06	20°–90°N, 180°W–180°E, $p<70$ hPa	$\lambda = 0.1$

Table 2 Summary of seasonal forecast experiments for the winter 2005/06 case study. All experiments are based on a T95L60 resolution using model cycle Cy32r1. Notice that TROP comprises different tropical regions.

stratospheric polar vortex can be successfully simulated by relaxing the tropics (Figures 9(c) and 9(d)). This suggests that the origin of the observed atmospheric anomalies associated with the cold European winter of 2005/06 as well as the sudden stratospheric warming in January/February 2006 lies in the tropics. It is possible, however, that once established, the stratospheric warming contributed to the persistence of Euro-Atlantic blocking throughout the latter part of December to February 2005/06. Our results highlight the danger of interpreting stratospheric relaxation experiments in terms of "cause and effect". This is particularly true, given that "sudden stratospheric warmings" are believed to be driven by planetary waves of tropospheric origin, which propagate in the stratosphere, where they break and slow down the polar vortex.

The notion that the stratospheric warming originated from the tropics is further supported by the realistic timing of the "ensemble mean" warming in the tropical relaxation experiment (Figure 10). The observational data show that the warming occurred at the end of January 2006. The control integration with observed SSTs, on the other hand, shows a gradual intensification of the stratospheric polar vortex. This "intensification" can largely be understood as a gradual development of a systematic model error. In fact, it is well-known that model cycle Cy32r1, which has been used in this study, produces an erroneously strong stratospheric polar vortex (*Bechtold et al.*, 2008). If considered relative to the control integration (in order to remove the influence of this bias) then it turns out that the timing of the stratospheric warming event in the tropical relaxation experiment is simulated quite realistically (Figure 10(d)). The relatively smooth warming (in contrast to the observed sudden warming) in the relaxation experiment may be explained by the fact that ensemble mean Z50 fields were used in Figures 10(b) to 10(d) which, by nature, are smoother than individual ensemble members (and the observational record).

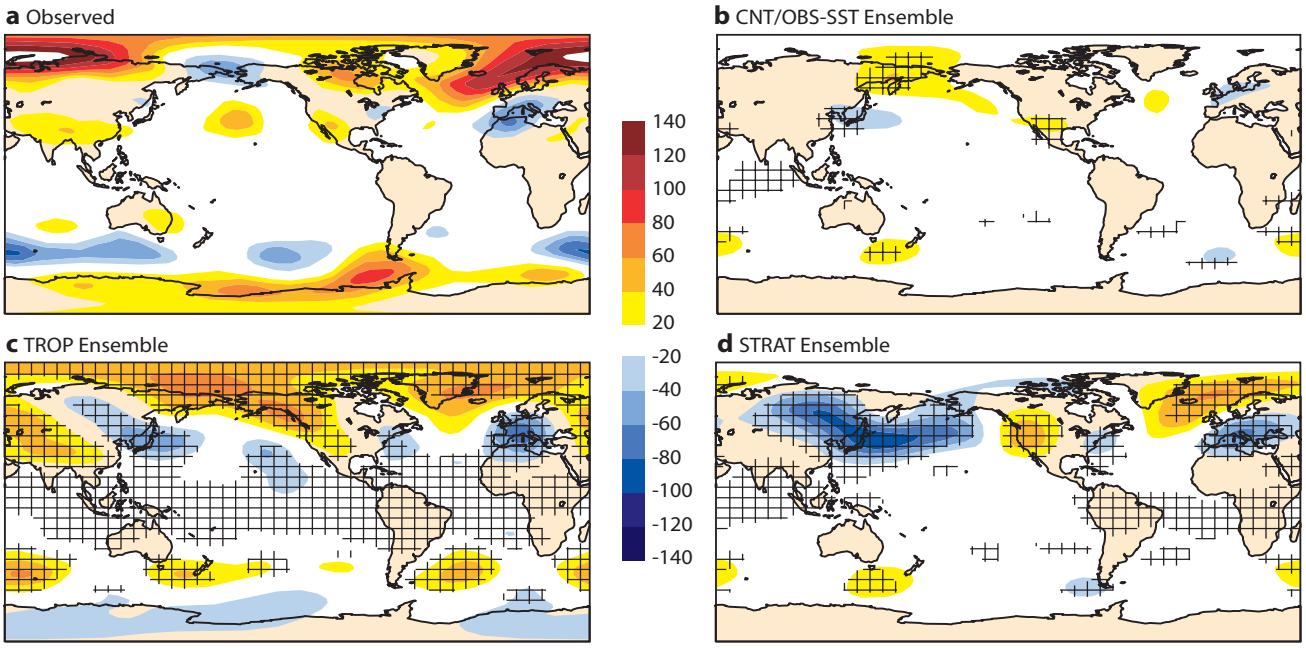

Figure 8 Mean 500 hPa geopotential height anomaly (in metres) for the winter December to February 2005/06: (a) observed, (b) control ensemble (CNT/OBS-SST), (c) tropical relaxation ensemble (TROP) and (d) ensemble with stratospheric relaxation over the northern hemisphere (STRAT). All integrations were carried out using observed SSTs as lower boundary. The anomalies in (b) to (d) are relative to a "calibration" run with observed SST covering winters of the period 1990/91 to 2005/06 and are based on ensemble mean fields (17 members). Statistically significant differences at the 95% confidence level are hatched.

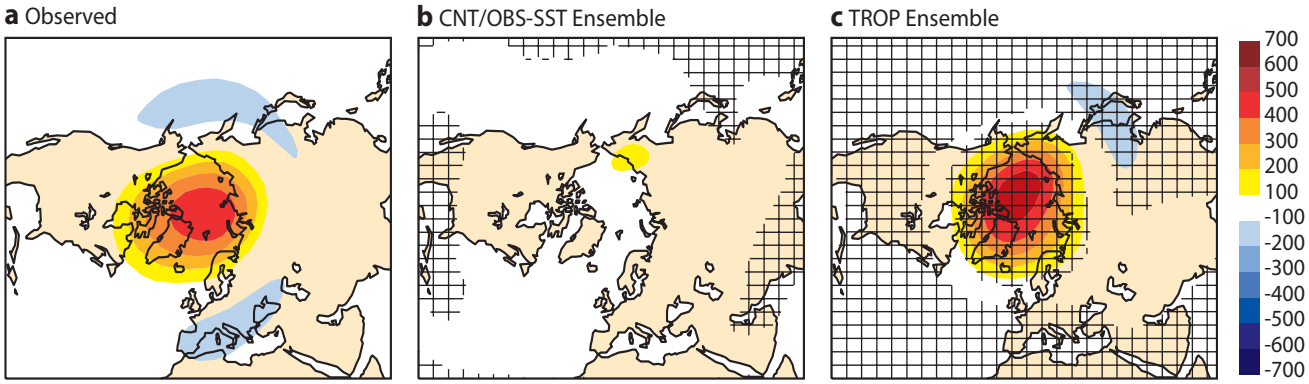

Figure 9 As in Figure 8, but for 50 hPa geopotential height fields: (a) observed, (b) control ensemble (CNT/OBS-SST) and (c) tropical relaxation ensemble (TROP).

Tropical-extratropical teleconnections

After having found evidence for the crucial role of the tropics in setting up the atmospheric circulation anomalies leading to the anomalously cold European winter 2005/06, it is worth briefly discussing the underlying teleconnections. Observed and simulated mean meridional components of the rotational wind (Vrot) in the upper troposphere for December to February 2005/06 are shown in Figure 11. Vrot is chosen here since it is a good parameter to characterise stationary Rossby waves.

Over the northern hemisphere the observations show the presence of a Rossby wave on the Asian Jet Stream, which appears to extend all the way across the North Pacific into the North Atlantic and Europe. The corresponding anomalies for the control ensemble with observed SSTs (Figure 11(b)) do not show the existence of the anomalous Rossby wave on the Asian wave guide. There is evidence, however, for a Rossby wave train propagating from the eastern tropical Pacific, through the Caribbean towards Europe. Although the

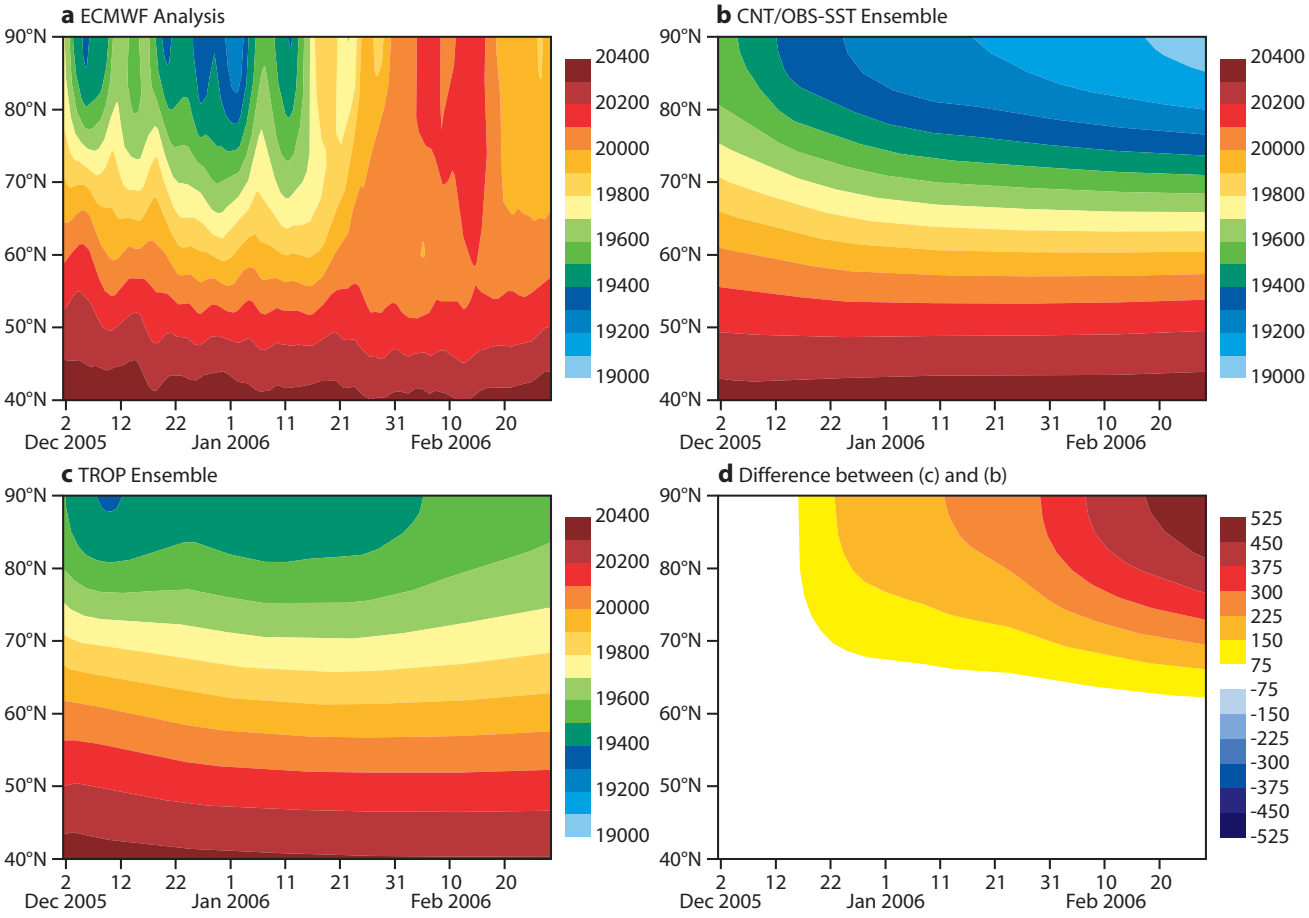

Figure 10 Time-latitude diagrams of zonally averaged daily 50 hPa geopotential height fields (in m) for (a) operational analysis data, (b) the control ensemble (CNT/OBS-SST) and (c) the tropical relaxation ensemble (TROP). (d) Difference between the tropical relaxation and control ensemble. Results in (b) to (d) are based on ensemble mean data (17 members).

spatial pattern of this wave appears to agree quite well with the observed anomalies in this region, the magnitude of this wave train, particularly over Europe, is much smaller than observed.

In the following, the relaxation experiments are discussed in terms of their departure from the control ensemble for the winter 2005/06. In this way it is possible to focus on the response which is not captured by prescribing observed SSTs. The first thing to notice is that the effect of relaxing the atmosphere is generally larger than that arising from specifying observed lower boundary conditions (Figure 11). Furthermore, Figure 11(c) shows that the tropical relaxation experiment is capable of reproducing most of the observed anomalous Rossby wave structure in the northern hemisphere extratropics; differences occur primarily in high latitudes. By confining the tropical relaxation to the area 0°–140°E (Africa, Indian Ocean and Maritime Continent) the Rossby wave on the Asian Jet Stream and its extension towards North America can be well simulated (Figure 11(d)).

The response over the North Atlantic and Europe, however, is much weaker than for the case in which the whole tropics are being relaxed. In fact, it turns out that in order to get the observed anomalous circulation over Europe correctly, it is necessary to relax the tropics from 140°E–0° (Pacific, South America and Atlantic, Figure 11(e)). One plausible explanation is that the correct atmospheric response to the La Niña conditions in the tropical Pacific (see Figure 7) was crucial for establishing the Rossby wave response capable of reaching Europe. In fact, this notion is consistent with results from a previous study in which it was shown that the response of the ECMWF model to a La Niña-type diabatic forcing tends to favour the negative phase of the North Atlantic Oscillation (*Greatbatch & Jung*, 2006), that is, anomalously cold European winters. Finally, Figure 11(f) confirms that the origin of the extratropical signal is primarily located in the tropical troposphere.

Using the relaxation technique

First results from using the relaxation technique to understand the origin of extratropical forecast error

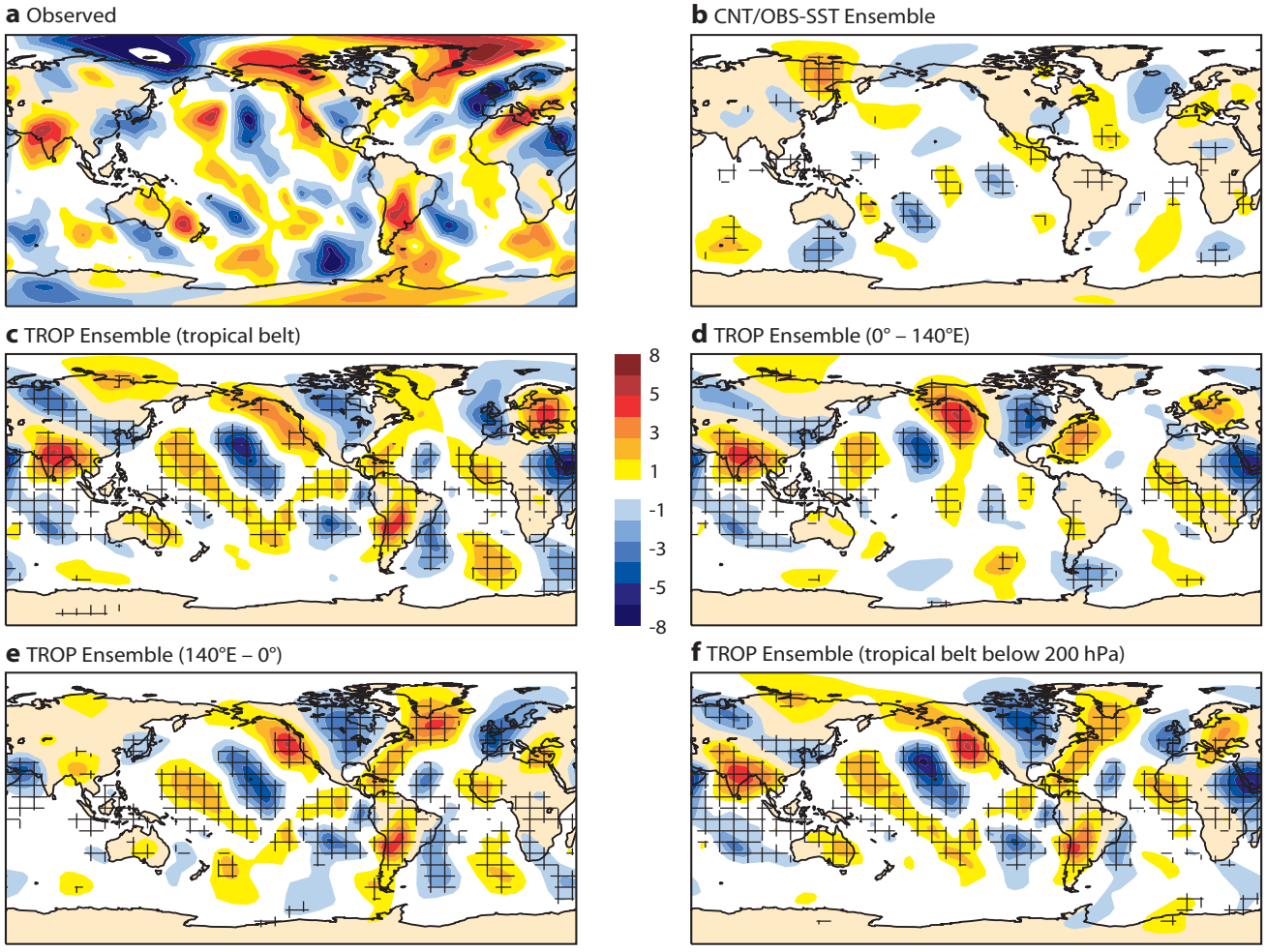

Figure 11 Mean meridional component of the rotational wind anomaly in the upper troposphere (in ms^{-1}) for the winter December to February 2005/06: (a) observed and (b) control ensemble. Also shown is the velocity potential response, which is defined as departure from the control ensemble for the winter of 2005/06, for relaxation (c) in the whole tropical belt, (d) in the tropics from 0°–140°E, (e) in the tropics from 140°E–0° and (f) in the whole tropical troposphere ($p > 200$ hPa). Results in (b) to (f) are based on ensemble mean fields (17 members). Statistically significant differences at the 95% confidence level are hatched. The data have been averaged in the vertical over three pressure levels (300, 250 and 200 hPa).

have been presented. The focus has been on "remote" influences from the tropics and the extratropical stratosphere. Most importantly, our results demonstrate the potential of the relaxation technique for understanding how forecast improvements in certain regions can lead to forecast error reductions in other regions. One question, that the relaxation technique leaves unanswered, however, is what level of predictability in the relaxation areas will actually be achievable by improving the forecasting system.

We feel that there is considerable scope for future forecast improvements in both, the tropics and the stratosphere. In both regions substantial systematic model errors are still present which are likely to hamper successful medium-range and extended-range forecasts. Results from the relaxation technique suggest that certain regions will benefit more from such improvements than others; and it seems that the Euro-Atlantic region will be at the "receiving end". Having said this, it should be kept in mind that possible model improvements will lead to modest improvements in the extended-range. Our results suggest, for example, that it is unlikely that in the future we will obtain the same level of forecast skill beyond D+20 in the Euro-Atlantic region that we presently obtain in the far medium-range (D+5 to D+10, Figure 3).

Furthermore, the relaxation technique is useful for understanding the "origin" of seasonal mean anomalies. Understanding the origin of such anomalies is important when evaluating the performance of ECMWF seasonal forecasts in predicting high impact events. The fact that the cold European winter 2005/06 most likely had its origin in the tropics suggests, for example, that there was some degree of predictability and that improvements of the ECMWF forecasting system would be beneficial when it comes to forecasting such events. By how much seasonal forecasts of the tropical atmosphere could be improved, however, remains unknown at the moment.

Finally, it is perhaps interesting to note that the relaxation technique is not a new diagnostic method. It has already been widely used at ECMWF in the 1980s (*Haseler*, 1982; *Klinker*, 1990; *Ferranti et al.*, 1990) to understand medium-range forecast error in the extratropics. Recently, it has been decided to (re-)implement the relaxation technique in recent model cycles (Cy32r1 and higher). This decision was motivated by different factors.

- It was felt that the relaxation technique could also be useful to understand forecast error in the extended-range, addressing the monthly and seasonal forecasting problem.
- The availability of larger computer resources allows the production of more forecasts, thereby increasing the robustness of the results.
- The availability of more realistic (re-)analyses (towards which to model is relaxed), particularly in the tropics, makes the relaxation technique much more powerful. This will be especially true with availability of the full ERA-Interim reanalysis in autumn 2008.

For the immediate future it is planned to carry out more case studies. This includes, for example, an investigation of the mechanisms giving rise to anomalously wet Western European summer of 2007. It is also planned to further refine the relaxation code. It would be helpful, for example, to be able to relax the model towards the analysis for specific spatial scales only (scale-dependent relaxation). In this way it would be possible, for example, to prescribe the MJO more directly during the course of the integration. Finally, it is planned to carry out a detailed investigation of the origin of the systematic model error, in particular the systematic underestimation of the frequency of occurrence of Euro-Atlantic blocking events in the extended-range.

FURTHER READING

Bechtold, **P.**, **M. Köhler**, **T. Jung**, **F. Doblas-Reyes**, **M. Leutbecher**, **M.J. Rodwell**, **F. Vitart** & **G. Balsamo**, 2008: Advances in simulating atmospheric variability with the ECMWF model: From synoptic to decadal time scales. *ECMWF Tech. Memo. No. 556.*

Branstator, **G.**, 2002: Circumglobal teleconnections, the Jet Stream waveguide, and the North Atlantic Oscillation. *J. Climate*, **15**, 1893–1910.

Ferranti, **L.**, **T.N. Palmer**, **F. Molteni** & **E. Klinker**, 1990: Tropical-extratropical interaction associated with the 30–60 day oscillation and its impact on medium and extended range prediction. *J. Atmos. Sci.*,, **47**, 2177–2199.

Greatbatch, **R.J.** & **T. Jung**, 2006: Local versus tropical diabatic heating and the winter North Atlantic Oscillation. *J. Climate*, **20**, 2058–2075.

Haseler, **J.**, 1982: An investigation of the impact at middle and high latitudes of tropical forecast errors. *ECMWF Tech. Report No. 31.*

Jones, **C.**, **D.E. Waliser**, **K.M. Lau** & **W. Stern**, 2004: The Madden-Julian Oscillation and its impact on Northern Hemisphere weather predictability. *Mon. Wea. Rev.*, **132**, 1462–1471.

Jung, **T.** & **J. Barkmeijer**, 2006: Sensitivity of the tropospheric circulation to changes in the strength of the stratospheric polar vortex. *Mon. Wea. Rev.*, **134**, 2191–2207.

Klinker, **E.**, 1990: Investigation of systematic errors by relaxation experiments. *Q. J. Roy. Meteorol. Soc.*, **116**, 573–594.

Shapiro, **M.** & **A. Thorpe**, 2004: THORPEX International Science Plan. *WMO/TD-No. 1246, WWRP/THORPEX No. 2.* (http://www.wmo.int/pages/prog/arep/thorpex/)

Vitart, **F.**, **S. Woolnough**, **M.A. Balmaseda** & **A.M. Tompkins**, 2007: Monthly forecast of the Madden-Julian Oscillation using a coupled GCM. *Mon. Wea. Rev.*, **135**, 2700–2715.

Zhang, **C.**, 2005: Madden-Julian Oscillation. *Rev. Geophys.*, **43**, RG2003, doi:10.1029/2004RG000158.

Progress in ozone monitoring and assimilation

ROSSANA DRAGANI, DICK DEE

SINCE the launch of the Environmental Satellite (Envisat) in March 2002, the number of remote sensors with the capability of performing measurements of atmospheric gas composition (in particular ozone) has progressively increased. These new instruments, on one hand, provide the much-wanted constraint to the corresponding model fields, whilst on the other hand they represent a real challenge. Apart from the technical issues such as data handling, complex observing systems require continuous monitoring of the ozone information derived from each of its components, as well as an assessment of their potential benefits to the operational ozone analyses.

This article describes the ozone observing system currently used in the ECMWF operational suite. It briefly discusses the quality of the ECMWF ozone analyses, and shows the potential benefits of using ozone products as well as ozone-sensitive radiances from these new instruments. Results from a number of Observing System Experiments (OSEs) are presented.

A full list of the instruments referred to in this article and their acronyms is given in Table 1.

The ozone observing system used at ECMWF

Table 2 presents the ozone observing system currently used at ECMWF. It includes a variety of instruments from both lower orbiting polar (LEO) and geostationary (GEO) satellites. These instruments provide information about total column ozone (TCO), ozone partial columns and ozone profiles.

The operational ozone assimilation at ECMWF includes the following.

- **SBUV/2**. Near-real-time ozone retrievals from the Solar Backscatter Ultra Violet (SBUV/2) instrument flying on board the NOAA-16 satellite have been assimilated since April 2002. Starting from 6 November 2007, the ECMWF ozone analyses also benefited from the active assimilation of ozone partial columns from the SBUV/2 instruments on board NOAA-17 and NOAA-18.
- **SCIAMACHY**. TCO produced in near-real-time by KNMI from the Scanning Imaging Absorption Spectrometer for Atmospheric Chartography (SCIAMACHY) nadir measurements has been assimilated since 28 September 2004. The SCIAMACHY retrievals, which are distributed via the ESA funded PROMOTE-2 consortium, are pre-thinned to a horizontal resolution of 1°×1° before the assimilation. This approach is taken to limit the contribution of the horizontal error correlations, as no account is taken of these.

Instrument		Satellite
AIRS	Advanced Infrared Sounder	AQUA
GOME-2	Global Ozone Monitoring Experiment-2	MetOp-A
GOME-1	Global Ozone Monitoring Experiment-1	ERS-2
GOMOS	Global Ozone Monitoring by Occultation of Stars	Envisat
HIRDLS	High Resolution Dynamic Limb Sounder	EOS-AURA
MIPAS	Michelson Interferometer of the Passive Atmospheric Sounding	Envisat
MLS	Microwave Limb Sounder	EOS-AURA
OMI	Ozone Monitoring Instrument	EOS-AURA
SBUV/2	Solar Backscatter Ultra Violet/2	NOAA-16, NOAA-17 and NOAA-18
SCIAMACHY	Scanning Imaging Absorption Spectrometer for Atmospheric Chartography	Envisat
SEVIRI	Spinning Enhanced Visible and Infra-Red Imager	Meteosat 9
TOMS	Total Ozone Mapping Spectrometer	ADEOS and Earth Probe

Table 1 Instruments on board satellites referred to in this article.

In addition to the actively assimilated ozone products, ECMWF also monitors ozone data from a number of different remote sensors on an operational basis. Currently (as in cycle Cy32r3 of ECMWF's Integrated Forecast System), the set of passively monitored ozone data includes:

- **GOMOS**. Ozone profiles from GOMOS (Global Ozone Monitoring by Occultation of Stars) on board Envisat.

Sensor	Satellite	Satellite type	Data provider	Product type
SCIAMACHY	Envisat	LEO	KNMI	TCO
SBUV/2	NOAA-16, -17,-18	LEO	NOAA	O_3 partial columns
SEVIRI	Meteosat-9	GEO	EUMETSAT	TCO
OMI	AURA	LEO	NASA	TCO
GOMOS	Envisat	LEO	ESA	O_3 Profile

Table 2 The ozone observing system currently used at ECMWF. The satellite types are lower orbiting polar (LEO) and geostationary (GEO).

- **SEVIRI**. TCO retrieved from the SEVIRI (Spinning Enhanced Visible and Infra-Red Imager) 9.7 μm channel on board Meteosat 9.
- **OMI**. TCO from OMI (Ozone Monitoring Instrument) on board AURA.

Monitoring statistics plots are available on-line for all the ozone products at

www.ecmwf.int/products/forecasts/d/charts/monitoring/satellite/o3/.

The quality of the operational ozone analyses

At the time this article was written, the ECMWF operational ozone analyses were only constrained by the SCIAMACHY TCO and the three SBUV/2 partial column ozone products. The bottom layer of the assimilated SBUV/2 data spans the atmosphere from surface up to about 16 hPa so that it can be almost regarded as a total column. The combination of these data generally provides a good constraint to the TCO analyses. Figure 1 shows the comparison between the time series of the zonal mean TCO analyses produced operationally at ECMWF and the retrieved TCO from OMI for January 2007 to February 2008. The level of agreement between the operational TCO analyses and OMI is generally good in terms of distribution, seasonal variability, and total ozone amount.

Although important, the ozone products that are currently assimilated are often not able to provide the information required to constrain the ozone vertical distribution. This is worse in regions where nadir ultraviolet instruments – largely used for ozone retrieval - cannot make measurements, such as the polar winter hemisphere.

Figure 2 shows the monthly mean comparisons between ozone sondes launched from the McMurdo station during the 2007 Match campaign in Antarctica (*Mercer et al.*, 2007), and their model equivalent derived from the operational ozone analyses during August. During the polar winter, the maximum of the ozone analyses is generally placed at a higher vertical level than that measured by the ozone sondes. In addition, the ozone analyses show deeper depletion in the mid-stratosphere just below the ozone

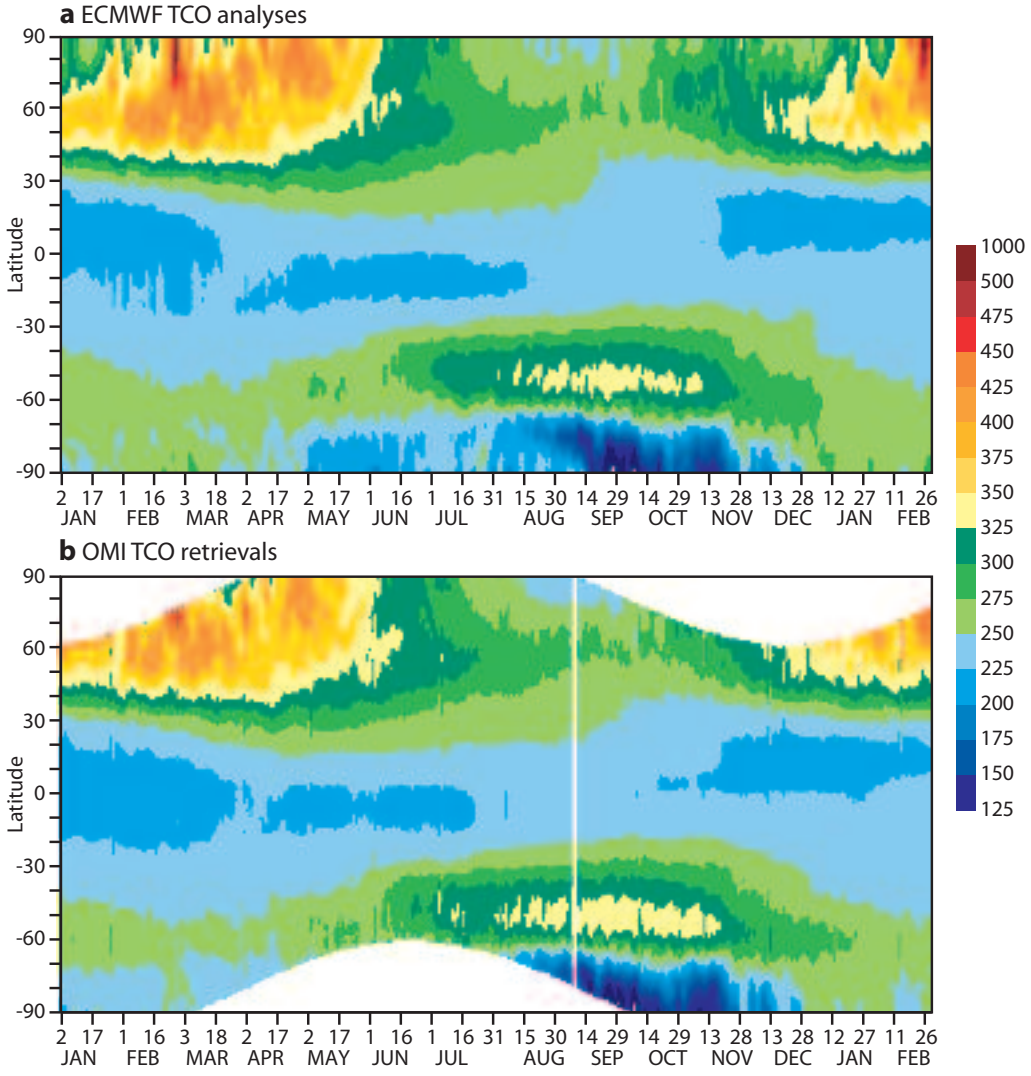

Figure 1 Comparison between the time series of the zonal mean of (a) ECMWF TCO analyses and (b) OMI TCO retrievals for 1 January 2007 to 29 February 2008.

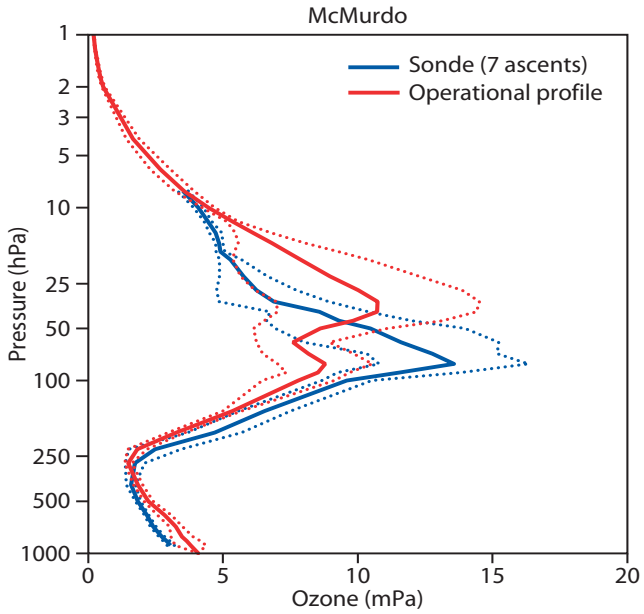

Figure 2 Comparison between the monthly mean operational ozone profiles (red) and co-located ozone sondes (black) launched from the McMurdo station (77.8°S, 166.7°E) in August 2007 as part of the 2007 Match campaign. Dotted lines limit the one standard deviation range about the mean. The Norwegian Institute for Air Research (NILU) provided the Match ozone sonde data.

maximum. This shortcoming is known and can be addressed by improving the quality of the ozone first guess as well as by assimilating ozone data retrieved from remote sensors employing different geometries and sounding different ozone-sensitive spectral regions.

The ozone first guess used at ECMWF is derived from an updated version of the *Cariolle & Deque* (1986) scheme. In this scheme the ozone continuity equation is expressed as a linear relaxation towards a photochemical equilibrium for the local value of the ozone mixing ratio, the temperature, and the overhead ozone column. An ozone destruction term is used to parametrize the heterogeneous chemistry as a function of the equivalent chlorine content for the actual year. Although this parametrization has undergone significant upgrades in recent years thanks to collaboration with Daniel Cariolle (Météo-France), undoubtedly the ozone analyses would benefit from any further increase in their accuracy (e.g. by using improved coefficients in the linear expansion of the ozone continuity equation).

As far as the assimilation of ozone observations is concerned, ozone profiles retrieved from a limb sounder could improve, for example, the vertical distribution of the ozone analyses. Infrared and microwave sounders can provide the required constraint where the ultraviolet sensors are practically blind. *Dethof* (2003) showed that the assimilation of ozone profiles from the Michelson Interferometer of the Passive Atmospheric Sounding (MIPAS) into the ECMWF system can substantially improve the quality of the ozone analyses. This is particularly apparent in the tropical lower stratosphere, where the ozone peak value is usually underestimated, as well as inside the winter vortex, where the stratospheric ozone transport and depletion are, in general, difficult to model accurately. Furthermore, microwave sounders offer the added advantage of providing measurements that are not affected by cloud contamination. The Microwave Limb Sounder (MLS), launched on the NASA's EOS-AURA satellite on July 2004, is a potential candidate to provide this kind of information. In addition to the standard level 2 ozone products, an investigation into the assimilation of the ozone-band in the infrared spectral range (about the 9.7 μm channel) has also started.

Observing System Experiments (OSEs)

The potential benefits of assimilating four ozone products will now be discussed.

- We first present some results from the assimilation of TCO from the ultraviolet nadir sounder OMI on board EOS-AURA.
- There follows a discussion of the monitoring and assimilation of TCO from the ultraviolet nadir sounder GOME-2 on board MetOp-A.
- Then, we will show some preliminary results from the assimilation of ozone profiles retrieved from MLS on board EOS-AURA.
- Finally, we will present some results from the assimilation of radiances in the infrared O_3-channels as measured by the Advanced Infrared Sounder, AIRS, on board AQUA.

Each OSE includes two experiments: a control experiment (always referred to as CTRL) used as reference, and a perturbation experiment which has the same configuration as CTRL except for the element under study. All the OSEs were performed using the 12-hour 4D-Var data assimilation scheme. Unless otherwise stated, the experiments were run at resolution T159 L91 using the current operational cycle (Cy32r3). In the following discussion an indication is given of when a different set up was used.

Assimilation of the OMI TCO

TCO retrieved from OMI has been passively monitored in the operational suite since 6 November 2007 (Cy32r3). The monitoring statistics shows that the agreement between these observations and the ECMWF analyses of TCO is generally within 3 DU.

The first assimilation trial of OMI TCO was performed using the current operational system at a resolution of T255L60 (from surface up to 0.1 hPa) for 1 July to 31 August 2006. With the exception of only the ozone data, both the control (CTRL) and the perturbation experiment (Exp/OMI) used the same observations as were assimilated operationally. As far as the ozone assimilation is concerned, SCIAMACHY TCO was used to constrain the CTRL ozone analyses. OMI TCO was added to that reference in Exp/OMI. The active assimilation of the SBUV/2 partial columns was, instead, turned off in both CTRL and Exp/OMI. Owing to data redundancy of a complex GOS, such as that used at

ECMWF, performing impact studies using the full operational dataset can only show very limited impact and does not necessarily highlight the intrinsic benefit of the element under study. Furthermore, having switched off their active assimilation, the three SBUV/2 instruments can be used for the ozone analysis validation.

It is found that there are small but statistically significant differences between the CTRL and Exp/OMI ozone analyses in the region of the atmosphere between 10 and 80 hPa. Comparisons with independent, unassimilated observations show improved levels of agreement of the Exp/OMI analyses. Figure 3 presents the global mean relative differences between MLS ozone profiles and the ozone analyses from CTRL and Exp/OMI averaged over the two month period July-August 2006. Overall, the assimilation of OMI TCO leads to a better level of agreement of the ozone analyses with MLS data in the region between 20 and 150 hPa.

Comparisons of the ozone analyses with ozone profiles from HIRDLS (HIgh Resolution Dynamic Limb Sounder on AURA) and the SBUV/2 data from NOAA-16, NOAA-17 and NOAA-18 (not shown here) also confirm these results by showing a better fit to the independent observations when OMI TCO is actively assimilated. Finally, comparisons with ozone sondes show a neutral or positive impact of the OMI data. The active assimilation of OMI TCO will start with the next operational cycle (Cy33r1).

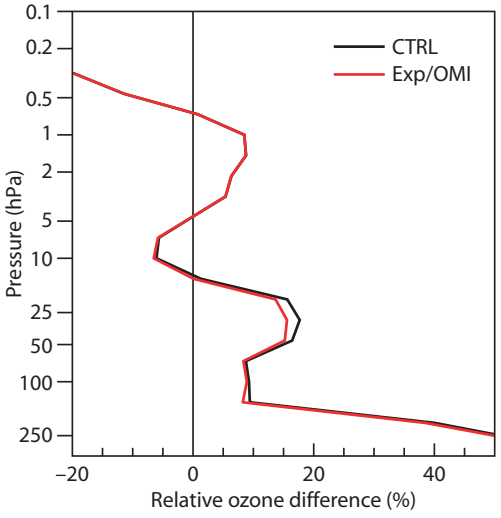

Figure 3 Relative ozone difference between MLS ozone profiles and their model equivalent obtained from CTRL and Exp/OMI. The plotted profiles were computed as 100×(MLS-A)/MLS, where A is the ozone analysis. The profiles were obtained as global mean over the period 1 July to 31 August 2006.

Monitoring and assimilation of GOME-2 TCO

On October 2006, the first of three satellites of the EUMETSAT Polar System (EPS), MetOp-A, was launched. On board this satellite was an ozone monitoring sounder, the second Global Ozone Monitoring Experiment, GOME-2. This instrument benefits from the inheritance of GOME-1, launched on board of ERS-2 in 1995, as well as from more recently launched sensors, such as SCIAMACHY and OMI. The passive monitoring of GOME-2 TCO is currently in a pre-operational status, and will start operationally with the next ECMWF cycle (Cy33r1). Preliminary comparisons between GOME-2 TCO and their model equivalent show a high level of agreement. As an example, Figure 4 shows the distribution of the first-guess departures (namely observations minus first-guess) for one-day's worth of GOME-2 data.

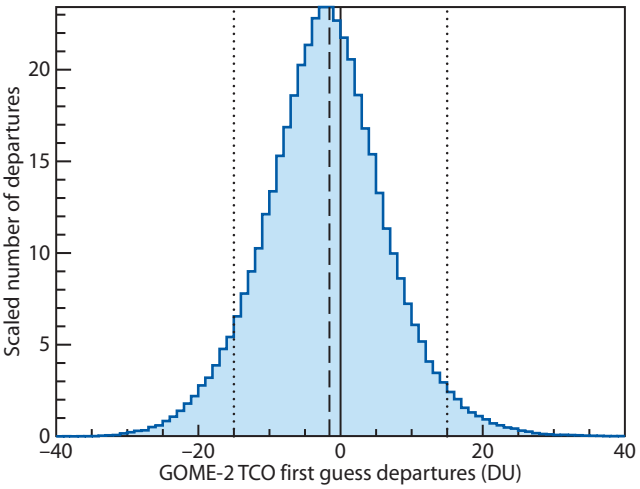

Figure 4 Distribution of the GOME-2 TCO first-guess departures over 24 hours for 25 July 2007. Values are in DU.

In addition to the passive monitoring, preliminary assimilation experiments of GOME-2 TCO have already started covering the period between 1 January and 28 February 2008. In the baseline experiment (CTRL), the SCIAMACHY TCO was the only ozone data actively assimilated. In the perturbation experiment (Exp/GOME2), the TCO from GOME-2 was also assimilated.

A complete assessment of the impact of GOME TCO on the ECMWF ozone analyses is not yet available. Comparisons with ozone sondes show some limited improvements in the upper troposphere and lower stratosphere when GOME-2 observations are assimilated. Two examples of monthly mean comparisons for January 2008 are shown in Figure 5 for one station at mid-latitudes in the northern hemisphere. The impact of the mean scores is generally negative, in particular in the southern hemisphere. Such a negative impact determined by the GOME-2 TCO assimilation contradicts, somehow, the good level of agreement found in the passive monitoring between these data and the ECMWF ozone analyses. However, if confirmed, these preliminary results seem to suggest that some extra care has to be taken before the assimilation. A potential problem in the assimilation, that requires further investigation, is the presence of systematic biases between different ozone products that have not yet been corrected.

Assimilation of MLS ozone profiles

There are a number of studies which have shown the potential benefit of assimilating the off-line ozone profiles retrieved from MLS data. For example, at the

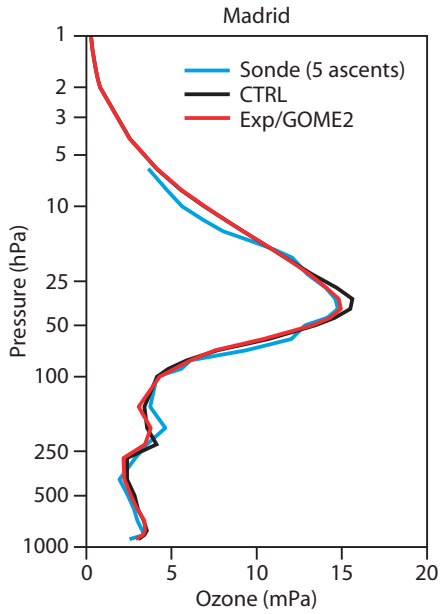

Figure 5 Comparison between the monthly mean ozone sonde profile launched from the Madrid station (40.5°N, 3.7°W) in January 2008 (blue) and co-located mean ozone profile from CTRL (black) and Exp/GOME2 (red).

NASA Goddard's Global Modeling and Assimilation Office (GMAO), assimilation trials of MLS ozone profiles in the GEOS-5 (Goddard Earth Observing System 5) data assimilation system produced a more realistic Antarctic ozone hole than, for example, SBUV/2 ozone data (*Sienkiewicz & Stajner*, 2007). Also *Feng et al.* (2008) found that the assimilation of MLS data using the ECMWF system had a positive impact on the stratospheric ozone analyses. However, the unavailability of MLS data in near-real-time, which is required by NWP centres, has enormously limited their usage. With the start of the near-real-time dissemination of this product, a further investigation of the potential benefits of MLS ozone profiles on the ECMWF ozone analyses using the most recent model is both timely and needed.

An assimilation trial of off-line MLS ozone profiles was performed for the period 1 July to 31 August 2007. In the CTRL experiment, SCIAMACHY TCO was the only ozone data actively assimilated. In the perturbation experiment (Exp/MLS), the MLS ozone profiles were also used to constrain the ozone analyses. Preliminary results are encouraging.

Figure 6 shows the comparison between the monthly mean ozone profiles obtained from the McMurdo ozone sondes and the corresponding mean ozone analyses from CTRL and Exp/MLS in August 2007. A similar comparison using the operational ozone analyses was shown in Figures 2. For clarity, Figure 6 does not show the one standard deviation range about each mean profile. As expected, the assimilation of MLS ozone profiles strongly improves the ozone vertical distribution, both in terms of vertical localization of the ozone maximum and its values, especially in a critical region like Antarctica.

Assimilation of AIRS infrared channels in the ozone-band

In addition to the traditional assimilation of ozone products, some attempts of assimilating radiances from the ozone-band in the infrared spectral region from infrared sounders, such as AIRS, are also under investigation. A huge amount of data is available from infrared sounders, currently not sufficiently exploited.

Two three-month long assimilation experiments (from 15 September to 14 December 2006) were run with cycle Cy31r2. CTRL made use of the operational set-up (i.e. all data used operationally in Cy31r2). In the perturbation experiment (Exp/AIRS), thirty-six channels in the spectral range between 1003 and 1286 cm^{-1} were also actively assimilated. Owing to emissivity problems, all radiances over land were blacklisted, and therefore not actively assimilated.

Comparisons between the two sets of ozone analyses showed little differences up to 7 to 8 DU in the total ozone. In the vertical, the assimilation of AIRS channels produces differences within –1 and +1 ppmm (parts per million mass), mainly in the lower stratosphere between 6 and 100 hPa. Comparisons with ozone sondes show negligible differences between the two experiments at mid-latitudes. In contrast, the assimilation of AIRS infrared channels generally leads to an improved level of agreement between the ozone sonde profiles and the collocated analyses in the tropics and at high latitudes in both hemispheres. As an example, Figure 7 shows the November monthly mean comparison for the sondes launched from Syowa (69°S), San Cristobal (0.9°S), and Eureka (80°N). The contribution of AIRS to the ozone analyses is particularly noticeable in the upper

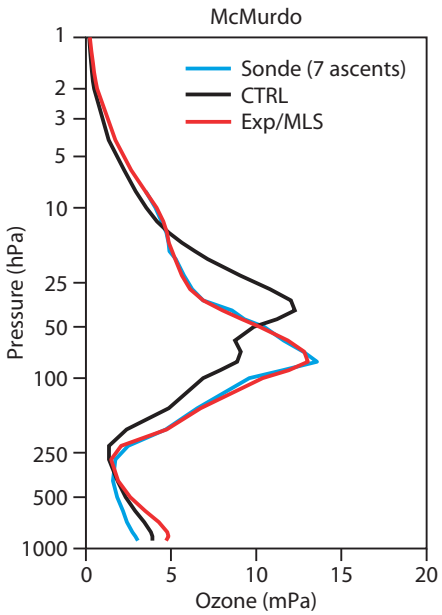

Figure 6 Comparison between the monthly mean ozone sonde profile launched from the McMurdo station (77.8°S, 166.7°W) in August 2007 (blue) and co-located mean ozone profile from CTRL (black) and Exp/MLS (red), respectively. All the ozone sondes were launched as part of the 2007 Match campaign.

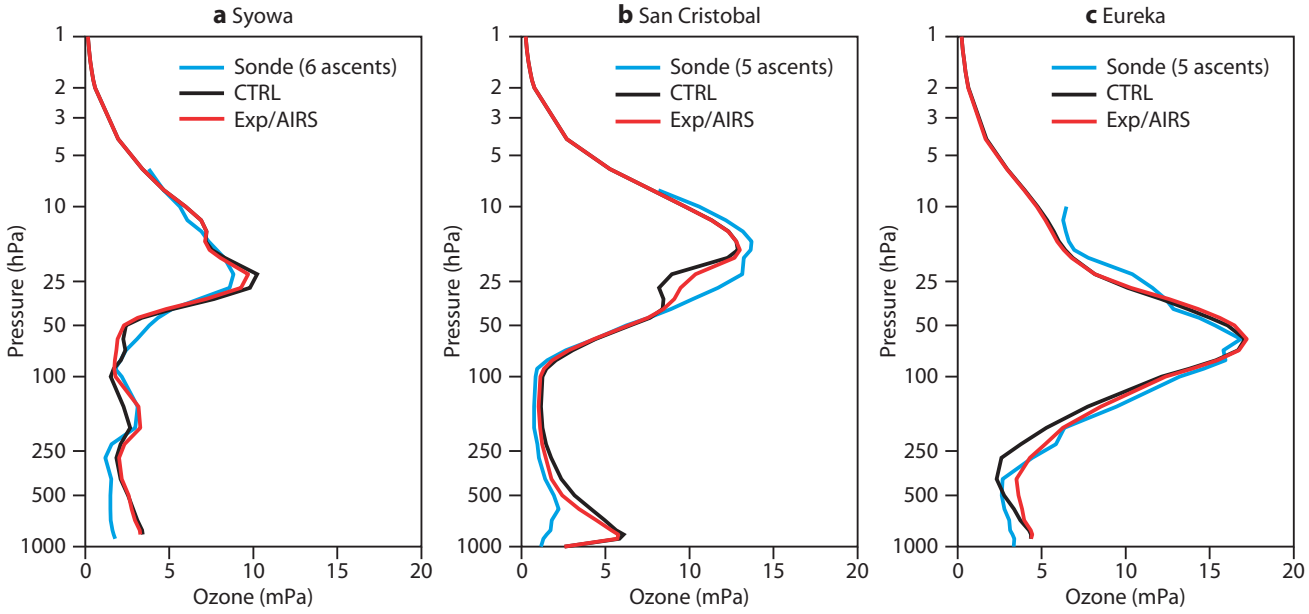

Figure 7 Comparison between the November monthly mean ozone sonde profile (blue) and co-located mean ozone profile from CTRL (black) and Exp/AIRS (red) for (a) a station at high latitudes in the southern hemisphere (Syowa, 69°S), (b) a station in the tropics (San Cristobal, 0.9°S), and (c) a station at high latitudes in the northern hemisphere (Eureka, 80°N).

troposphere and lower stratosphere. Comparisons with MLS ozone profiles also exhibit some improvements in the upper troposphere.

The impact of AIRS assimilation on the mean scores is generally positive, as shown by the mean geographical normalized rms (48-hour) forecast error difference between Exp/AIRS and CTRL for the total column ozone (Figure 8). Negative values (green) have to be regarded as an improvement determined by the assimilation of AIRS radiances over the CTRL analyses.

Table 3 summarises the mean normalized rms difference of the 24-, 48-, 72-, 96-, 120- and 240-hour forecast error of TCO between Exp/AIRS and CTRL for different regions. Indeed, the assimilation of AIRS channels in the ozone-band leads to improvements in the ozone field, especially within the first 96 hours of the forecasts. Particularly noticeable is the improvement in the mean scores over the southern hemisphere that still shows a positive impact (negative value) at day 10.

Ozone bias correction

Observations (and models) are prone to be affected by biases which, if uncorrected, can introduce systematic errors in the final analyses. In addition, non-negligible

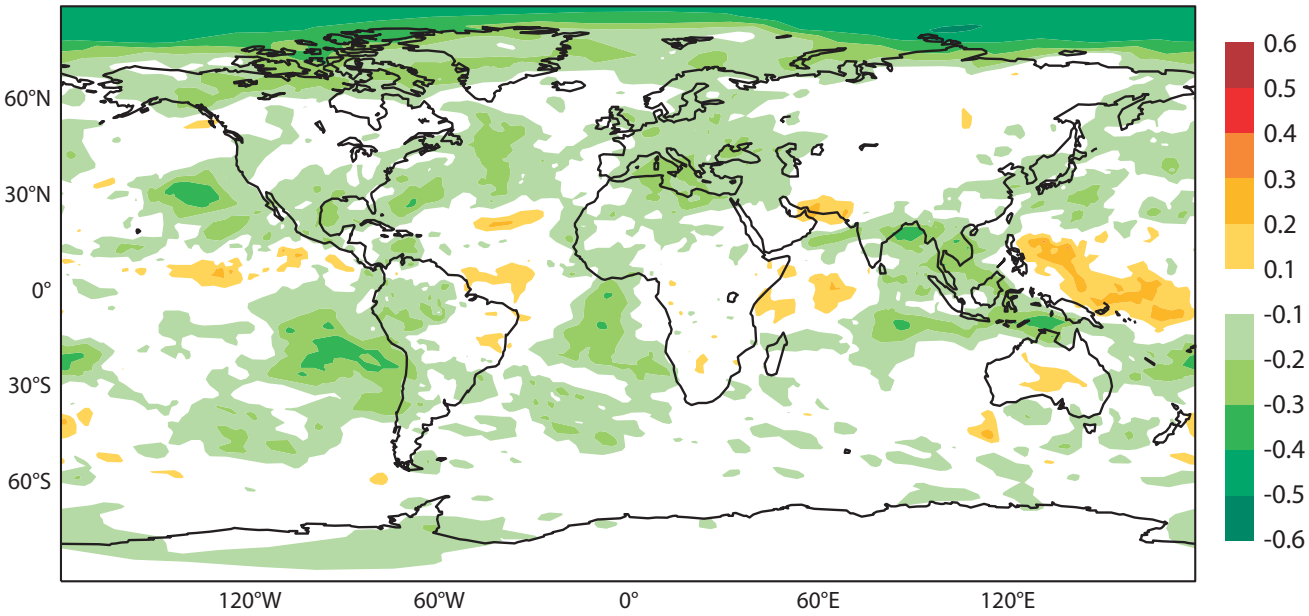

Figure 8 Mean normalized rms difference of the 48-hour forecast error between Exp/AIRS and CTRL for the total column ozone. Negative values (green) indicate an improvement due to the assimilation of AIRS radiances over the CTRL analyses.

	T+24	T+48	T+72	T+96	T+120	T+240
Northern hemisphere	-0.17	-0.11	-0.06	-0.03	-0.01	0.02
Southern hemisphere	-0.09	-0.06	-0.05	-0.03	-0.03	-0.01
Europe	-0.20	-0.14	-0.09	-0.04	-0.03	0
East Asia	-0.15	-0.08	-0.03	-0.01	-0.01	0.02
North America	-0.11	-0.09	-0.04	-0.02	0	0.01
Tropics	-0.12	-0.05	-0.02	0	0.02	0.08
North Atlantic	-0.18	-0.11	-0.07	-0.05	-0.03	0
North Pacific	-0.19	-0.10	-0.05	-0.01	0	0

Table 3 Summary of the mean normalized rms difference of the 24-, 48-, 72-, 96-, 120- and 240-hour total ozone forecast errors between Exp/AIRS and CTRL for different regions. Negative values (black) refer to a reduction (i.e. improvement) of the rms forecast error when AIRS radiances are actively assimilated. Positive values (blue) refer to an increase of the rms forecast error when AIRS radiances are actively assimilated. Zero values (red) correspond to neutral impact of the AIRS assimilation on the total ozone forecast error.

inter-instrumental biases can make the simultaneous assimilation of data from different sensors highly inefficient; the contribution from one instrument can, in principle, cancel that of another one. When increasing the number of sensors that provide the same data product, it becomes crucial to account for and correct these mutual biases. An operational bias correction for ozone (and retrieved products, in general) is not yet available at ECMWF, but development work is currently ongoing.

Based on the adaptive scheme of *Derber & Wu* (1998), a variational bias correction for radiances, VarBC, was introduced in the ECMWF operational suite (Cy31r1) on 11 September 2006 (*McNally et al.*, 2006). This scheme successfully corrects for systematic biases in the Level-1 data. In VarBC the bias correction is computed as a linear regression of a number of predictors. These predictors have to be carefully defined for each sensor and according to the data type. As far as the radiance bias correction is concerned, the predictors may include correction for air-mass or scan angle dependence, in addition to a global offset. The coefficients of the linear regression are included in a modified state vector, and therefore they are computed during the assimilation minimization. VarBC has recently been extended to correct for systematic errors in retrievals. This feature is currently being tested but is not yet operational.

The monitoring of satellite ozone products, which is routinely performed at ECMWF, shows that the observational systematic biases can vary in amplitude with season and location (with a strong latitudinal dependence), and with the vertical level for profiles. Using the solar elevation at the location and time of the observations, in addition to a global constant offset as a bias predictor, a two-month long ozone bias correction experiment (Exp/SOE) has already been completed. A second experiment with no ozone bias correction (CTRL) has been run for reference. The period under study is January and February 1997. The ozone products actively assimilated in both experiments were TOMS TCO retrieved from the ADEOS and Earth

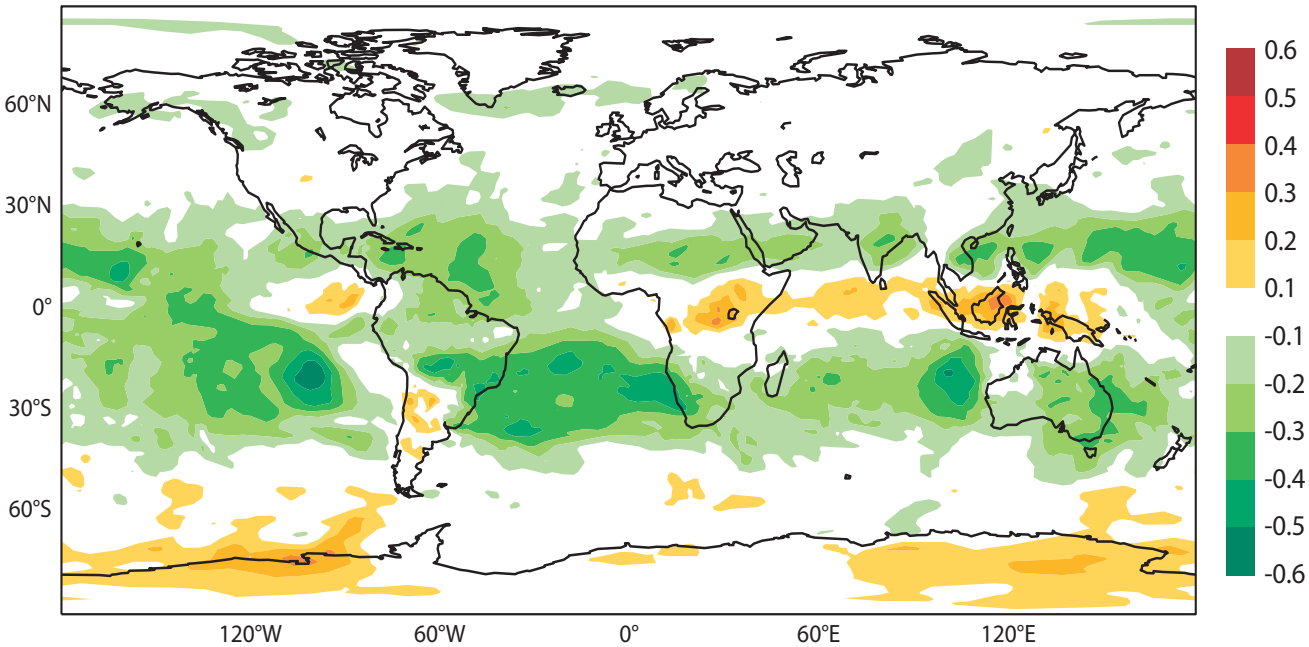

Figure 9 Mean normalized difference of the rms of the 24-hour forecast error between Exp/SOE and CTRL for the total column ozone. Negative values (green) indicate a reduction (i.e. improvement) of the rms error of the 24-hour forecast when the ozone bias correction is applied.

Probe measurements, SBUV/2 ozone partial columns from NOAA-9 and NOAA-14, and GOME ozone profiles from ERS-2. All the ozone data were simultaneously bias corrected in Exp/SOE.

Preliminary results show that for the ozone products both the first-guess and analysis departures are generally reduced in Exp/SOE compared with those of CTRL. In some cases this results in an increase of the number of data actively assimilated. Improvements were also found in the mean scores. Figure 9 shows the mean normalized difference of the rms error of the 24-hour forecasts of TCO between Exp/SOE and CTRL averaged over January and February 1997. Negative values (green) refer to a reduction (i.e. improvement) of the rms error of the 24-hour forecast when the ozone bias correction is applied. These preliminary results highlight some problems at high latitudes in the southern hemisphere – these require further investigation. Here the various sources of ozone information seem to be less consistent with each other when the bias correction is applied. In contrast, the consistency between the various sources of ozone information is substantially improved in the tropics due to the ozone bias correction.

Improving ozone products

A number of OSEs have been performed to assess the potential benefits of ozone products from a number of recently launched remote sounders on the ECMWF ozone analyses. Indeed, all the sensors and data products used in these studies have shown that they can potentially improve the quality of the ozone analyses. TCO retrieved from ultraviolet nadir sensors, such as OMI, showed a small but statistically significant positive impact on the ozone analyses especially in the lower stratosphere where there is improved agreement with independent, unassimilated observations.

Despite of this potential enhancement, constraining the ozone vertical distribution with such sensors is generally still a challenge. Comparisons of the operational ozone products with ozone sonde profiles clearly show that the ozone observations that are currently assimilated at ECMWF (mainly TCO from ultraviolet sounders) can provide an appropriate constraint to the analysis of total column ozone. However, they are still inadequate to fully constrain the ozone vertical distribution. In addition, the high latitude region in the winter hemisphere can also suffer from a lack of data, as at this time of the year nadir ultraviolet instruments – largely used for ozone retrieval – cannot make measurements. Preliminary results from the assimilation of MLS ozone profiles using the latest suite are very promising.

An additional source of information in critical regions, such as the high latitudes in the winter hemisphere, and yet not fully exploited is represented by infrared sensors. A first attempt of assimilating radiances in the infrared ozone-band from the AIRS sounder has also been performed. Preliminary results show that, although small, the assimilation of the AIRS ozone-band has a positive impact on the ozone analyses. There is an improvement in the comparison with independent observations (ozone sondes and MLS) mainly in the upper troposphere and lower stratosphere, as well as improving the mean forecast scores. As for future plans, the investigation of the potential benefits of the assimilation of infrared ozone-channels from AIRS will be completed and extended to other sounders, such as IASI.

As the number of ozone instruments actively used increases, systematic inter-instrumental biases start to be important, and in some cases the potential benefits of one instrument are cancelled by the assimilation of another one. Work on limiting, if not completely removing, these biases in the ozone observations is currently ongoing. Preliminary results from the first ozone bias correction trial performed within the reanalysis framework are encouraging. Some problems were seen at high latitudes in the southern hemisphere that require further investigation. However, the preliminary results show a general reduction of the first-guess and analysis departures of all the ozone products, as well as a substantial reduction in the rms error of the 24-hour forecast in the tropics.

FURTHER READING

Cariolle, **D.** & **M**. **Deque**, 1986: Southern hemisphere medium-scale waves and total ozone disturbances in a spectral general circulation model, *J. Geophys. Res.*, **91**, 10825–10846.

Derber, **J**.**C**. & **W**.-**S**. **Wu**, 1998: The use of TOVS cloud-cleared radiances in the NCEP SSI analysis system. *Mon. Wea. Rev.*, **126**, 2287–2299.

Dethof, **A**., 2003: Assimilation of ozone retrievals from the MIPAS instrument on board ENVISAT. *ECMWF Tech. Memo. No. 428.*

Feng, **L**., **R**. **Brugge**, **E**. **V**. **Holm**, **R**. **S**. **Harwood**, **A**. **O'Neill**, **M**. **J**. **Filipiak**, **L**. **Froidevaux** & **N**. **Livesey**, 2008: Four-dimensional variational assimilation of ozone profiles from the Microwave Limb Sounder on the Aura satellite. In press in *J. Geophys. Res.*, **113**, doi:10.1029/2007JD009121.

McNally, **T**., **T**. **Auligné**, **D**. **Dee** & **G**. **Kelly**, 2006: A variational approach to satellite bias correction. *ECMWF Newsletter No. 107*, 18–23.

Mercer, **J**.**L**., **C**. **Kruger**, **B**. **Nardi**, **B**.**J**. **Johnson**, **M**.**P**. **Chipperfield**, **S**.**W**. **Wood**, **S**.**E**. **Nichol**, **M**.**L**. **Santee** & **T**. **Deshler**, 2007: Comparison of measured and modelled ozone above McMurdo station, Antarctica, 1989–2003, during Austral winter/spring. *J. Geophys. Res.*, **112**, D19307, doi:10.1029/2006JD007982.

Sienkiewicz, **M**. & **I**. **Stajner**, 2007: Assimilation of MLS ozone observations improves Antarctic ozone hole depiction. *JCSDA Quarterly Newsletter No. 18*, March 2007, www.jcsda.noaa.gov.

Improving the radiative transfer modelling for the assimilation of radiances from SSU and AMSU-A stratospheric channels

SHINYA KOBAYASHI, MARCO MATRICARDI, DICK DEE, SAKARI UPPALA

STRATOSPHERIC analyses using satellite observations have been available for almost three decades. They provide important information about the dynamical behaviour of the upper atmosphere. There has been a growing concern about the changing amounts of trace constituents in the upper atmosphere, where they protect life from solar ultraviolet radiation. The abundance of trace constituents is controlled by their transport as well as the chemical processes. Thus high quality stratospheric analyses are required for the accurate analysis and prediction of trace constituents. Another role of stratospheric analyses is to provide numerical weather prediction (NWP) systems with "boundary conditions". The radiances observed by the tropospheric channels are partly sensitive to the temperature structure in the stratosphere, because their weighting functions extend to the stratosphere. Thus accurate stratospheric analyses are important to produce good quality initial conditions for NWP.

Stratospheric temperature analyses, dominated by satellite data, are strongly affected by the possible biases in stratospheric channels. Changing bias characteristics are often reflected in stratospheric temperature analyses as jumps that correspond to satellite transitions or drifts due to slower changes in biases. These artificial features can mask the true climate signals and make it difficult to estimate reliable long-term temperature trends. Thus biases in observations have to be accounted for to produce a consistent atmospheric dataset that is appropriate for climate research.

Satellites make indirect observations of physical properties of the earth system. Use of satellite data in an assimilation system requires a fast radiative transfer model (RTM) to simulate radiances using model fields. Several different RTMs are in use at NWP centres, e.g. the radiative transfer model for TOVS (RTTOV) (*Saunders et al.*, 1999) and the Community Radiative Transfer Model (CRTM) (*Kleespies et al.*, 2004). Especially for early satellite instruments, biases can be generated by improper characterization of the spectral response functions or by changes in the concentration of radiatively active constituents that are unaccounted for in the RTMs. Those biases in the RTMs have to be addressed when using satellite observations for atmospheric reanalysis.

Inter-satellite biases

Stratospheric temperatures have been retrieved from radiance observations made by the NOAA polar orbiting satellites since 1978. Data from infrared channels of the Stratospheric Sounding Unit (SSU) on the TIROS-N to NOAA-14 satellites has been used to retrieve stratospheric temperature information. From NOAA-15 onward the SSU was replaced by a higher vertical resolution microwave instrument, the Advanced Microwave Sounding Unit (AMSU-A). Raw SSU radiances were first assimilated in a reanalysis carried out at ECMWF (ERA-40) and more recently in the Japanese 25-year Reanalysis (JRA-25). Both reanalyses encountered difficulties in fully utilising the SSU radiance data due to large biases in the background temperatures combined with inadequate data coverage for much of the period. Particularly problematic periods are the early 1980s, when SSUs had large inter-satellite biases, and the late 1990s, when AMSU-A data first became available.

Figure 1 shows time series of inter-satellite biases between NOAA-6 and NOAA-7 for SSU channel 3 over the Antarctic, estimated using the Simultaneous Nadir Overpass (SNO) technique (*Cao et al.*, 2005). This technique compares observations made by different satellites at the same time and location. Since both instruments sense the same atmospheric profiles, this comparison produces reliable estimates of the inter-satellite biases that are entirely attributable to differences in the radiometric and spectroscopic performance of the instruments. The seasonal dependence of the relative

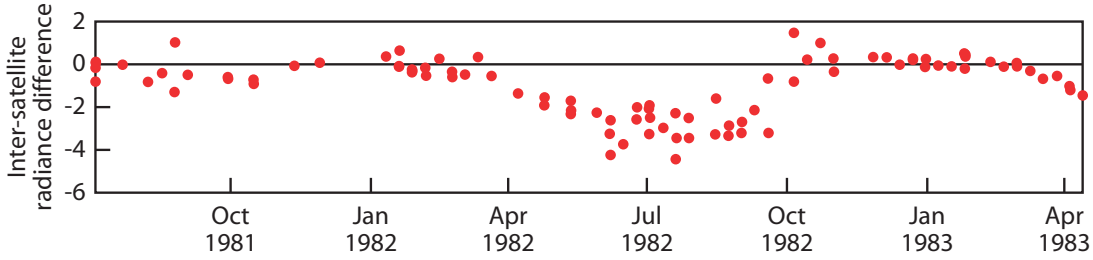

Figure 1 Inter-satellite differences between radiance measurements from SSU channel 3 on NOAA-6 and NOAA-7 over the Antarctic, obtained with the SNO technique.

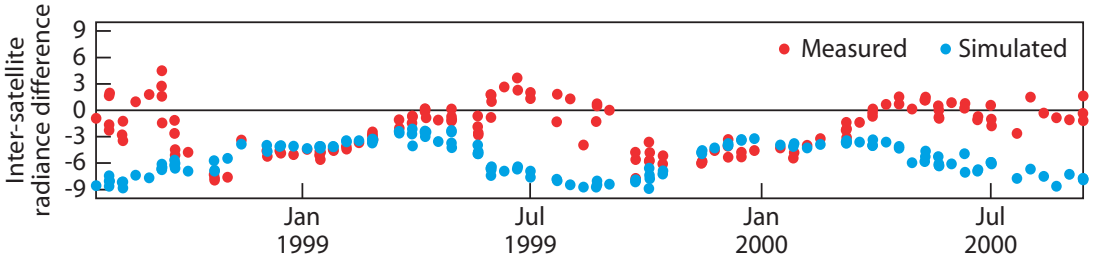

Figure 2 Inter-satellite differences between radiance measurements from SSU channel 3 on NOAA-11 and AMSU-A channel 14 on NOAA-15 over the Antarctic, obtained with the SNO technique (red) and the corresponding simulated differences using RTTOV (blue).

biases evident in Figure 1 can be correlated with the lapse rate in the upper stratosphere, indicating that the weighting functions are not identical.

The inter-satellite radiance differences between SSU and AMSU-A were also estimated with the SNO technique – see Figure 2. The discrepancy between the measured radiance differences and the differences simulated using RTTOV is especially significant in spring and winter. This is not easily explained by instrument errors alone, which suggests that the RTTOV radiance simulations themselves might be inaccurate.

Radiative transfer modelling – SSU

SSU is a three-channel infrared radiometer designed to measure radiances in the 15 μm carbon dioxide absorption band. The SSU uses a pressure modulation technique where the pressure in a cell of carbon dioxide gas in the instrument's optical path is varied in a cyclic manner. The spectral performance of the instrument depends on the mean cell pressure whose long-term stability is crucial for time-consistent observations. As it turned out, a sealing problem caused cell pressures to increase during storage on the ground and then to decrease after launch. The Met Office, which produced the instrument, has routinely monitored and recorded the mean cell pressure at six-month intervals subsequent to the launch of each spacecraft. Figure 3 shows daily values of the mean cell pressures estimated from these records. The gradual reduction of cell pressure affects the level of peak energy for the SSU channels. Figure 4 shows typical changes to the weighting functions. The channels most affected are channels 2 and 3, which both peak in the upper stratosphere.

We studied the impact of the recorded SSU cell pressure changes by accurately modelling their effect on the radiances using the LBLRTM line-by-line model (*Clough et al.*, 2004). Figure 5 shows time series of the line-by-line simulated inter-satellite biases for the same pair of satellites shown in Figure 1, together with the actual biases obtained with the SNO technique. Although

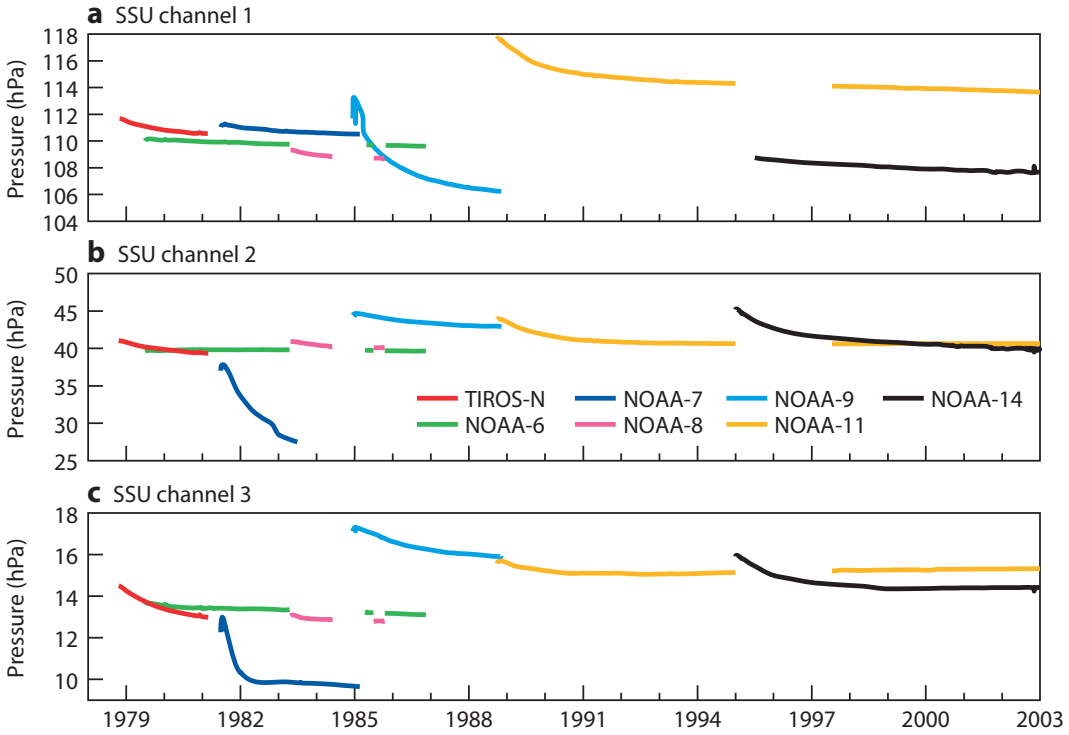

Figure 3 Daily values of the mean cell pressures for channels 1, 2 and 3 of all the SSU instruments are shown as time series. The values have been interpolated from the Met Office's six-monthly estimates using a linear relationship between the mean cell pressure and the modulation frequency.

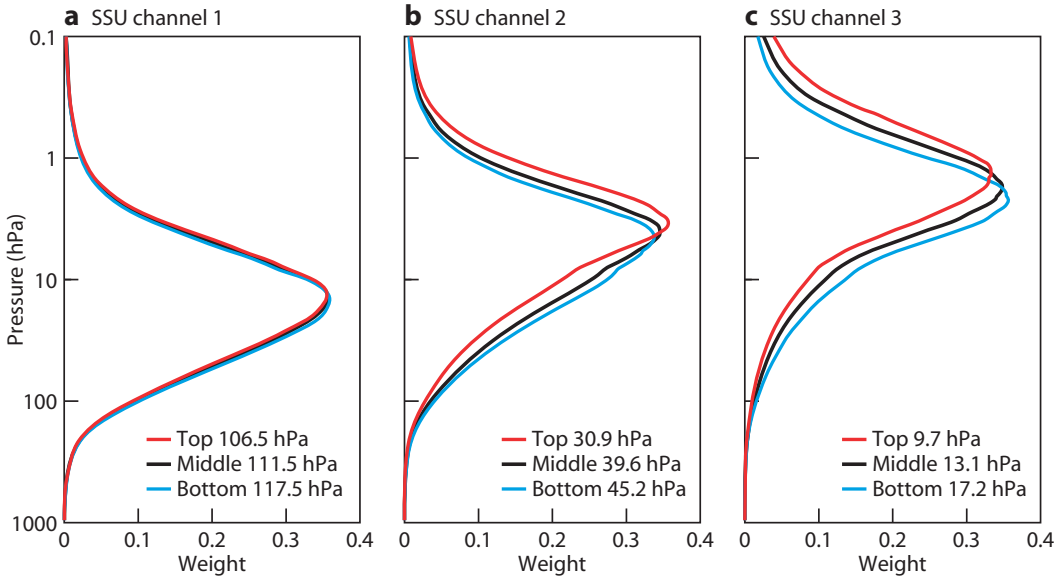

Figure 4 Impact of the changes in mean cell pressure on the weighting functions for (a) channel 1, (b) channel 2 and (c) channel 3 of the SSU for the US Standard Atmosphere 1976 with carbon dioxide at 330 ppmv (parts per million by volume).

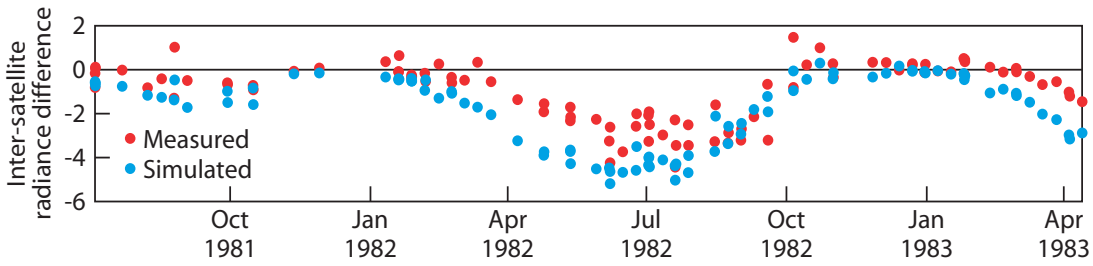

Figure 5 Inter-satellite differences between the radiance measurements from SSU channel 3 on NOAA-11 and AMSU-A channel 14 on NOAA-15 over the Antarctic, obtained with the SNO technique (as shown in Figure 1) and the corresponding simulated differences using the LBLRTM model to account for the pressure loss in the carbon dioxide cell.

discrepancies between the observed and simulated inter-satellite biases still exist (possibly due to uncertainties in the band-pass filter and the calibration algorithm), the seasonal cycle is much better captured in the line-by-line calculations. On this basis, new RTTOV coefficients for the SSU have been generated that properly take into account the variation of the mean pressure in the carbon dioxide cell.

Radiative transfer modelling – AMSU-A

AMSU-A is a multi-channel microwave radiometer designed to retrieve vertical profiles of temperature from about 3 hPa (45 km) to the surface. The AMSU-A stratospheric channels measure the radiance originating from the 60-Ghz oxygen absorption lines. These magnetic-dipole absorption lines are split by the terrestrial magnetic field. This splitting is due to the Zeeman effect which is particularly important at low pressures when the magnitude of the line splitting is comparable to or smaller than the line width and can thus affect the high-peaking stratospheric channels of AMSU-A.

RTTOV represents the Zeeman effect by a scalar approximation described in *Liebe et al.* (1993), which models the effect simply by increasing the line-broadening parameter for the oxygen absorption lines. We compared attenuation rates at frequencies that include the pass bands of AMSU-A channel 14, using three alternative representations of the Zeeman effect: the RTTOV scalar approximation; explicit simulation using a line-by-line model; and omission of the Zeeman effect. Figure 6 shows that the scalar approximation is accurate at the frequencies near the centre of the oxygen absorption line, but overestimates the attenuation rates within the pass bands of AMSU-A channel 14. As shown in Figure 7, this results in an anomalous upward shift of its weighting function.

Figure 7 also shows that for AMSU-A channel 14 the RTTOV weighting function computed without the Zeeman effect is much closer to that obtained by explicit simulation. Therefore the scalar approximation of the Zeeman effect results in radiance simulations that are less accurate than would be obtained by omitting it completely. Although the optimal solution would be to include an explicit model for Zeeman splitting in RTTOV, this would require a long-term effort. As a practical short-term solution to improve the RTTOV simulation of AMSU-A radiance data, we have trained RTTOV by performing new line-by-line computations

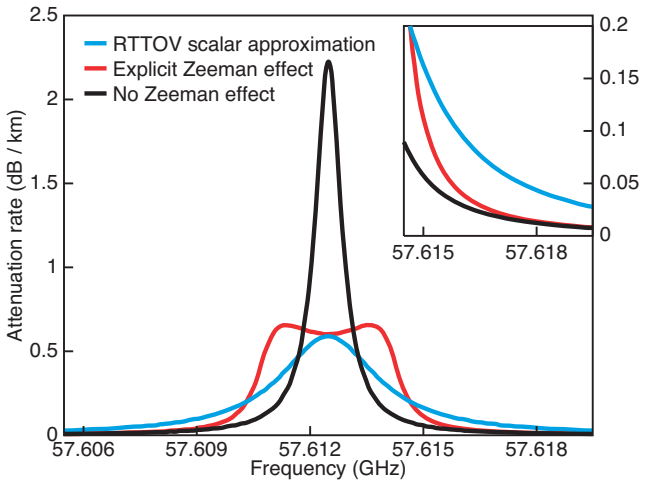

Figure 6 Simulation of attenuation rates at the frequencies around the pass bands of AMSU-A channel 14 at 0.29 hPa using the RTTOV scalar approximation, an explicit representation of the Zeeman effect, and no Zeeman effect.

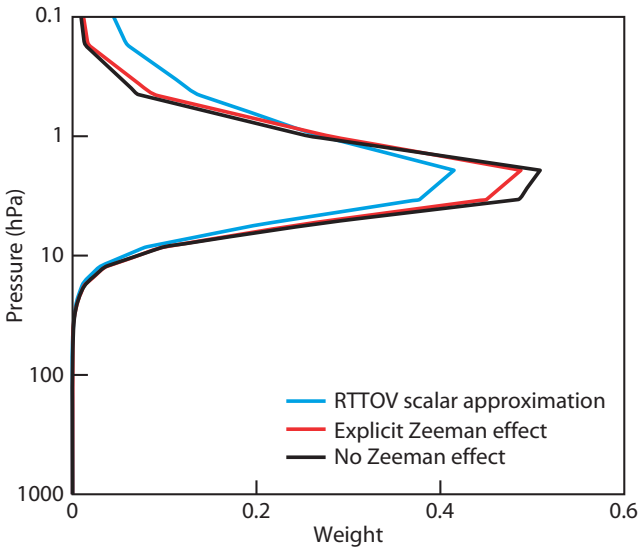

Figure 7 Weighting functions for AMSU-A channel 14 based on the US Standard Atmosphere 1976, using the RTTOV scalar approximation, an explicit representation of the Zeeman effect, and no Zeeman effect.

which include cell pressure variations but exclude Zeeman splitting.

Figure 8 shows the time series of the inter-satellite radiance differences calculated with the revised radiative transfer model for the same pair of satellites shown in Figure 2, together with the actual inter-satellite radiance differences obtained with the SNO technique. The remarkable agreement between the measured and the computed radiance differences indicates a significant improvement of the accuracy of the revised RTTOV radiative transfer simulations.

Impact on the stratospheric temperature analysis

Assimilation experiments for testing the new AMSU-A coefficients have been performed. The period of the experiments is one year starting August 1998, which is when AMSU-A data first became available. The experiments utilised the ERA-Interim configuration (T255L60 with the top level at 0.1 hPa; for details see *ECMWF Newsletter No. 110*), using the current AMSU-A coefficients for the control assimilation and the revised AMSU-A coefficients for the new radiative transfer experiment. All satellite radiance data were subject to variational bias correction (VarBC; see *ECMWF Newsletter No. 107*).In order to constrain the upper-stratospheric temperature analysis in the presence of a large, warm, forecast model bias, radiances from AMSU-A channel 14 were corrected for scan biases only.

Figure 9 shows the evolution of the vertical temperature structures in polar regions. The control assimilation tends to create spurious peaks around model levels 6 and 10 (2 and 5 hPa respectively) when the strong polar vortex develops in winter. This is because the weighting function for AMSU-A channel 14 in the operational RTTOV is located too high, which results in too warm radiance simulations when the mesosphere is warmer than the stratosphere. Such a situation occurs in the polar regions in winter. In the experiment performed with the revised RTTOV model, these spurious peaks have been reduced and the vertical temperature structure varies more smoothly with the seasons.

Assimilation experiments for testing the new SSU coefficients are currently underway. Preliminary results show a significant reduction in the standard deviations of first-guess departures (observations minus their modelled equivalents) for SSU data. This suggests an improvement of the accuracy of the RTTOV radiative transfer simulations. The impact on the long-term temperature trends of the stratospheric temperature analysis is now being investigated.

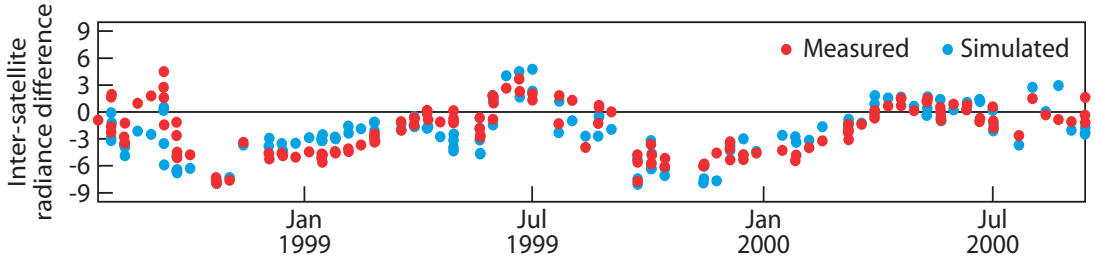

Figure 8 Inter-satellite differences between radiance measurements from SSU channel 3 on NOAA-11 and AMSU-A channel 14 on NOAA-15 over the Antarctic, obtained with the SNO technique (red, as shown in Figure 2) and the corresponding simulated differences using the revised version of RTTOV (blue).

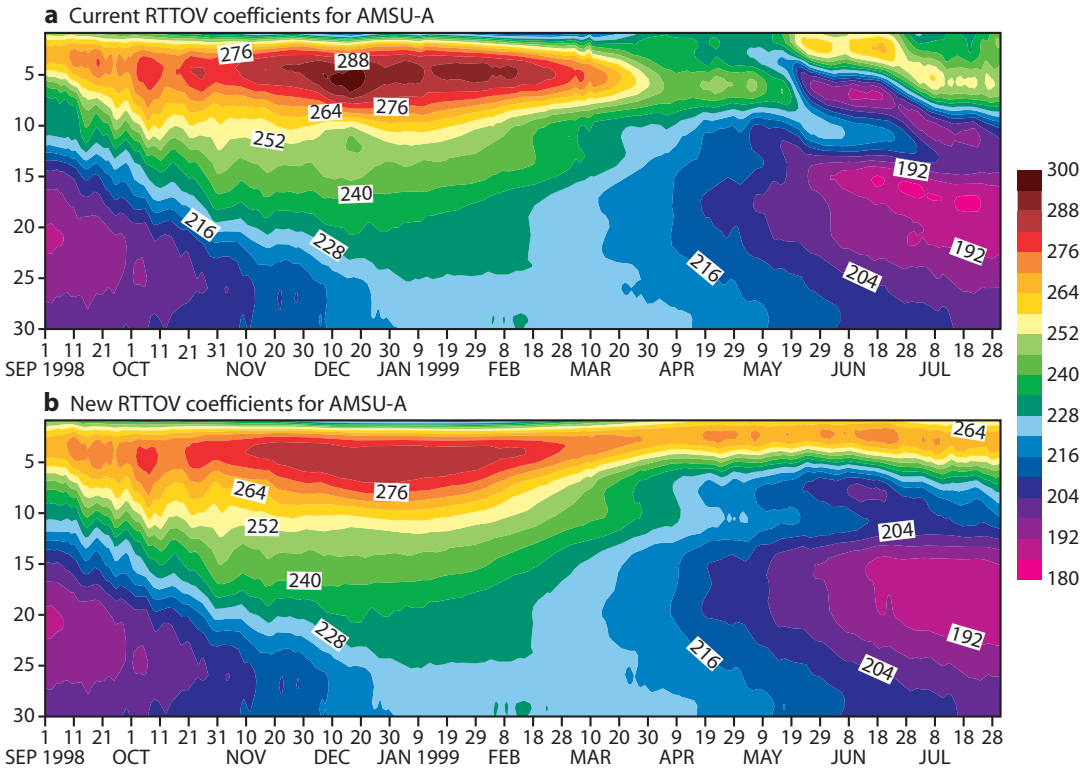

Figure 9 Evolution of the vertical temperature structures over the Antarctic (60° to 90°S) from September 1998 to July 1999 for assimilations using (a) the current RTTOV coefficients for AMSU-A and (b) the new RTTOV coefficients for AMSU-A. The vertical axes represent model levels.

Current and future improvements

For a better use of the SSU and AMSU-A observations in reanalyses, the radiative transfer modelling for these instruments has been re-examined. This has led to a revision of the RTTOV coefficients based on more accurate radiative transfer computations. Forward calculations using the revised coefficients have proved to be more accurate than those using the operational RTTOV coefficients. While the new SSU coefficients are still being tested in assimilation experiments, the new AMSU-A coefficients are soon to be released with the RTTOV-9 package. We expect that the revised RTTOV modelling for SSU and AMSU-A will significantly improve the time consistency of upper-stratospheric temperature analyses.

Looking ahead, a proper representation of the Zeeman splitting effect in fast radiative transfer models was studied by *Han et al.* (2007) with the aim of improving the accuracy of the SSMI/S upper atmosphere channel simulations. This scheme has already been implemented in the CRTM fast model and has been selected for implementation in RTTOV-10 for SSMI/S (Special Sensor Microwave Imager/Sounder) and possibly AMSU-A channels. This development is expected to further improve our understanding of the dynamical behaviour of the upper atmosphere.

FURTHER READING

Cao, **C.**, **H. Xu**, **J. Sullivan**, **L. McMillin**, **P. Ciren** & **Y.T. Hou**, 2005: Intersatellite Radiance Biases for the High-Resolution Infrared Radiation Sounders (HIRS) on board NOAA-15, -16, and -17 from simultaneous nadir observations. *J. Atmos. Oceanic Technol.*, **22**, 381–395.

Clough, **S.A.**, **M.W. Shephard**, **E.J. Mlawer**, **J.S. Delamere**, **M.J. Iacono**, **K. Cady-Pereira**, **S. Boukabara** & **P.D. Brown**, 2004: Atmospheric radiative transfer modeling: a summary of the AER codes. *J. Quant. Spectrosc. and Radiat. Transfer*, **91**, 233–244.

Han, **Y.**, **F. Weng**, **Q. Liu** & **P. van Delst**, 2007: A fast radiative transfer model for SSMIS upper atmosphere sounding channels. *J. Geophys. Res.*, **112**, D11121, doi:10.1029/2006JD008208.

Kleespies, **T.J.**, **P. van Delst**, **L.M. McMillin** & **J. Derber**, 2004: Atmospheric Transmittance of an Absorbing Gas. 6. OPTRAN Status Report and Introduction to the NESDIS/NCEP Community Radiative Transfer Model. *Appl. Optics*, **43**, 3103–3109.

Liebe, **H.J.**, **G. A. Hufford** & **M.G. Cotton**, 1993: Propagation modeling of moist air and suspended water/ice particles at frequencies below 1000 GHz. In *Proc. NATO/AGARD Wave Propagation Panel, 52nd Meeting, Paper No. 3/1–10*, Mallorca, Spain, May 1993.

McNally, **A.P.**, **T. Auligné**, **D. Dee** & **G. Kelly**, 2006: A variational approach to satellite bias correction. *ECMWF Newsletter No.107*, 18–23.

Saunders, **R.**, **M. Matricardi** & **P. Brunel**, 1999: An improved fast radiative transfer model for assimilation of satellite radiance observations. *Q. J. R. Meteorol. Soc.*, **125**, 1407–1425.

Simmons, **A.**, **S. Uppala**, **D. Dee** & **S. Kobayashi**, 2006: ERA-Interim: New ECMWF reanalysis products from 1989 onwards. *ECMWF Newsletter No. 110*, 25–35.

ECMWF Calendar 2008

Sep 1–4	Seminar on "Parametrization of Subgrid-scale Physical Processes"
Sep 16–17	Trilateral Meeting of the Co-ordinating Committee on Remuneration
Sep 22–26	Training Course – Use of supercomputing resources
Oct 6–8	Scientific Advisory Committee (*37th Session*)
Oct 8–10	Technical Advisory Committee (*39th Session*)
Oct 13–17	Training Course – Use and interpretation of ECMWF products for WMO Members
Oct 13–14	Finance Committee (*81st Session*)
Oct 14–15	Policy Advisory Committee (*27th Session*)
Oct 20	Advisory Committee of Co-operating States (*14th Session*)
Nov 3–7	13th Workshop on "High Performance Computing in Meteorology"
Nov 10–12	Workshop on "Ocean-atmosphere Interaction"
Dec 2–3	Council (*70th Session*)

ECMWF publications

(see http://www.ecmwf.int/publications/)

Technical Memoranda

566 **Drusch, M., T. Holmes, P. de Rosnay & G. Balsamo**: Comparing ERA-40 based L-band brightness temperatures with Skylab observations: A calibration/validation study using the Community Microwave Emission Model. *July 2008*

565 **de Rosnay, P., M. Drusch, A. Boone, G. Balsamo, B. Decharme, P. Harris, Y. Kerr, T. Pellarin, J. Polcher & J.-P. Wigneron**: The AMMA Land Surface Model Intercomparison Experiment coupled to the Community Microwave Emission Model: ALMIP-MEM. *July 2008*

564 **Matricardi, M.**: The generation of RTTOV regression coefficients for IASI and AIRS using a new profile training set and a new line-by-line database. *May 2008*

563 **Balsamo, G., P. Viterbo, A. Beljaars, M. Hirschi, B. van den Hurk, A.K. Betts & K. Scipal**: A revised hydrology for the ECMWF model: Verification from field site to terrestrial water storage and impact in the Integrated Forecast System. *April 2008*

562 **Daget, N., A.T. Weaver & M.A. Balmaseda**: An ensemble three-dimensional variational data assimilation system for the global ocean: sensitivity to the observation- and background-error variance formulation. *June 2008*

561 **Fisher, M., J. Nocedal, Y. Trémolet & S.J. Wright**: Data assimilation in weather forecasting: A case in PDE-constrained optimization. *April 2008*

554 **Hersbach, H.**: CMOD5.N: A C-band geophysical model function for equivalent neutral wind. *April 2008*

Proceedings

ECMWF Workshop on Ensemble Prediction, 7–9 November 2007.

Index of past newsletter articles

This is a selection of articles published in the ECMWF Newsletter series during the last five years. Articles are arranged in date order within each subject category. Articles can be accessed on the ECMWF public website – www.ecmwf.int/publications/newsletter/index.html

Useful names and telephone numbers within ECMWF

Telephone
Telephone number of an individual at the Centre is:
International: +44 118 949 9 + three digit extension
UK: (0118) 949 9 + three digit extension
Internal: 2 + three digit extension
e.g. the Director's number is:
+44 118 949 9001 (international),
(0118) 949 9001 (UK) and 2001 (internal).

E-mail
The e-mail address of an individual at the Centre is:
firstinitial.lastname@ecmwf.int
e.g. the Director's address is: D.Marbouty@ecmwf.int
For double-barrelled names use a hyphen
e.g. J-N.Name-Name@ecmwf.int

Internet web site
ECMWF's public web site is: http://www.ecmwf.int

	Ext
Director	
Dominique Marbouty	001
Deputy Director & Head of Research Department	
Philippe Bougeault	005
Head of Operations Department	
Walter Zwieflhofer	003
Head of Administration Department	
Ute Dahremöller	007
Switchboard	
ECMWF switchboard	000
Advisory	
Internet mail addressed to Advisory@ecmwf.int	
Telefax (+44 118 986 9450, marked User Support)	
Computer Division	
Division Head	
Isabella Weger	050
Computer Operations Section Head	
Sylvia Baylis	301
Networking and Computer Security Section Head	
Rémy Giraud	356
Servers and Desktops Section Head	
Richard Fisker	355
Systems Software Section Head	
Neil Storer	353
User Support Section Head	
Umberto Modigliani	382
User Support Staff	
Paul Dando	381
Anne Fouilloux	380
Dominique Lucas	386
Carsten Maaß	389
Pam Prior	384
Computer Operations	
Call Desk	303
Call Desk email: calldesk@ecmwf.int	
Console – Shift Leaders	803
Console fax number +44 118 949 9840	
Console email: newops@ecmwf.int	
Fault reporting – Call Desk	303
Registration – Call Desk	303
Service queries – Call Desk	303
Tape Requests – Tape Librarian	315

	Ext
Meteorological Division	
Division Head	
Erik Andersson	060
Meteorological Applications Section Head	
Alfred Hofstadler	400
Data and Services Section Head	
Baudouin Raoult	404
Graphics Section Head	
Stephan Siemen	375
Meteorological Operations Section Head	
David Richardson	420
Meteorological Analysts	
Antonio Garcia-Mendez	424
Anna Ghelli	425
Claude Gibert (web products)	111
Fernando Prates	421
Meteorological Operations Room	426
Data Division	
Division Head	
Jean-Noël Thépaut	030
Data Assimilation Section Head	
To be announced	–
Satellite Data Section Head	
Peter Bauer	080
Re-Analysis Section Head	
Dick Dee	352
Probabilistic Forecasting & Diagnostics Division	
Division Head	
Tim Palmer	600
Seasonal Forecasting Section Head	
Franco Molteni	108
Model Division	
Division Head	
Martin Miller	070
Numerical Aspects Section Head	
Agathe Untch	704
Physical Aspects Section Head	
Anton Beljaars	035
Ocean Waves Section Head	
Peter Janssen	116
GMES Coordinator	
Adrian Simmons	700
Education & Training	
Renate Hagedorn	257
ECMWF library & documentation distribution	
Els Kooij-Connally	751